TECHNISCHE UNIVERSITÄT WIEN
Vienna University of Technology

ESEA
Institut für Energiesysteme
und Elektrische Antriebe

MASTER THESIS

Influence of the Reactive Power Control on the Voltage of the Next Higher Voltage Level Grid

In partial fulfillment of the requirements for the degree
Diplom-Ingenieur (Dipl.-Ing.)

committed by
Univ.-Prof. Dr. techn. Wolfgang Gawlik
Univ.-Ass. Dr. techn. Albana Ilo
of the

Vienna University of Technology
Faculty of Electrical Engineering and Information Technology
Institute of Energy Systems and Electrical Drives

by
Alexander Oman, BSc

29.09.15, Vienna

Department: Energy Systems
A-1040 Vienna, Gusshausstr. 25-29/370-1, http://www.ea.tuwien.ac.at

Acknowledgment

In this acknowledgment I would like to thank all those people who made this Thesis possible.

First of all I gratefully acknowledge the Salzburg Netz GmbH for kindly providing the data for the real grid.

I would like to express my deepest sense of gratitude to Dr. Albana Ilo who continually offered advice and assistance in the course of this Thesis.

I am thankful to Prof. Wolfgang Gawlik who aroused my interest in this topic during his excellent lectures and who always takes time to help and support his students.

Finally my very sincere thanks to my family and friends for the encouragement and support whenever I was in need.

Abstract

The penetration of distributed generation is increasing continuously in all voltage levels of the distribution networks. The use of reactive power consumption and injection to suppress voltage violations in the medium voltage level has caused an uncontrolled reactive power flow over the HV/MV transformer. This Master Thesis investigates the volatile power effects and the resulting voltage interdependencies between the high voltage level and the medium voltage level in the presence of a high share of distributed generation.

Firstly, the impact on the medium- and the high voltage grid of the IEEE 30 Bus Test Network, is analyzed. Secondly, the investigations are extended to a real European distribution grid, which already incorporates a high share of distributed generation in its medium voltage grid. The analyses are performed by varying the level of distributed generation in the medium voltage grid. The $Q(U)$ local controllers are taken into account and their effect is analyzed in detail. The analyses of the medium- and high voltage grid are performed by load flow simulations in PSS Sincal.

Results have shown that with an increasing share of distributed generation the voltage and reactive power flow on the superordinate grid are affected. This phenomenon is not visible for a small distributed generation share. The reactive power flow in the superordinate grid is unpredictable because the local reactive power controller in the medium voltage grid induces it. The reaction of the local controller in the case of wind and photovoltaic distributed generations is a function of the voltage level and the weather conditions.

Kurzzusammenfassung

Mit stetig steigender Verbreitung dezentraler Erzeugung in allen Spannungsebenen des Verteilnetzes steigt auch der Einsatz lokaler *Q(U)* Regler, um gegen Spannungslimitüberschreitungen vorzugehen, immer weiter an. Dies bewirkt einen unkontrollierten Blindleistungsfluss über den Transformator. Diese Masterarbeit untersucht die Effekte der volatilen Einspeisung bei einem hohen Anteil an dezentraler Erzeugung und die daraus resultierenden Zusammenhänge der Spannungen aus dem Hoch- und Mittelspannungsnetz.

Zu beginn dieser Arbeit wird der Einfluss eines großen Anteils dezentraler Erzeugung auf das Hoch- und Mittelspannungsnetz des IEEE 30 Bus Test Netzwerks analysiert. Danach wird die Analyse auf ein reales europäisches Verteilnetz ausgeweitet. Dieses hat bereits einen hohen Anteil an dezentraler Erzeugung in einem seiner Mittelspannungsnetze. Die Analyse erfolgt durch Variation der dezentralen Einspeisung. Dabei wird auch ein lokaler *Q(U)* Regler für die dezentrale Erzeugung eingesetzt und dessen Einfluss auf die Spannungen genau untersucht. Für die Analyse des Mittel- und Hochspannungsnetzes werden Lastflusssimulationen in PSS Sincal durchgeführt.

Ergebnisse dieser Arbeit haben gezeigt, dass mit der Erhöhung der dezentralen Einspeisung die Spannung und der Blindleistungsfluss der übergeordneten Spannungsebene beeinflusst werden. Bei einem kleinen Anteil an dezentraler Einspeisung der Gesamterzeugung konnte dieser Effekt nicht beobachtet werden. Der Blindleistungsfluss in der nächsthöheren Spannungsebene ist nicht vorhersehbar, da er von einem lokalen Blindleistungsregler im Mittelspannungsnetz verursacht wird. Dieser Regler ist im Falle von dezentraler Erzeugung aus Wind und Sonne von der aktuellen Spannung im Netz und dem derzeitigen Wetter abhängig.

Contents

Abbreviations

b	shunt susceptance in p.u.
CDF	Common Data Format
DER	Distributed Energy Resource
DG	Distributed Generation
HV	High Voltage
I_{La}	real current of one phase
I_{Lre}	reactive current of one phase
LV	Low Voltage
MV	Medium Voltage
OLTC	On load tap changer
p.u.	per unit
P_n	nominal Power
PV	Photovoltaic
R_T	Transformer resistance
S_{base}	Power base for per unit calculations
STATCOM	Static Synchronous Compensator
SVC	Static VAr Compensator
TSP	Transformer Step Position
U_1	Primary transformer Voltage
U_2'	Secondary transformer Voltage referred to the primary side
U_{base}	Voltage base for per unit calculations
V_{di}	dielectical losses
x	reactance in p.u.
X	reactance in Ω
X_T	Transformer stray reactance

1 Introduction

1.1 Background

In the campaign against climate change, not only the European Union has set its goal to increase the share of renewable energy sources to 20% by 2020 [**1**] but also Obamas Clean Power Plan has a goal of 28% renewables by 2030 [**2**]. Also China, the biggest economy of the world, is spending as much as Europe and the US put together on clean power and has increased its share of renewable energy sources to 25% in the last decade [**3**]. These policy objectives are propelling the further integration of distributed energy resources in Europe and worldwide.

1.2 Motivations

The political decisions and the advances in technology have caused the implementation of a large number of distributed generators in all voltage levels of distribution networks, which increases by the day. Therefore power systems are experiencing a noticeable decentralization of the generation, which is impacting their operation. It has become very difficult to predict and control the total electricity generation. The uncontrolled operation of them has caused severe uncontrolled reactive power flow through the high-medium voltage transformer [**4**]. Subsequent studies have shown that also the local injection or consumption of the reactive power, used to suppress the voltage violations in medium voltage level, has an impact on the voltage of the superordinate grid [**5**]. In this Master Thesis volatile power effects and the resulting voltage interdependencies between HV and MV in presence of a high DG share are investigated.

1.3 Objectives

The main objective of this Master Thesis is the investigation of the impact of the locally injected reactive power in distribution grid on the next higher voltage level. This study will examine the effects of uncontrolled reactive power on the grid resulting from a very high DG share.

1.4 Scope of Work

The scope of this Thesis is the high and medium voltage grid. Low voltage grid is modeled through a lumped load. The distributed generation is modeled though a lumped generation and a local $Q(U)$ control. First the analysis is performed in the

IEEE 30 Bus test network, which includes three medium-high voltage substations with 9 feeders. Secondly the analysis is performed in a real European distribution network, which includes a medium voltage region with a high share of DG dispersed on 12 feeders. The simulations are done as load flow simulations in PSS Sincal.

1.5 Thesis Structure

- Chapter 1: Introduction
  This chapter contains the background, motivations, the objectives and the scope of this Master Thesis.

- Chapter 2: Volt-var control – Theoretical background
  This is the theoretic part of this Thesis. Besides the "Technical Organizational Rules" for operators and users, the impact of the reactive power on the voltage, reactive power control strategies and PQ capabilities for different kind of power plants are discussed.

- Chapter 3: Reactive power and voltages in the presence of a high DG share
  The investigations are performed in two different networks.
    o Chapter 3.1: IEEE 30 Bus Test Network
      This chapter starts with a description the IEEE 30 Bus Test Network in all its detail. To verify the built test network, a verifying simulation is done to compare the results with IEEE results.
      In the next part six different test scenarios are defined and simulated. At the end of this sub chapter the results of the Test Scenarios are compared and discussed.
    o Chapter 3.2: Simulations in a real network
      After a detailed description of real European distribution network, three different test scenarios are defined, simulated and investigated.

- Chapter 4: Conclusion and Future Work
  The conclusion of this Master Thesis can be found in this chapter.

- Chapter 5: References
- Chapter 6: Appendix
  The Appendix includes a description of how a Common Data Format (CDF) File can be read. This information is necessary for using the data provided by IEEE for the 30 Bus Test Network. Furthermore the Appendix includes Charts and Tables from simulations.

2 Volt-var control – Theoretical background

The operation of electrical power systems has become a very complex issue with the rising penetration of variable generation and the move towards smart grids. This includes new technologies like advancing generation, transmission and distribution coupled with customer enablement. One of the major functions for operating an electrical power system are generation load balance, reactive power and voltage management [6]. Reactive power control is of special interest for decreasing the voltage boost that is caused by distributed generation (DG) in the MV grid.

The European Norm EN 50160 [7] requires that voltage changes should not be bigger than ±10% of the nominal voltage for supplying normal customers and +10%/-15% for supplying customers in remote areas. Voltage regulation is done nowadays mostly with tap changers with control characteristics adapted to it's environment. But with the rising number of DG this centric approach does not necessarily lead to it's desired result. With the combination of OLTCs and reactive power control of the DG the voltage can be kept within its limits more effectively [8].

The Technical and Organizational Rules for Operators and Users (TOR) in Austria require a *cos(φ)* between 0,95 under- (lagging) and 0,95 overexcited (leading). If the distributed generator power exceeds 13,8 kVA the grid-Operator can require a *cos(φ)* between 0,9 under- and 0,9 overexcited under special circumstances [9].

Subchapters will discuss the following topics:

- "Impact of reactive power on the voltage" will describe the impact of reactive power injection on the grid voltage will be explained.
- "Transformer secondary voltage dependence on the phase angle" is important for explaining the relation between the primary and secondary voltage of a transformer in dependence of the phase angle and therefore the reactive power flow.
- "Reactive power control strategies" will discuss possible reactive power control strategies in dependence of different parameters.
- "*PQ* characteristics" explains the *PQ* characteristic of different DGs.

2.1 Impact of reactive power on the voltage

Figure 2.1 shows a section of a power system containing a HV/MV substation, a line, DG supplying the MV grid and a load. Every line has a resistance R and a reactance X which is affected by circuit length, conductor size and spacing.
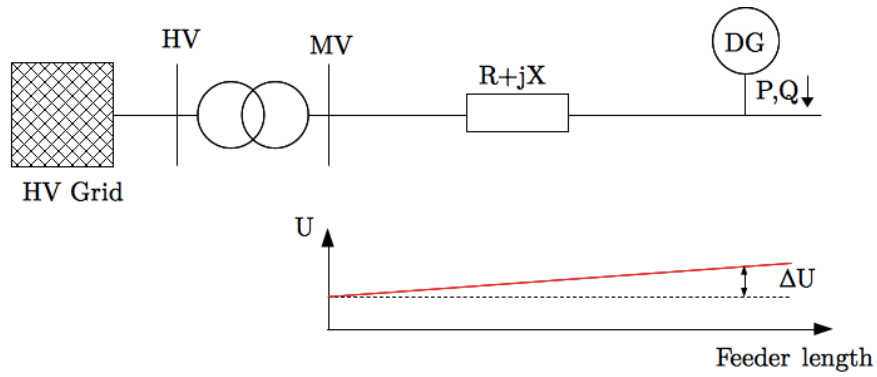
Figure 2.1 Voltage profile of a power system with DG in the MV grid

The voltage boost caused by DG can be dealt with in two ways, either by limiting the active power output (curtailment) or by feeding reactive power into the grid with the installation of coils for example (under excited operation). Of course a reduction of active power also means a loss in revenue so reactive power control is the preferred method. The impact of reactive power on the voltage can be explained with the following equation [**10**]:

$$\Delta U \approx \frac{R \cdot P}{U_N^2} \cdot \left[1 - \tan(\varphi) \cdot \frac{1}{R/X}\right] = \frac{R \cdot P}{U_N^2} \cdot \left[1 - \frac{Q}{P} \cdot \frac{1}{R/X}\right] \qquad (2.1)$$

where:
R ... real part of the Networkimpedance
X ... imaginary part of the Networkimpedance
$tan(\varphi)$ ... ratio of Q to P
U_N ... nominal voltage at the connection point
ΔU ... relative voltage boost

Figure 2.1 shows the voltage profile along the feeder and ΔU. The bigger the ratio R/X, the more reactive power Q is needed to reduce the voltage boost. In other words: The smaller the R/X ratio is the greater is the impact of the reactive power on the voltage. For this definition power consumption is counted positive.

2.2 Transformer secondary voltage dependence on the phase angle

Figure 2.2 illustrates the general load case of a transformer. It can be modeled with the Kap-triangle when appropriate conversion of the secondary values is used. The size of the Kap-triangle depends on the load current $\underline{I}$, the short circuit resistance R_K and the short
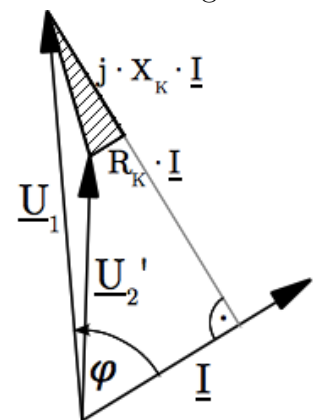

Figure 2.2 Relation between $\underline{U}_1$ and $\underline{U}_2$', Kap-triangle is hatched [11]

circuit reactance X_K. The values of R_K and X_K can be determined over the short circuit experiment of the transformer. Figure 2.3 shows the equivalent circuit diagram of this operating condition.
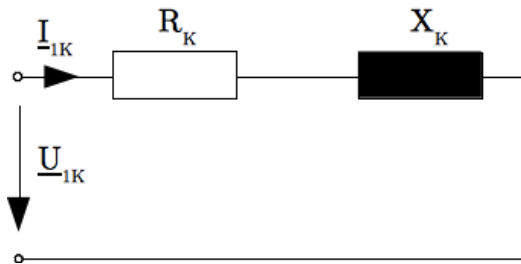

Figure 2.3 Equivalent circuit diagram of a transformer in the case of a short circuit

U_1 is the primary Voltage and U_2' is the secondary Voltage, referred to the primary side of the transformer. The size of U_2' is not only depending on the absolute value of the current, but also on the phase angle of the current. Figure 2.4 shows an example of how the phase angle influences the secondary voltage. Inductive behavior (lagging current) results in a smaller absolute secondary voltage while capacitive behavior (leading current) results in a higher absolute secondary voltage. [11]
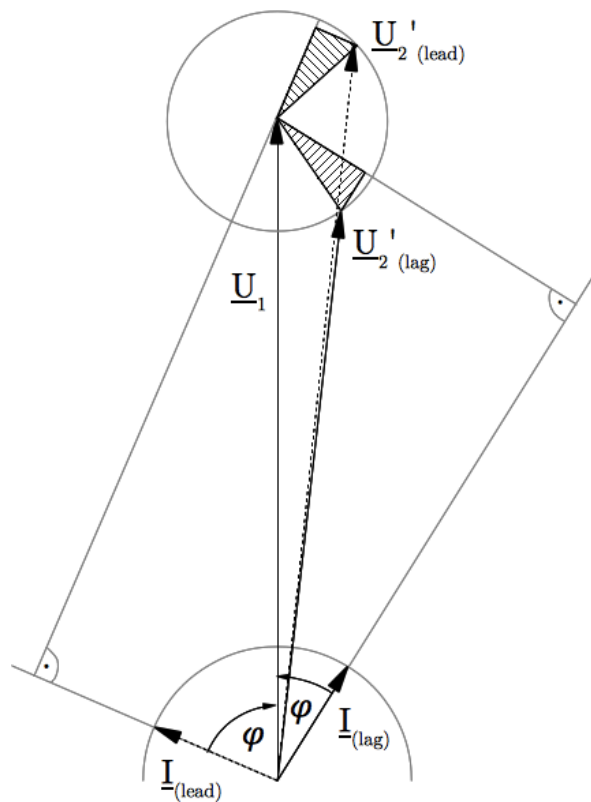

Figure 2.4 Leading and lagging load case at the same absolute current [11]

2.3 Reactive power control strategies of distributed generation

There are several different control strategies how reactive power should be supplied from DG to the grid:

- Fixed *cos(φ)*: No control of reactive power at all
- Power factor depending on the active power *cos(φ)(P)*
- Reactive power control depending on the voltage *Q(U)*
- Combination of *Q(U)* and *P(U)* control

2.3.1 Fixed *cos(φ)*

Nowadays it is common that distributed generation use a fixed *cos(φ)* of 1, 0,95 under- or 0,95 overexcited. For example DG that was installed in the medium voltage grid before 2009 in the south of Germany had a fixed *cos(φ)* of 1. A fixed *cos(φ)* of 1 is the simplest way for a photovoltaic owner because the inverter only needs to be designed for a fixed active power value which makes it cheaper and thereby more profitable. DG, which is implemented directly into an industrial facility and doesn't have a great impact on the grid voltage, is still required to feed into the network with a fixed *cos(φ)* of 1 [12].

2.3.2 Reactive power control depending on the voltage *Q(U)*

The power output of the DG does not necessarily correlate with the grid voltage. This is not true for photovoltaics (PV) because of the high share of PV of all the DG. If the voltage is less than the desired voltage the DG is overexcited and tries to boost the voltage. However if the voltage is higher than the desired voltage the DG is underexcited to decrease the voltage.
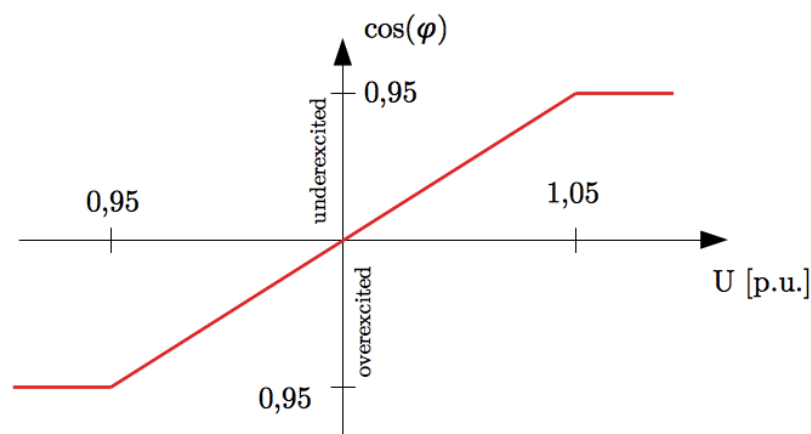

Figure 2.5 *Q(U)* reactive power control

Figure 2.5 shows an example *Q(U)* characteristic [12].

2.3.3 Combination of *Q(U)* and *P(U)* control

In special cases with a very high density of DG it is possible to combine the *Q(U)* control with a *P(U)* active power control. If the *Q(U)* control strategy reaches the limits where it is still useful a *P(U)* control can limit the active power output [13]. This combination enables to have a very high number of DG without the need of switching any power plant off and keep the system stable. Figure 2.6 shows an illustration of this control strategy.
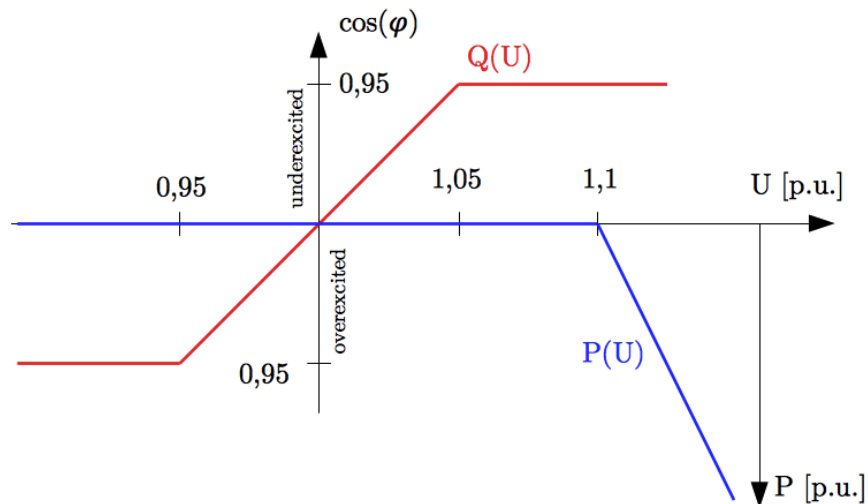

Figure 2.6 Combination of *Q(U)* and *P(U)* control

2.4 *PQ* characteristics of distributed generation

Previously the share of volatile generation plants was small and the system voltage and reactive power control was done by the following components [14]:

- Synchronous-generators to supply and absorb reactive power
- Synchronous condensers are synchronous-generators which don't have mechanical leads with the only purpose to supply or absorb reactive power
- Shunt reactors to absorb reactive power
- Shunt capacitors to supply reactive power
- Static var compensators can replace the functionality of synchronous condensers but have lower losses and do not need mechanical maintenance
- Static Synchronous Compensator (STATCOM)

With the rising penetration of distributed generation, it is essential that these new technologies contribute to the voltage regulation. But in the past it was common that wind generation was using an induction generator and PV was using line-commuted inverters with no reactive power control capabilities. Newly built wind plants use

doubly fed asynchronous generators or full-conversion machines with self-commuted inverters with good reactive power control capabilities. For an inverter to support reactive power control at full real power output it has to built for a higher apparent power output than at real power output only. It is also possible to add a Static var Compensator (SVC) or a Static Synchronous Compensator (STATCOM) next to the inverter to enhance its reactive power capabilities as it was stated before [**15**].

2.4.1 Conventional Power Plants

Figure 2.7 shows the PQ characteristic of synchronous generator. There is a minimum active power P_{min} limit due to turbine operation and a maximum active power limit P_{max} that is originating from the maximum permissible temperature of the stator winding [**16**] [**17**]. Some synchronous generators have the capability to operate in a synchronous condenser mode and to provide reactive power at zero active power output. But even these generators cannot operate between zero and the minimum active power limit (green hatched area in Figure 2.7) [**15**].
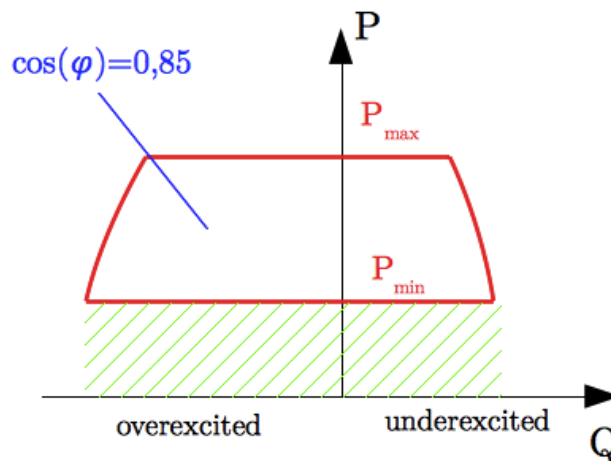

Figure 2.7 PQ characteristic of a synchronous generator [16] [17] [18]

2.4.2 PQ characteristic of Wind Power Plants and PV Inverters

Figure 2.8 shows that Wind power plants with doubly fed asynchronous generators or full-conversation machines can have a "D-Shape", "triangular" or "rectangular" PQ characteristic.
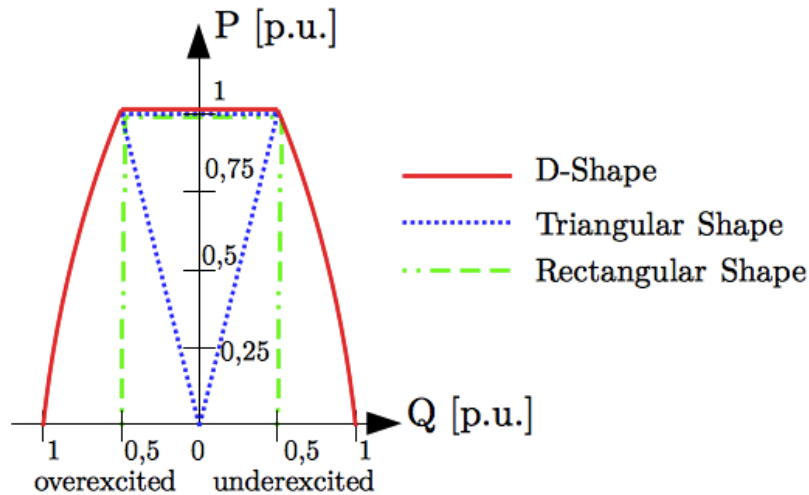
Figure 2.8 Possible *PQ* characteristic of wind generators at nominal Voltage

It is possible to operate some machines with a "D-Shape" or "Rectangular-Shape" *PQ* characteristic in a reactive power only mode when they are not producing any active power due to the lack of wind. The same works with PV inverters when there is no sun. However induction generators don't have the capability to control the reactive power output without an AC/AC converter [**15**]. An AC/AC converter consists of an AC/DC rectifier and a DC/AC inverter to adapt the machine frequency to the grid frequency. Figure 2.9 shows an overview diagram of a wind turbine using an AC/AC converter.
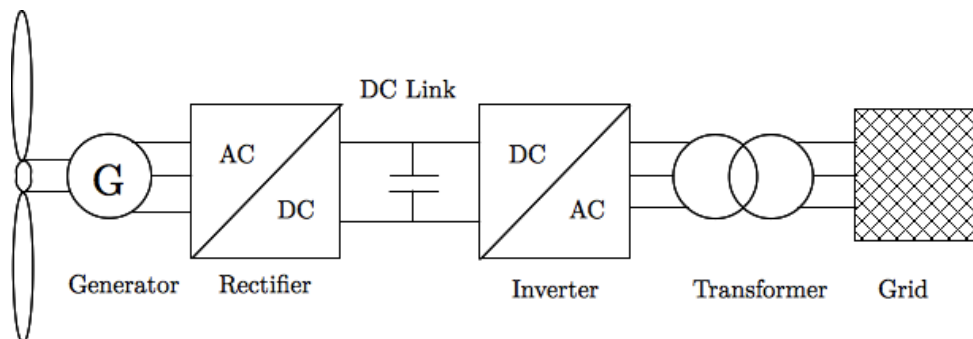

Figure 2.9 Overview diagram of a wind turbine using an AC/AC converter

PV inverters are very similar to AC/AC converter wind generators and have similar reactive power capabilities with a "Triangular Shape" *PQ* characteristic. It should be noted that inverters are designed to operate at unity factor. If an inverter has to provide reactive power at nominal active power output the current is higher than in operation at unity factor. The cost of an inverter is related to its current rating and therefore more expansive [**15**].

It is possible to operate the inverter as a STATCOM when there is no sun during the night. But at present it is common practice to disconnect the PV inverters. In this case the reactive power capability is not available. [**15**]

3 Reactive power and voltages in the presence of a high DG share

The volatile power effects and the resulting voltage interdependencies between the HV and the MV grid in the presence of a high DG are investigated in two network types:

- IEEE 30 Bus Test Network
- Real European Distribution Network

In the next subchapter 3.1 and 3.2 there will be an explanation of each test network followed by an examination of the effects of uncontrolled reactive power resulting from a high DG share on the grid.

3.1 IEEE 30 Bus Test Network

Figure 3.1 shows the IEEE 30 bus test system. It has been chosen as the first test network to investigate the impact of reactive power control on the next higher voltage level. This network represents a portion of the American Electric Power System in Virginia as of December 1961. It consists of a 132 kV high voltage (HV) grid and a 33 kV medium voltage (MV) grid. The HV grid consists out of 3 supplying substations from 132kV to 33 kV and 11 HV lines. The MV grid consists of 12 feeders supplied from the substation in Hancock (3 Feeders), Roanoke (6 Feeders) and Cloverdale (3 Feeders). The shortest feeder is in Roanoke and is about 15 km and the longest feeder is in Hancock and is about 50 km long. There are two Generators in the grid, a bigger one at Glen Lyn (260,2 MW) and a smaller one at Claytor (40 MW). Furthermore there are several synchronous condensers in the HV grid and two capacitor banks in the MV grid for reactive power control. Impedances of the lines, load-, generation-, transformer- and synchronous condenser data of the network can be found at **[19]** in a text file that is formatted in the "common data format" (CDF) by IEEE. More information about the common data format and how it should be read can be found in Appendix 6.1 Common Data Format.
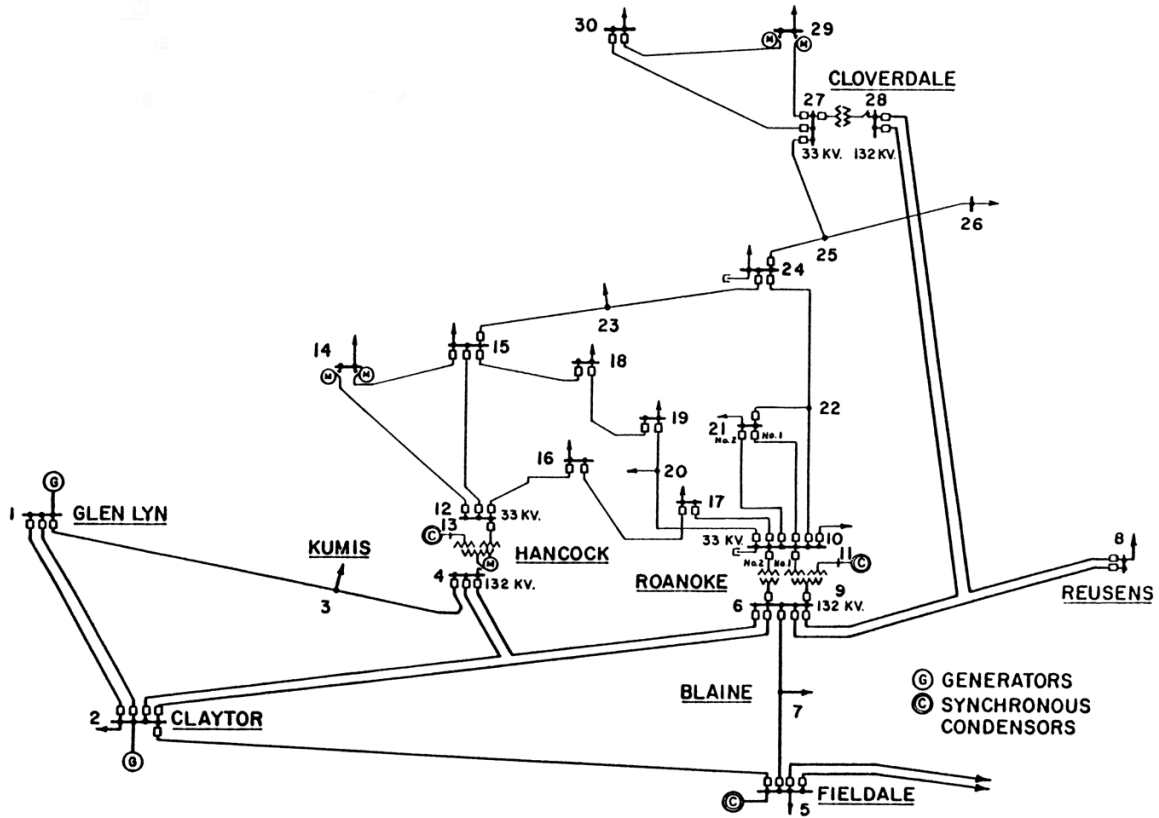
Figure 3.1 IEEE 30 bus test system [19]

3.1.1 Network data description

In this chapter all the necessary information for modeling the IEEE 30 Bus Network is collected. Data about the Capacitor Banks, the Generators and the Synchronous Condensers comes from the CDF file. Information about the length of the lines, the vector group and the power rating of the transformers, the position of circuit breakers and switches and the load characteristics are not included in the CDF File. To have an accurate network model the missing parameters have to be taken from other sources.

Capacitor Banks at bus bar 10 and 24

In the MV grid there are two static capacitors installed at the bus bar 10 and bus bar 24. The value of each shunt susceptance is given in the CDF File in p.u.. To calculate the size of the actual capacitor from the given susceptance the following formulas are used:

$$b_{10} = 0,19 \, p.u.$$
where b_{10} is the susceptance at bus bar 10

$$x_{10} = \frac{1}{b_{10}} = 5,26\,pu.$$

where x_{10} is the reactance in per unit at bus bar 10

$$X_{10} = x_{10} \cdot \frac{U_{base}{}^2}{S_{base}} = 5,26 \cdot \frac{33kV^2}{100\,MVA} = 57,3158\,\Omega$$

where X_{10} is the reactance in Ω at bus bar 10

and U_{base} is the base voltage

(3.1)

and S_{base} is the base apparent power

$$X_{10} = \frac{1}{\omega \cdot C_{10}} \rightarrow C_{10} = \frac{1}{\omega \cdot X_{10}} = \frac{1}{2 \cdot \pi \cdot 60\,Hz \cdot 57,3158\,\Omega} = 46,28\,\mu F$$

where C_{10} is the value of the capacitor at bus bar 10

and ω is the angular frequency

The calculation of the capacitor at bus bar 24 is similar and it has the size of 10,47µF.

For the simulation in PSS Sincal it is necessary to provide the reactive power values for the two capacitors at bus bar 10 and 24. According to the PSS Sincal Help file the shunt capacitor will be modeled as an impedance $\underline{Z}$ as shown in equation (3.2).

$$\underline{Z} = \frac{U_n}{V_{di} \cdot 10^{-3} - j \cdot Q_n}$$

(3.2)

where $\underline{Z}$ is the impedance

U_n the nominal voltage

V_{di} the dielectrical losses

Q_n the nominal reactive power

We already know the impedance of the capacitor but we need the reactive power so we have to rearrange equation (3.2). Furthermore the dialectical losses will be neglected.

$$\underline{Z} = j \cdot X = j \cdot \frac{U_n{}^2}{Q_n} \rightarrow Q_n = \frac{U_n{}^2}{X}$$

where X is the Reactance

(3.3)

$$Q_{n,10} = \frac{33kV^2}{57,32\,\Omega} = 19\text{Mvar}$$

and $Q_{n,10}$ is the reactive power at bus bar 10

The capacitor at bus bar 10 will provide 19 Mvar capacitive reactive power and the Capacitor at bus bar 24 will provide 4,3 Mvar in nominal conditions.

Generators and Synchronous Condensers

The two Generators at bus bar 1 in Glen Lyn and 2 at Claytor are trying to keep the voltage at 1,06 p.u. and 1,045 p.u.. The synchronous condensers at bus bar 5, 8, 11 and 13 try to keep the voltage at 1,01 p.u., 1,01 p.u., 1,082 p.u. and 1,071 p.u..

Transformer power rating and line ratings

The paper by Alsac and Stott [20], which is also using the IEEE 30 bus test system as a test network, has more information about the power rating of the branches, the data can be found in Appendix: Charts and Tables in Table 6.3 Branch data .
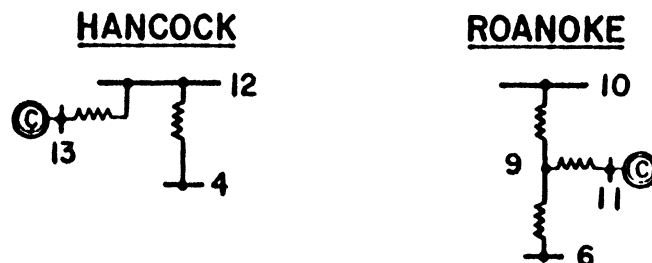

Figure 3.2 Three winding transformer equivalent for the transformers in Hancock and Roanoke [19]

There are two different types of branches: Transformer branches and transmission lines. The transformer power ratings can be used for the three winding equivalents from Figure 3.2. The line power ratings need to be converted to the maximum thermal current $I_{th,\max}$ of the line with the equation (3.4).

$$I_{th,\max} = \frac{S_n}{U_n}$$

where S_n is the nominal apparent power of the line

and U_n is the nominal voltage of the line

(3.4)

With the knowledge of the maximum thermal current the usage rate of the cables can be calculated for the simulations.

Comment: In the CDF File the branch type (as described in the Appendix in Table 6.2) was set to 0 for all branches, which stands for Transmission line. But it is obvious that this is a mistake and the correct branch types can be easily determined with Figure 3.1. The branch types in Table 6.3 are already corrected.

Transformer tap ranges

Parameters for the transformer tapping ranges have also been taken from [20]. They propose tapping ranges of $\pm$ 10 with steps of 1%.

Position of circuit breakers and switches

There is no information in the CDF File of the IEEE 30 bus test system about the topology of the network and the position of the circuit breakers. But usually transmission networks are meshed [21] and distribution networks have a radial topology [22]. The feeders in the distribution network have been selected as following:

Substation Hancock:

- Feeder H1: Bus 12 – Bus 14
- Feeder H2A: Bus 12 – Bus 15 – Bus 23 – Bus 24
- Feeder H2B: Bus 12 – Bus 15 – Bus 18

Substation Roanke:

- Feeder R1: Bus 10 – Bus 20 – Bus 19
- Feeder R2: Bus 10 – Bus 17 – Bus 16
- Feeder R3: Bus 10 – Bus 21 – Bus 22

Substation Cloverdale:

- Feeder C1: Bus 27 – Bus 29
- Feeder C2: Bus 27 – Bus 30
- Feeder C3: Bus 27 – Bus 25 – Bus 26

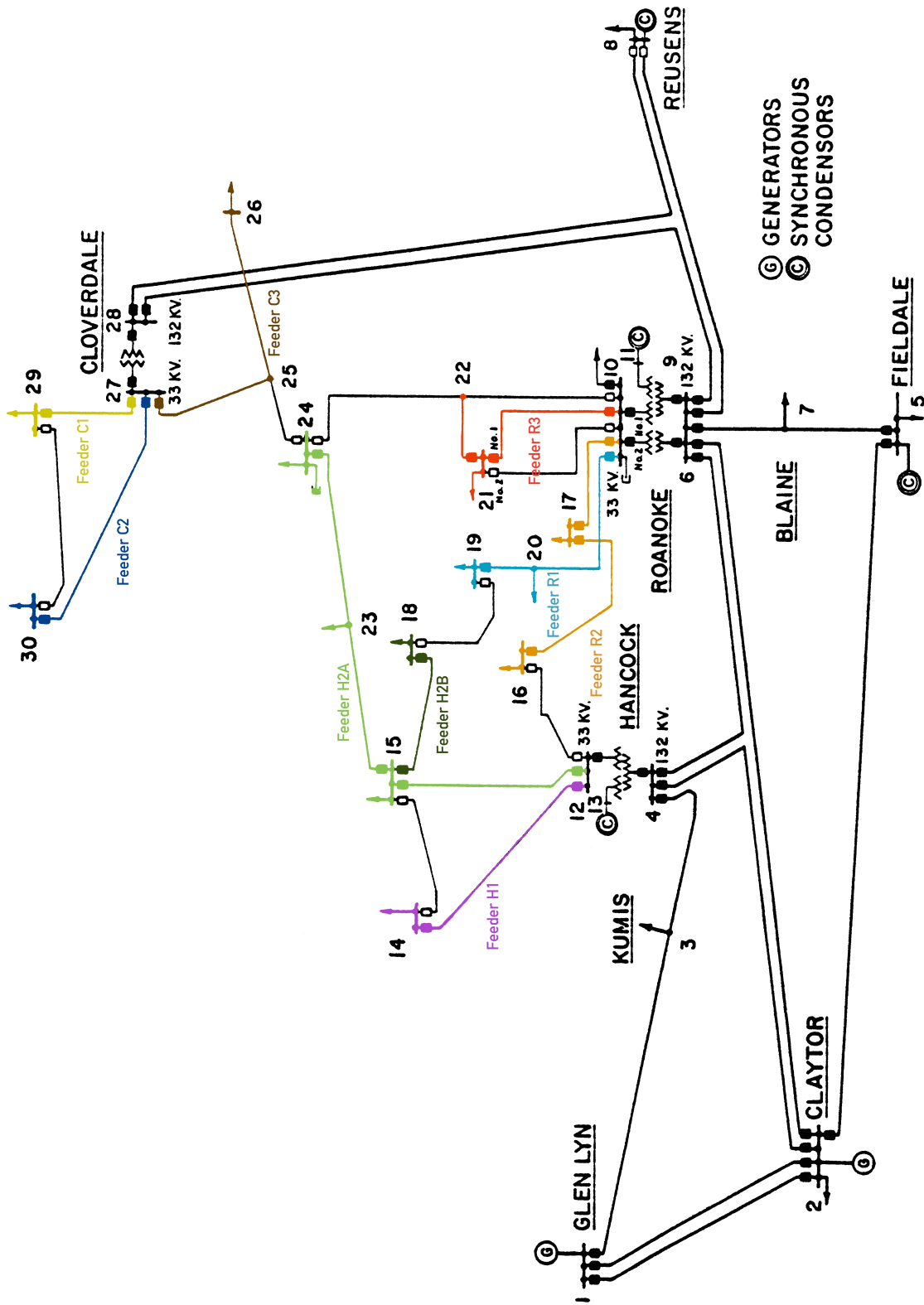Figure 3.3 shows a picture of the grid with highlighted feeders.

Figure 3.3 IEEE 30 Bus Test grid with highlighted Feeders

Line length

It is necessary to know the length of the lines to illustrate the voltage profiles of the feeders. With available information of the maximum thermal current and the nominal voltage of the line, a cable that fitted the requirements was chosen out of an industrial catalogue [23].

In the distribution network of the IEEE 30 bus test system two different cable types are used. For the first type the maximum thermal current is 0,97 kA and for the second type it is 0,48 kA. It is assumed that the cables will be laid direct into the ground. For the first cable type the conductor with a cross section of 1000 mm^2 has been chosen because it is the biggest available conductor from Table 9 in [23] and it fitted the thermal current best. The second cable type was chosen with a cross section of 300 mm^2 because the current rating is in an acceptable range. Cable parameters have been summarized in Table 3.1.

		Cable Type 1	Cable Type 2
Branch data	Power Rating [MW]	32	16
	$I_{th,max}$ [kA]	0,97	0,48
Chosen cable from cable catalogue	Cross section [mm^2]	1000	300
	Current rating[1] [kA]	0,74	0,49
	Approximate AC resistance of Conductor at 90°C [ohm/km]	0,029	0,0791
	Approximate Reactance at 50 Hertz [ohm/km]	0,09	0,12
	Approximate Capacitance of Cable [µF/km]	0,44	0,26
[1] laid Direct, Ground Temp. 30°C & g = 1.2°C m/W, depth of laying 0,8m			

Table 3.1 Cable properties

The approximate reactance X_{50} in Table 3.1 needs to be transformed for the American frequency of 60 Hz to X_{60}:

$$X_{60} = X_{50} \cdot \frac{60\,Hz}{50\,Hz}$$

(3.5)

where X_{60} is the reactance at 60 Hz

and X_{50} is the reactance at 50 Hz

With the knowledge of the resistance and the reactance of the whole line and the approximate resistance and reactance of the conductor the length of the line is calculated with the formula.

$$\text{Line length} = \frac{\dfrac{R}{R'} + \dfrac{X}{X'}}{2}$$

where R is the resistance of the line

R' is the resistance per km

(3.6)

X is the reactance of the line

X' is the reactance per km

Susceptance of the medium voltage lines

The database for the IEEE test network neglected the susceptance B in the Medium Voltage grid. To get more accurate simulation results the susceptance parameters have been calculated from the capacitance values in Table 3.1 with the Formula (3.7). This information has been added for the second simulation in 3.1.2.2 Simulation of the completed network. Figure 3.4 illustrates the equivalent circuit for a line with all parameters.

$$B = C \cdot \omega$$

where B is the susceptance

C is the capacitance

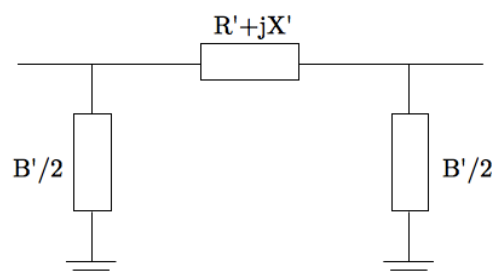(3.7)

ω is the angular frequency

Figure 3.4 Equivalent circuit of a line

Transformer vector group

The vector group was chosen as YY0 for all transformers.

Transformer short circuit impedance

It has to be said that the given active part of the relative short circuit voltage u_R is zero for all transformers, this means that the copper losses are neglected.

The reactive part of the relative short circuit voltage u_X is given in p.u.. This p.u. value needs to be transformed to fit the apparent power of the transformer. An example calculation for u_X of the transformer between Busbar 6 and Busbar 10 from data of the CDF File is shown below:

Base apparent power S_{base}: 100 MVA

Branch Reactance x: 0,556 p.u.

nominal apparent power S_n of the transformer: 32 MVA

$$u_x = x \cdot \frac{U_{base}{}^2}{S_{base}} \cdot \frac{S_n}{U_{base}{}^2} = x \cdot \frac{S_n}{S_{base}} = 0,556 \cdot \frac{32 MVA}{100 MVA} = 0,178 \text{ p.u.} \qquad (\ 3.8\ )$$

where u_x is the reactive part of the relative short circuit voltage in p.u.

x is the branch reactance in p.u.

U_{base} is the base voltage

S_{base} is the base apparent power

S_n is the nominal apparent power of the transformer

For the transformer between Busbar 27 and 28 the u_X of 0,257 per unit is much higher than the usual values of a transformer with this power rating. This could be either because there is an extra reactance along the branch or maybe the transformer rating given in [20] is wrong. But as calculated in 3.1.2.1 Data verification simulation the values seem to be correct.

3.1.2 Model verification

For a load flow analysis the data of the IEEE 30 bus test system has been entered into the program PSS Sincal. The three winding Transformers in Hancock and Roanoke were modeled as two winding equivalents (see Figure 3.2).

The IEEE Network will be simulated twice. In the first simulation the network will have the exact values as stated in the CDF file. This is done for verification purposes to compare the simulation results with the desired results that are stated in the CDF file too. In this grid the Medium Voltage grid has a meshed structure, which is very untypical.

In the second simulation of the IEEE Network all the changes and missing information that have been proposed earlier in this chapter were taken into account.

3.1.2.1 Data verification simulation

This simulation was done with the network data provided only by the CDF File to verify the simulation results and to compare them with the results from the CDF File. Only the transformer power rating has been taken from [20]. The results are summarized in Table 3.2. The biggest Voltage difference is about 1,6% and the average difference is about 0,45%. This simulation results are a good approximation of the original results.

		IEEE Data		PSS Sincal Results		Difference	
Bus Number	Bus Name	Final Voltage [%]	Final Angle [°]	Final Voltage [%]	Final Angle [°]	Δ Voltage [%]	Δ Angle [°]
1	Glen Lyn	106	0	106,000	0,000	0,000	0,000
2	Claytor	104,3	-5,48	104,222	-5,346	0,078	0,134
3	Kumis	102,1	-7,96	101,960	-7,514	0,140	0,446
4	Hancock	101,2	-9,62	101,036	-9,263	0,164	0,357
5	Fieldale	101	-14,37	101,000	-14,209	0,000	0,161
6	Roanoke	101	-11,34	100,625	-11,037	0,375	0,303
7	Blaine	100,2	-13,12	99,999	-12,869	0,201	0,251
8	Reusens	101	-12,1	100,709	-11,806	0,291	0,294
9	Roanoke	105,1	-14,38	106,690	-14,058	1,590	0,322
10	Roanoke	104,5	-15,97	105,823	-15,674	1,323	0,296
11	Roanoke	108,2	-14,39	108,199	-14,058	0,001	0,332
12	Hancock	105,7	-15,24	105,766	-14,807	0,066	0,433
13	Hancock	107,1	-15,24	107,100	-14,807	0,000	0,433
14	Bus 14	104,2	-16,13	104,418	-15,695	0,218	0,435
15	Bus 15	103,8	-16,22	104,090	-15,815	0,290	0,405
16	Bus 16	104,5	-15,83	105,032	-15,461	0,532	0,369
17	Bus 17	104	-16,14	105,084	-15,811	1,084	0,329
18	Bus 18	102,8	-16,82	103,494	-16,451	0,694	0,369
19	Bus 19	102,6	-17	103,454	-16,639	0,854	0,361
20	Bus 20	103	-16,8	103,968	-16,455	0,968	0,345
21	Bus 21	103,3	-16,42	104,493	-16,104	1,193	0,316
22	Bus 22	103,3	-16,41	104,512	-16,089	1,212	0,321
23	Bus 23	102,7	-16,61	103,230	-16,215	0,530	0,395
24	Bus 24	102,1	-16,78	102,919	-16,407	0,819	0,373
25	Bus 25	101,7	-16,35	102,000	-15,955	0,300	0,395
26	Bus 26	100	-16,77	100,237	-16,373	0,237	0,397
27	Cloverdale	102,3	-15,82	102,281	-15,421	0,019	0,399
28	Cloverdale	100,7	-11,97	100,373	-11,664	0,327	0,306
29	Bus 29	100,3	-17,06	100,296	-16,652	0,004	0,408
30	Bus 30	99,2	-17,94	99,148	-17,536	0,052	0,404
						∅ 0,452	∅ 0,336

Table 3.2 Comparison of the simulation results and the results from the CDF File

3.1.2.2 Simulation of the completed network

In this simulation the IEEE 30 bus test network is basically the same as in 3.1.2.1 but was enhanced with these small changes:

- The maximum reactive power limit from the generator at bus bar 2 has been increased from 50 Mvar to 60 Mvar. Now it is possible for the generator to reach its desired voltage goal of 1,045 p.u. which is required by the CDF file
- The Medium Voltage grid is radial instead of meshed
- The Transformers have the possibility to control their tap positions automatically
- The missing susceptances of the medium voltage grid lines have been added

In Figure 3.5 - Figure 3.8 the results of the load flow simulation are illustrated. The bus bar voltages always stay within their limits, which were set to ±7%.

Figure 3.5 shows the voltage profile of all feeders supplied from the Hancock substation. All three feeders (H1, H2A, H2B) have the same behavior; the voltage is continuously decreasing with increasing feeder length from the Hancock substation. The voltage at the MV bus bar of Hancock is $U_{Hancock}^{MV} = 1,045\,pu.$.
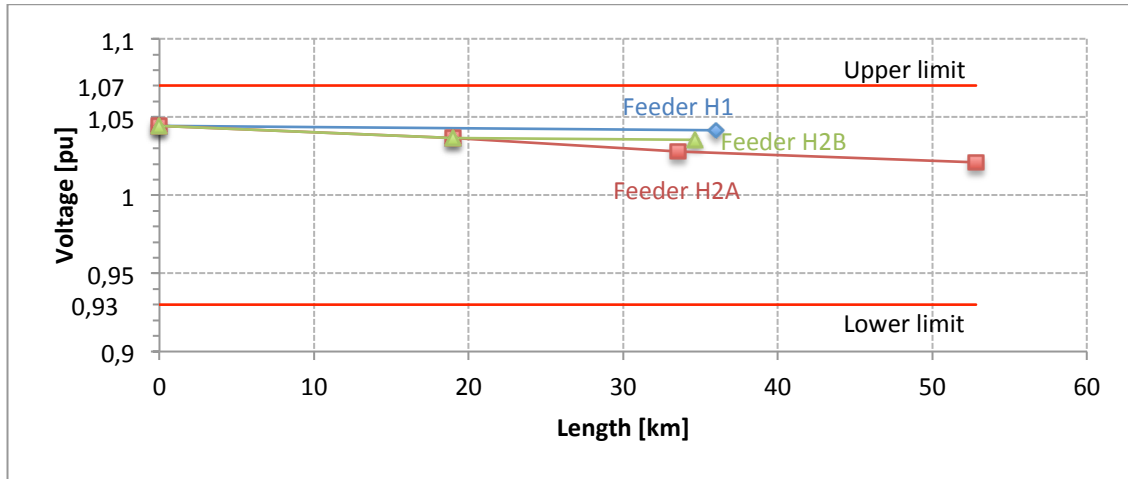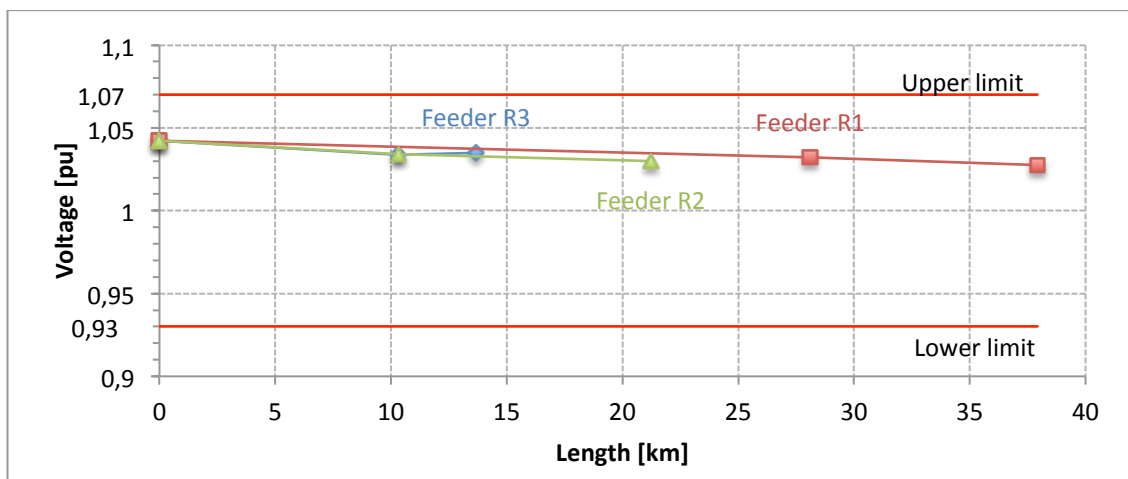

Figure 3.5 Voltage profile of all feeders supplied from the Hancock substation (U_n=33kV)

Figure 3.6 shows the voltage profile of the three feeders R1, R2 and R3 supplied by Roanoke substation. All three feeders have the same behavior of decreasing voltage with increasing distance from the Roanoke transformer. The voltage at the MV bus bar of Roanoke is $U_{Roanoke}^{MV} = 1,042\,pu.$.

Figure 3.6 Voltage profile of all feeders supplied from the Roanoke substation (U_n=33kV)

Figure 3.7 illustrates the voltage profile of the three feeders supplied by the Cloverdale transformer. While feeder C2 and C3 show similar behavior of decreasing voltage with increasing feeder length however the bus bar at the end of feeder C1 has a higher voltage than the feeder head. An explanation for this can be found when comparing the loads at the end of the feeders. The load at the end of feeder C2 is 10,6 MW and

1,9 Mvar, at the end of feeder C3 3,5 MW and 2,3 Mvar and at the end of feeder C1 2,4 MW and 0,9 Mvar. While the difference in active power consumption between the load at the end of C3 and C1 isn't that big, just 31%, the difference between the reactive power consumption of the loads at the end of the feeder is 61%. Because the reactive power consumption at bus bar 29 (the end of C1) consumes less of the active power produced by the cable there is a voltage increase with increasing feeder length. The voltage at the MV bus bar of Cloverdale is $U_{Cloverdale}^{MV} = 1,015\,p.u.$.
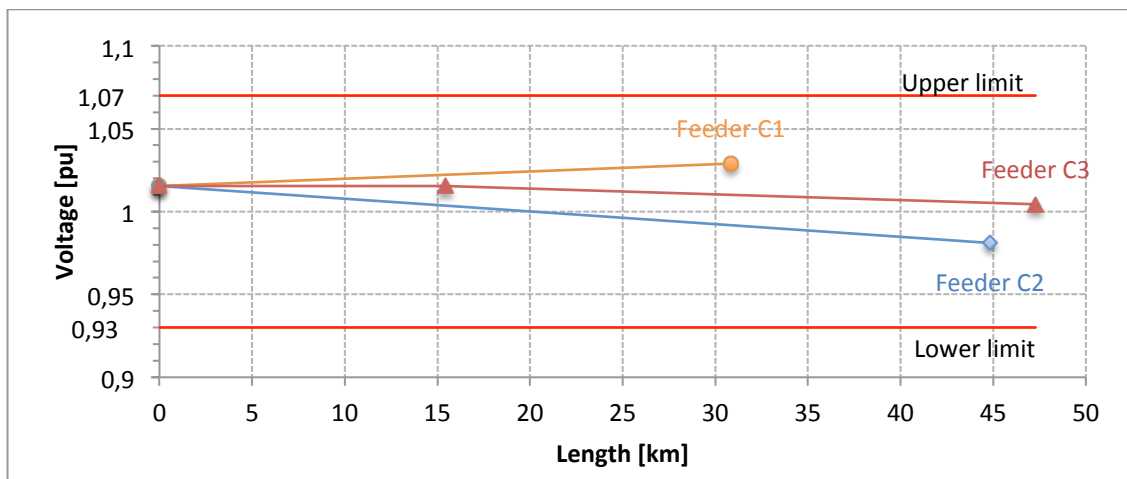
Figure 3.7 Voltage profile of all feeders supplied from the Cloverdale substation (U_n=33kV)

Figure 3.8 shows the calculated voltages in different buses of the HV grid. Because the HV grid is meshed a different type of chart was chosen. The height of the pyramids represent the voltage level, the position represents their approximate position in the grid (see Figure 3.3). The color blue indicates voltages between 0,92 p.u. and 0,96 p.u., red indicates voltages between 0,96 p.u. and 1 p.u., green indicates voltages between 1 p.u. and 1,04 p.u. and violet indicates voltages between 1,04 p.u. and 1,08 p.u.. Because all the bus bar voltages in the HV grid are above 1 p.u., every pyramid has a green top. Glen Lyn, where the biggest generator of the grid is located, is defined as the slack of the grid and has a violet top because the generator keeps the bus bar voltage to the pre defined value of 1,06 p.u.. The minimal bus bar voltage is in Blaine with a value of 1,002 p.u.. All the HV bus bar voltages stay within their limits.
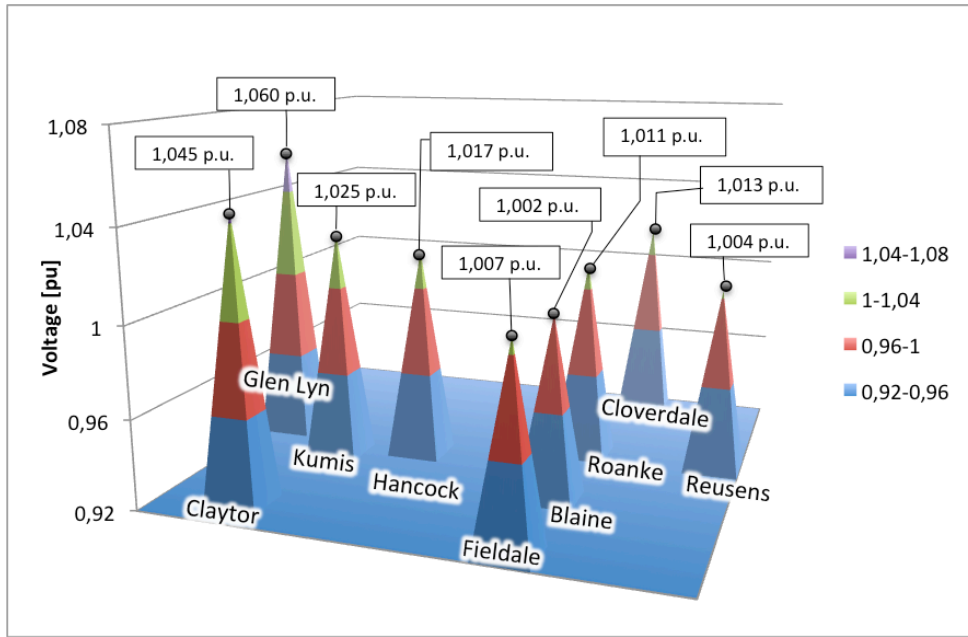
Figure 3.8 Voltage levels in the HV grid of the IEEE 30 Bus Test Network

3.1.3 Simulations in the IEEE 30 Bus Test Network

The impact of DG production at different power factors in the MV grid on the bus bar voltages in the MV and the HV grid is analyzed. Before turning to these test scenarios some minor modifications to the IEEE 30 Bus Test Network are discussed. The test scenarios that were carried out consist of a base scenario with no DG, two scenarios with installed DG limited to one region at two different power factors and two scenarios with installed DG in every region at two different power factors. The result evaluation for each test scenario is split into two parts: The impact on the MV grid and the impact on the HV grid.

3.1.3.1 Base case establishment
The following modifications were made in order to be able to simulate different test scenarios with distributed generation installed in the MV grid and to get meaningful results.

3.1.3.1.1 Medium Voltage grid
In Hancock and Roanoke at the bus bars 13 and 11 the synchronous condensers were switched off. The Capacitors at bus bars 24 and 10 were also switched off.

The transformer tap position has an impact on the reactive power flow over the transformer. To analyze the impact of the uncontrolled reactive power, which is supplied by the installed DG, the transformer is set to a fixed tap position.

Distributed Generation has been added in parallel to each load to the feeders in Hancock, Roanoke and Cloverdale. The loads represent the maximum loads and are a

combination of the load in the MV grid and all native loads from the LV grid. In the base case there will be no DG production. Test Scenario 1 and Test Scenario 2 will examine the impact of the DG production in the Hancock region at two different power factors. In the test scenarios, Test Scenario 3 and 4, the DG production will additionally be activated in the feeders of Roanoke and Cloverdale at two different power factors. In the last two scenarios for the IEEE Test grid a *Q(U)* controller is used to control the reactive power output of the DG in Hancock for Test Scenario 5 and for all three test regions for Test Scenario 6.

Distributed Generation in Hancock

To test the impact of the uncontrolled reactive power Distributed Energy Resources (DER) were installed in Hancock. The maximum power of the DER was chosen that there is a power flow from the MV grid to the HV grid and the Transformer is loaded 60% at full DG production. The DER production is distributed along the Feeders in Hancock (Figure 3.9) and adds up to 69 MW:
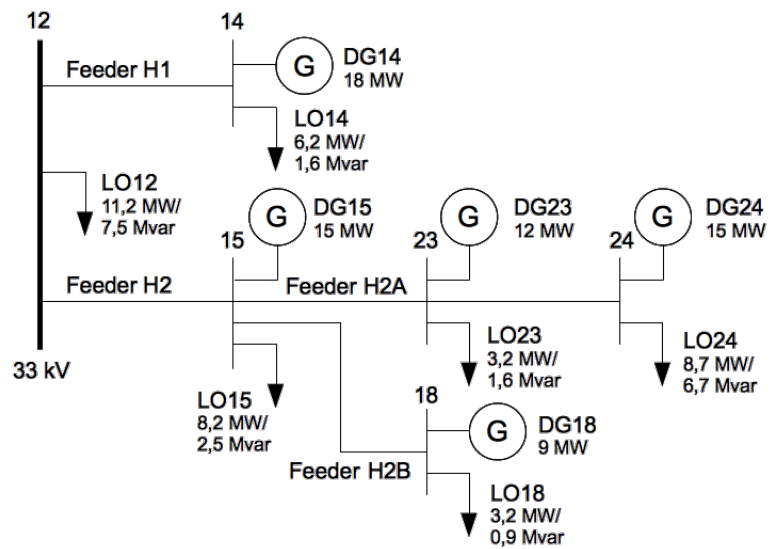
Figure 3.9 Loads and Distributed Generation in Hancock

- Feeder H1:
    - DG14: $P_{DG14,base}$=18 MW
- Feeder H2A:
    - DG15: $P_{DG15,base}$=15 MW
    - DG23: $P_{DG23,base}$=12 MW
    - DG24: $P_{DG24,base}$=15 MW
- Feeder H2B:
    - DG18: $P_{DG18,base}$=9 MW

Test Scenario 1: The sum of all distributed generation in Hancock represents the base DG production for Test Scenario 1 at a power factor of 1:

$$P_{DG,base} = P_{DG,Hancock,base} = 69\,MW$$

$$S_{base} = \frac{P_{DG,base}}{\cos(\varphi)} = \frac{69\,MW}{1} = \underline{\underline{69\,MVA}}$$

Test Scenario 2 and Test Scenario 5: The sum of all distributed generation in Hancock represents the base DG production for these Test Scenarios at a power factor of 0,95:

$$P_{DG,base} = P_{DG,Hancock,base} = 69\,MW$$

$$S_{base} = \frac{P_{DG,base}}{\cos(\varphi)} = \frac{69\,MW}{0,95} = \underline{\underline{72,63\,MVA}}$$

Distributed Generation in Roanoke and Cloverdale

Similar to DG in Hancock the size of the maximum DG production was chosen to have a power flow from the MV grid to the HV grid at a Transformer load of about 60%.

The installed DG in Roanoke (Figure 3.10) adds up to 75 MW:

- Feeder R1:
    - DG20: $P_{DG20,base}$=10 MW
    - DG19: $P_{DG19,base}$=15 MW
- Feeder R2:
    - DG17: $P_{DG17,base}$=15 MW
    - DG16: $P_{DG16,base}$=5 MW
- Feeder R3:
    - DG21: $P_{DG21,base}$=20 MW
    - DG22: $P_{DG22,base}$=10 MW

The installed DG in Cloverdale (Figure 3.11) adds up to 50 MW:

- Feeder C1:
    - DG29: $P_{DG29,base}$=10 MW
- Feeder C2:
    - DG30: $P_{DG30,base}$=20 MW
- Feeder C3:
    - DG25: $P_{DG25,base}$=10 MW

    - DG26: $P_{DG26,base}$=10 MW
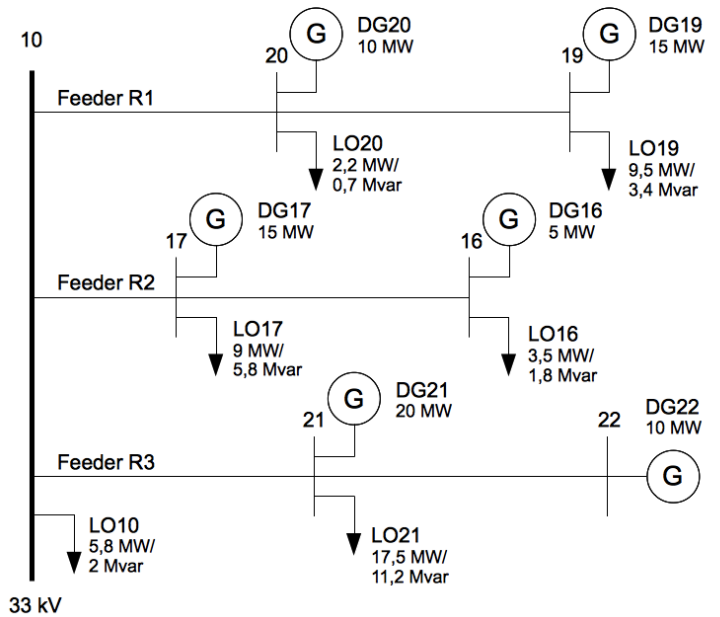
Figure 3.10 Loads and Distributed Generation in Roanoke
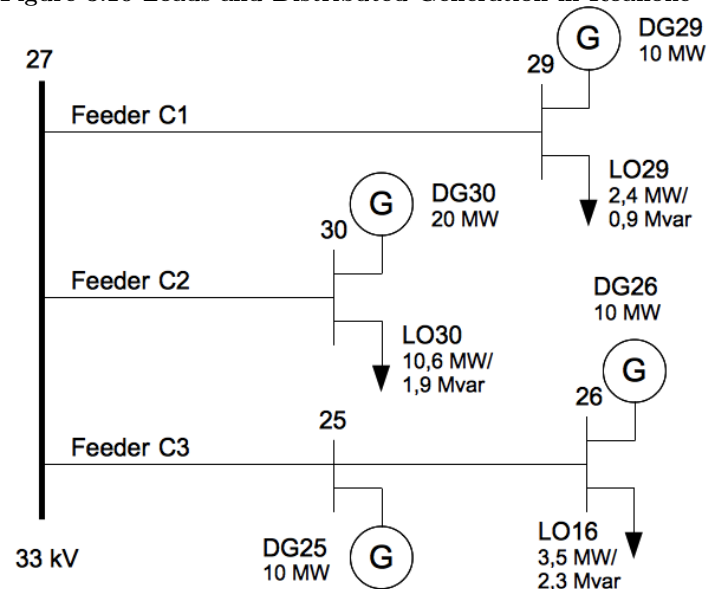
Figure 3.11 Loads and Distributed Generation in Cloverdale

Test Scenario 3: The sum of all distributed generation in Hancock, Roanoke and Cloverdale represents the base DG production in this Test Scenario at a power factor of 1:

$$P_{DG,base} = P_{DG,Hancock,base} + P_{DG,Roanoke,base} + P_{DG,Cloverdale,base} = 194\,MW$$

$$S_{base} = \frac{P_{DG,base}}{\cos(\varphi)} = \frac{194\,MW}{1} = \underline{\underline{194\,MVA}}$$

Test Scenario 4 and Test Scenario 6: The sum of all distributed generation in Hancock, Roanoke and Cloverdale represents the base DG production in this Test Scenario at a power factor of 0,95:

$$P_{DG,base} = P_{DG,Hancock,base} + P_{DG,Roanoke,base} + P_{DG,Cloverdale,base} = 194\,MW$$

$$S_{base} = \frac{P_{DG,base}}{\cos(\varphi)} = \frac{194\,MW}{0,95} = \underline{\underline{204,21\,MVA}}$$

3.1.3.1.2 High Voltage grid

No modifications were applied to the High Voltage grid.

3.1.3.2 Test Scenarios

Five different test scenarios for the IEEE 30 Bus Test Network were simulated. A base scenario without any DG production to compare the results, a scenario where the DER in Hancock are operated at a power factor of 1 and another simulation with a power factor of 0,95 lagging. Scenario number four is a simulation of DER in Hancock, Roanoke and Cloverdale operating at a power factor of 1 and the last scenario is testing the impact on the grid for DER operated at a power factor of 0,95 lagging.

- Base Scenario: No distributed generation production
  - P_{DG}=0 p.u.
  - Q_{DG}=0 p.u.
- Test Scenario 1: Distributed generation in Hancock at $cos(\varphi)$=1
  - $P_{DG,Hancock} \neq 0$ p.u.
  - $P_{DG,Roanoke}=P_{DG,Cloverdale}$=0 p.u.
  - Q_{DG}=0 p.u.
- Test Scenario 2: Distributed generation in Hancock at $cos(\varphi)$=0,95 lagging
  - $P_{DG,Hancock} \neq 0$ p.u.
  - $P_{DG,Roanoke}=P_{DG,Cloverdale}$=0 p.u.
  - $Q_{DG,Hancock} \neq 0$ p.u.
  - $Q_{DG,Roanoke}=Q_{DG,Cloverdale}$=0 p.u.
- Test Scenario 3: Distributed generation in Hancock, Roanoke and Cloverdale at $cos(\varphi)$=1
  - $P_{DG} \neq 0$ p.u.
  - Q_{DG}=0 p.u.
- Test Scenario 4: Distributed generation in Hancock, Roanoke and Cloverdale at $cos(\varphi)$=0,95 lagging
  - $P_{DG} \neq 0$ p.u.
  - $Q_{DG} \neq 0$ p.u.
- Test Scenario 5: Distributed generation in Hancock, $Q(U)$ controller activated
  - $P_{DG,Hancock} \neq 0$ p.u.
  - $P_{DG,Roanoke}=P_{DG,Cloverdale}$=0 p.u.
  - $Q_{DG,Hancock} \neq 0$ p.u.
  - $Q_{DG,Roanoke}=Q_{DG,Cloverdale}$=0 p.u.

- Test Scenario 6: Distributed generation in Hancock, Roanoke and Cloverdale, *Q(U)* controller activated
  - $P_{DG} \neq 0$ p.u.
  - $Q_{DG} \neq 0$ p.u.

The test method that was used was a load flow simulation done in Sincal. The voltage limits were set to ±7%.

3.1.3.3 No distributed generation production

This test case represents a situation where no energy is supplied by DG, e.g. when no wind is blowing for wind power plants and no sun is shining for PV.

3.1.3.3.1 Voltage profiles in the Medium Voltage grid

Figure 3.12 shows an illustration of the voltage profile of the feeders in Hancock in the base scenario. The voltage at the MV bus bar of Hancock is $U_{Hancock}^{MV} = 1,011\,p.u.$. In each bus of all three feeders the voltages are within their limits. The voltage decrease along the H2A feeder is higher (5,7%) because it has a larger feeder length and serves a higher load. The voltage decrease along feeders H1 and H2B is 0,34% and 1,73% respectively.
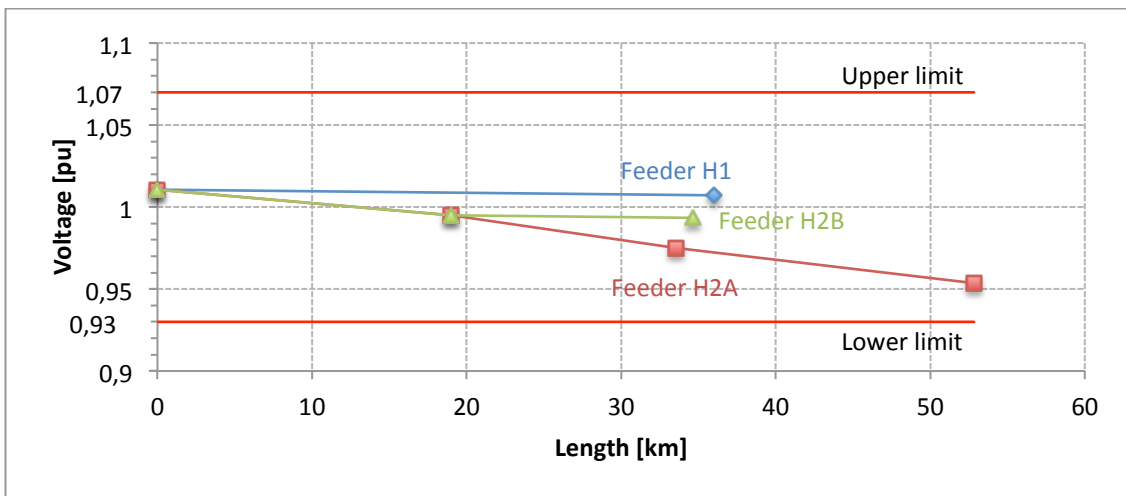
Figure 3.12 Voltage profile of all feeders supplied from the Hancock substation (U_n=33kV) at no DG production

In comparison with the MV grid voltage profile of "Simulation of the completed network" in Figure 3.5 the bus voltages in Figure 3.12 are lower. The feeder head voltage is lower in this test case: 1,011 p.u. vs. 1,045 p.u., and the voltage decreases along the feeders are higher especially in the feeder H2A (5,7% vs. 2,33%). An explanation for this can be found in the deactivation of the capacitor at the end of feeder H2A at bus bar 24. The supply of reactive power to the grid has the effect of voltage boost.

3.1.3.3.2 Voltages in the High Voltage grid

Figure 3.13. shows an illustration of the HV grid voltages. The height of the pyramids represents the voltage, the color gives a visual indication of the voltage band and the position represents the approximate physical position of the bus bar in the HV grid (see Figure 3.3). The voltage of all the bus bars in the High Voltage grid is above 1 p.u.. Glen Lyn is the location of the main generator of the grid which also acts as the Slack. The generator keeps the bus bar voltage in Glen Lyn to the desired value of 1,06 p.u..

In comparison with the voltage profile of "Simulation of the completed network" the voltages at the bus bars in Glen Lyn and Claytor are the same in the two simulations because the generators set them to desired values (1,06 p.u. and 1,045 p.u.). The deactivation of the capacitor at the end of feeder H2A in Hancock and at the MV bus bar of Roanoke results in less reactive power supply to the MV grid. This results in a slightly lower voltage at the HV bus bar of the Hancock substation (1,016 p.u. vs. 1,017 p.u.) and a slightly lower voltage at the HV bus bar of the Roanoke substation (1,010 p.u. vs. 1,011 p.u.). In the "Simulation of the completed network" the synchronous condensers at bus bar 11 and 13 are activated and in this simulation they aren't. To keep the reactive power balanced the synchronous condensers at bus bar 5 (Fieldale) and 8 (Reusens) need to inject more reactive power, which results in higher voltages at these two bus bars for this test case (1,01 p.u. vs 1,007 p.u. for Fieldale and 1,01 p.u. vs. 1,004 p.u. for Reusens).
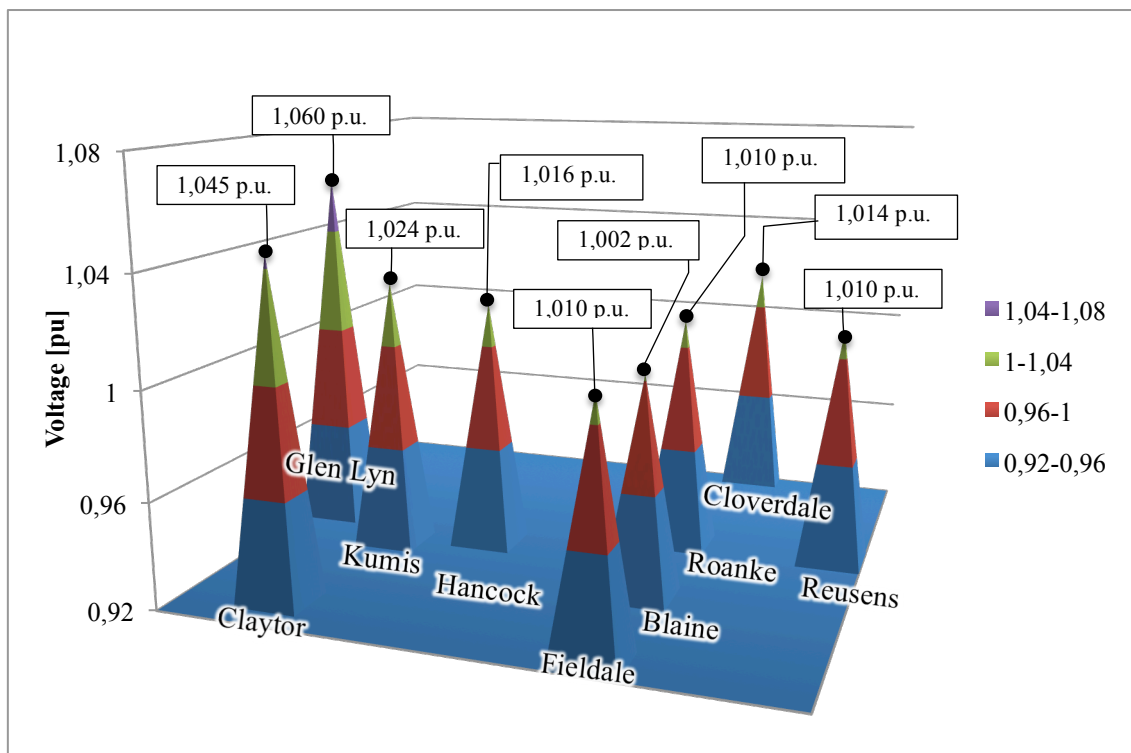
Figure 3.13 Voltage levels in the High Voltage grid (U_n=132 kV) at no DG production

3.1.3.4 Distributed generation in Hancock at cos(φ)=1

This test scenario is a simulation of DG enabled in Hancock that operates at three different production levels at a power factor of 1. Figure 3.14 shows the operation points.
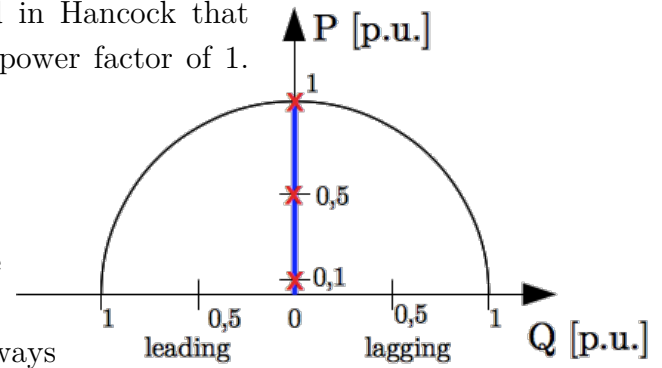
3.1.3.4.1 Impact on the Medium Voltage grid

Figure 3.15, Figure 3.16 and Figure 3.17 show the voltage profile of the feeders in Hancock at three different DG production levels. The voltages always stay within their limits. The DG has an impact on the feeder head Voltage. It rises from 1,017

Figure 3.14 PQ characteristic of the DG, red crosses mark the operation points

p.u. at P_{DG}=0,1 p.u. to 1,032 p.u. at P_{DG}=0,5 p.u. and declines slightly to 1,031 p.u. at full DG production. This corresponds to a Voltage rise at the feeder head of 682V from no DG production to full DG production.

Figure 3.15 illustrates that all three feeders have the same behavior at P_{DG}=0,1 p.u.. The voltage decreases with increasing feeder length. The voltage at the MV bus bar of the Hancock substation is $U_{Hancock}^{MV} = 1,017 p u..$
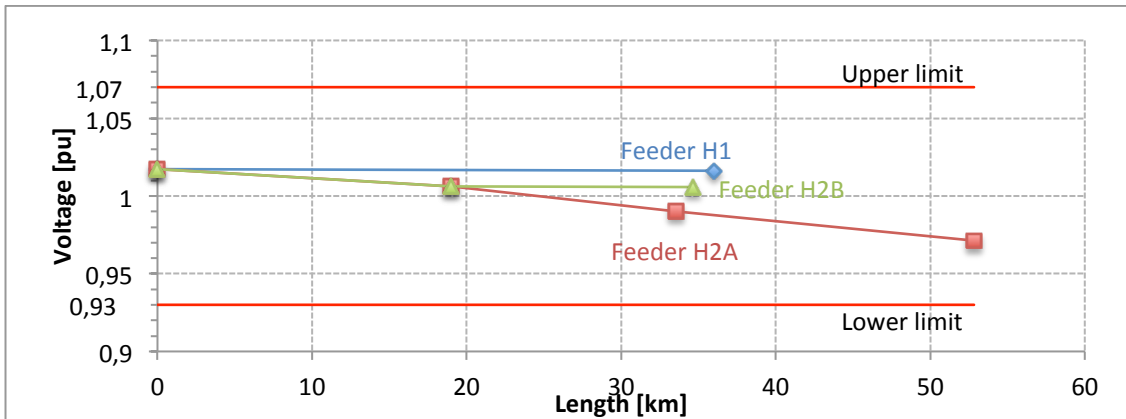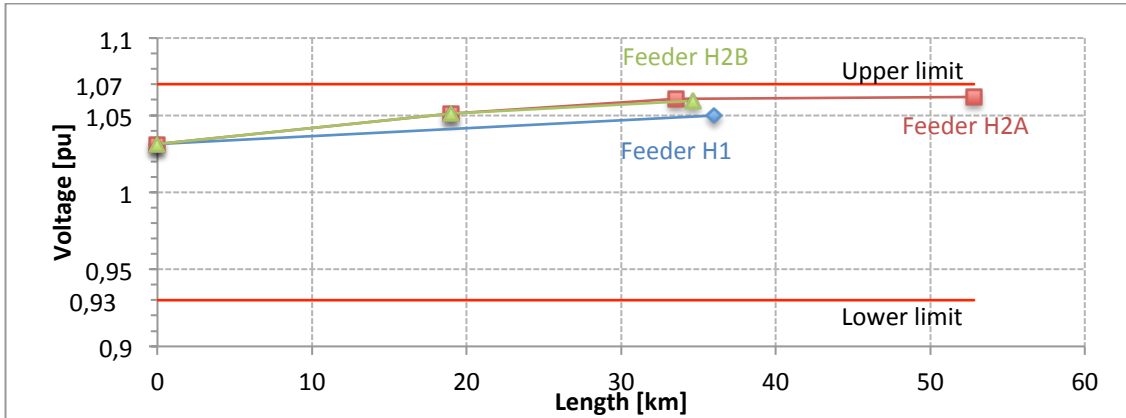

Figure 3.15 Voltage profile of all feeders supplied from the Hancock substation (U_n=33kV) at a DG production level of P_{DG}=0,1 p.u. at $cos(φ)$=1

Figure 3.16 shows that at P_{DG}=0,5 p.u. the feeders H1 and H2B show a behavior of rising voltage with increasing feeder length. The voltage along Feeder H2A rises until bus bar 15, after this the voltage declines again. The voltage at the bus bar on the end of the feeder is lower (1,025 p.u.) than at the MV bus bar of the Hancock substation $U_{Hancock}^{MV} = 1,032 p u.$.
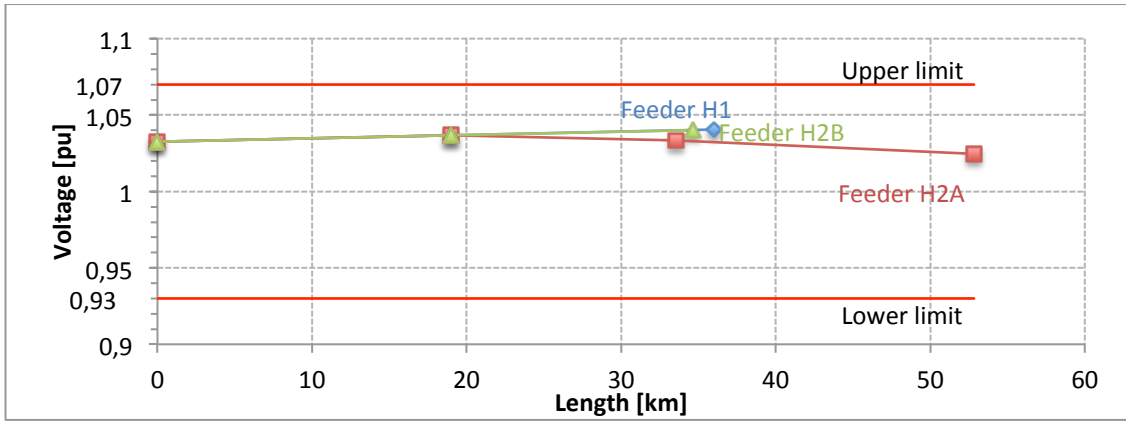
Figure 3.16 Voltage profile of all feeders supplied from the Hancock substation (U_n=33kV) at a DG production level of P_DG=0,5 p.u. at $cos(\varphi)$=1

Figure 3.17 illustrates the voltage profile at full DG production. All feeders supplied from the Hancock substation have the same behavior. The DG production causes a voltage boost and therefore an increasing voltage with increasing feeder length. The voltage at the MV bus bar of the Hancock substation is $U_{Hancock}^{MV} = 1,031 p.u.$.

Figure 3.17 Voltage profile of all feeders supplied from the Hancock substation (U_n=33kV) at a DG production level of P_DG=1 p.u. at $cos(\varphi)$=1

		no DG production		P_DG=0,1 pu, $cos(\varphi)$=1		P_DG=0,5 pu, $cos(\varphi)$=1		P_DG= 1 pu, $cos(\varphi)$=1	
		Voltage [p.u.]	Angle [°]	Voltage [p.u.]	Angle [°]	Voltage [p.u.]	Angle [°]	Voltage [p.u.]	Angle [°]
Feeder	H1								
Bus bar	12	1,011	-15,316	1,017	-13,891	1,032	-8,522	1,031	-2,187
Bus bar	14	1,007	-16,328	1,016	-14,635	1,040	-8,266	1,050	-0,718
Feeder	H2A								
Bus bar	12	1,011	-15,316	1,017	-13,891	1,032	-8,522	1,031	-2,187
Bus bar	15	0,995	-17,083	1,006	-15,268	1,037	-8,452	1,051	-0,381
Bus bar	23	0,975	-18,316	0,990	-16,165	1,033	-8,149	1,061	1,292
Bus bar	24	0,954	-19,496	0,971	-17,075	1,025	-8,127	1,062	2,322
Feeder	H2B								
Bus bar	12	1,011	-15,316	1,017	-13,891	1,032	-8,522	1,031	-2,187
Bus bar	15	0,995	-17,083	1,006	-15,268	1,037	-8,452	1,051	-0,381
Bus bar	18	0,993	-17,544	1,006	-15,610	1,040	-8,362	1,059	0,208

Table 3.3 Voltages in Hancock depending on the DG production, feeder head is shaded in grey

The biggest impact on the voltage is along the H2A feeder. At P_{DG}=0,1 p.u., as shown in Figure 3.15, there is a voltage decline of 4,59%, at P_{DG}=0,5 p.u., as shown in Figure 3.16 the voltage declines 0,79% along the feeder and at P_{DG}=1 p.u., as shown in Figure 3.17, the voltage rises 3,07% from the feeder head to the end of the feeder. The exact results can be found in Table 3.3.

3.1.3.4.2 Impact on the High Voltage grid

Figure 3.18 illustrates the relation of the reactive (in green) and active (in blue) power flow over the Transformer in Hancock depending on the DG production in Hancock. The active power flow is 41,44 MW from the High Voltage to the Medium Voltage grid at no DG production. However, at full DG production the MV grid supplies the HV grid with 27,38 MW active power.

As discussed in chapter "3.1.3.4.1 Impact on the Medium Voltage grid" the voltage rises with rising DG supply. This in turn means that the cables in the Medium Voltage grid are producing more reactive power. The reactive power supply from the MV grid to the HV grid rises up until a DG production level of P_{DG}=0,5 p.u. is reached. The reactive power flow decline from P_{DG}=0,5 p.u. to P_{DG}=1 p.u. has been investigated with further simulations at the operation points P_{DG}=0,6 p.u., P_{DG}=0,7 p.u., P_{DG}=0,8 p.u. and P_{DG}=0,6 p.u..
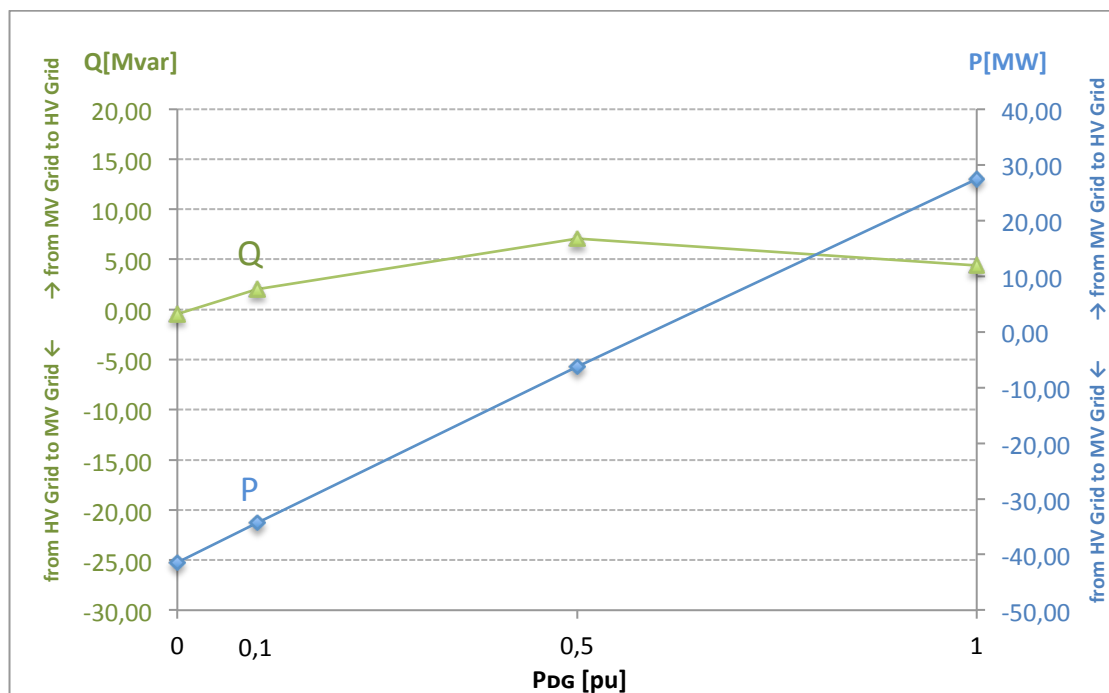
Figure 3.18 Power flow over the MV/HV transformer in Hancock for different DG production levels at $cos(\varphi)$=1

As shown in Figure 3.19 the reactive power flow rises up until a DG production of P_{DG}=0,6 p.u. to 7,31 Mvar. At P_{DG}=0,7 p.u. it is the first time the Medium Voltage

grid supplies the High Voltage grid with active power (0,59 MW). With the rising active power flow into the HV grid the reactive power flow declines. The power flow Data can be found in Table 3.4.

	no DG production	$P_{DG}=0,1$ pu, $cos(\varphi)=1$	$P_{DG}=0,5$ pu, $cos(\varphi)=1$	$P_{DG}=0,6$ pu, $cos(\varphi)=1$	$P_{DG}=0,7$ pu, $cos(\varphi)=1$	$P_{DG}=0,8$ pu, $cos(\varphi)=1$	$P_{DG}=0,9$ pu, $cos(\varphi)=1$	$P_{DG}=1$ pu, $cos(\varphi)=1$
P [MW]	-41,44	-34,25	-6,26	0,59	7,37	14,09	20,77	27,38
Q [Mvar]	-0,46	2,04	7,10	7,31	7,13	6,58	5,66	4,37

Table 3.4 Power flow over the Hancock substation in dependence of the DG
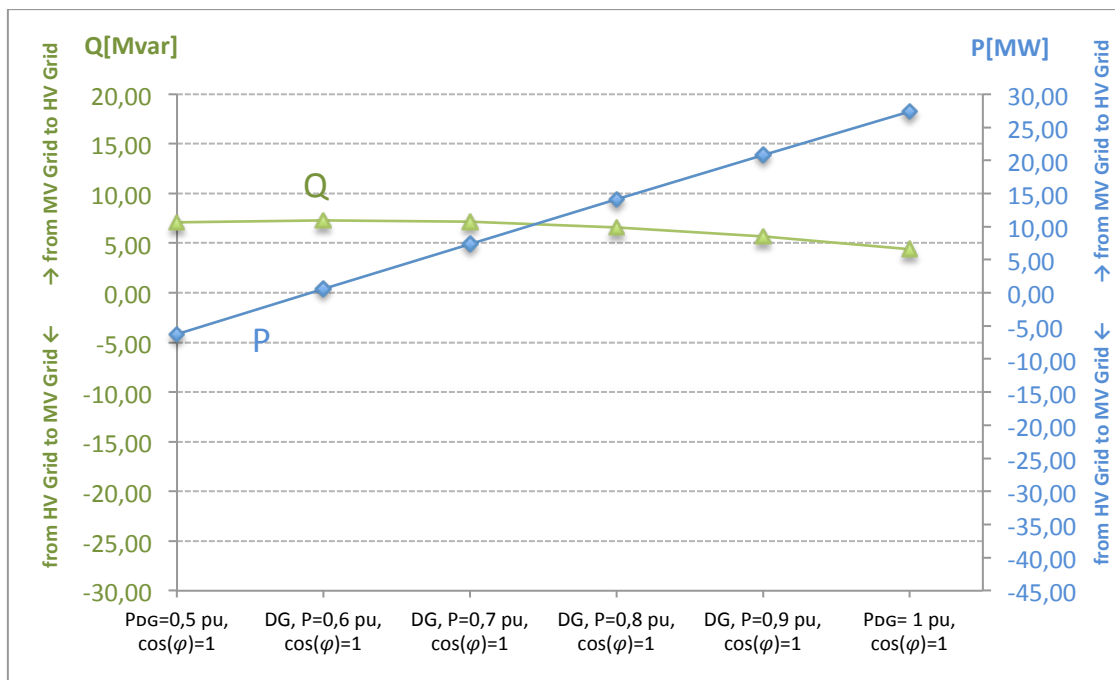
Figure 3.19 Further simulations for the power flow over the MV/HV transformer in Hancock for different DG production levels between $P_{DG}=0,5$ p.u. to $P_{DG}=1$ p.u. at $cos(\varphi)=1$

The rising DG production in Hancock has an impact on the High Voltage grid Voltages as shown in Figure 3.20. The voltage rise is most significant at the bus bar in Hancock, where the voltage rises from 1,0163 p.u. at no DG production to 1,0282 p.u. at full DG production which corresponds to a Voltage rise of 1571V. In Kumis, where the second biggest rise occurs, there is a voltage boost of 1360V at the same circumstances. This can be explained because the DG supply is in the MV grid of the Hancock substation and Kumis is not far away from Hancock. The DG production has no impact on the bus bars of Fieldale and Reusens because the Synchronous Condensors connected to these bus bars keep the voltage to desired values. The exact values can be found in Table 3.5.
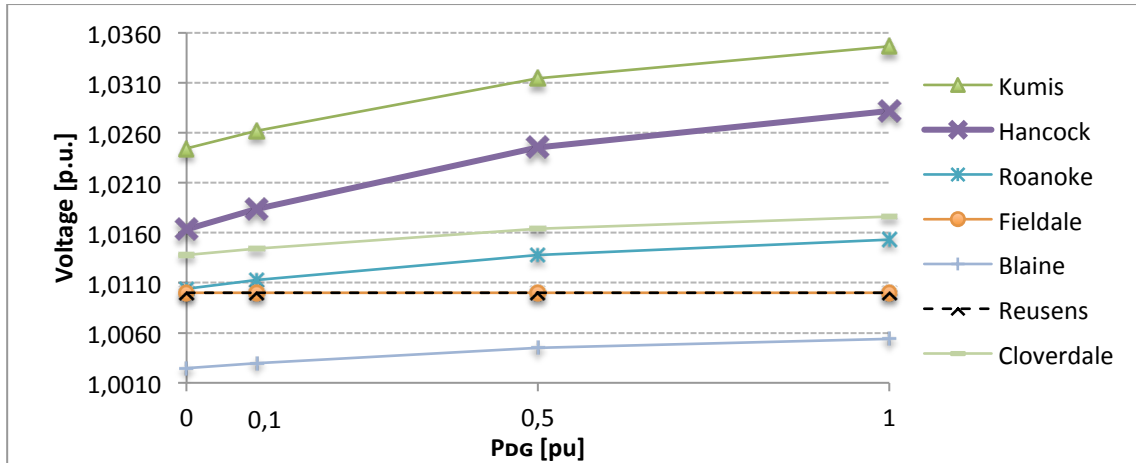
Figure 3.20 High Voltage grid (U_n=132 kV) Voltages depending on the DG production in the Medium Voltage grid at $cos(\varphi)$=1

	no DG production		P_{DG}=0,1 pu, $cos(\varphi)$=1		P_{DG}=0,5 pu, $cos(\varphi)$=1		P_{DG}=1 pu, $cos(\varphi)$=1	
	Voltage [p.u.]	Angle [°]	Voltage [p.u.]	Angle [°]	Voltage [p.u.]	Angle [°]	Voltage [p.u.]	Angle [°]
Glen Lyn	1,060	0,000	1,060	0,000	1,060	0,000	1,060	0,000
Claytor	1,045	-5,389	1,045	-5,234	1,045	-4,641	1,045	-3,948
Kumis	1,024	-7,572	1,026	-7,298	1,031	-6,223	1,035	-4,911
Hancock	1,016	-9,329	1,018	-8,987	1,025	-7,646	1,028	-6,015
Roanoke	1,010	-11,098	1,011	-10,787	1,014	-9,588	1,015	-8,164
Fieldale	1,010	-14,178	1,010	-13,938	1,010	-13,023	1,010	-11,961
Blaine	1,002	-12,890	1,003	-12,607	1,004	-11,523	1,005	-10,245
Reusens	1,010	-11,836	1,010	-11,511	1,010	-10,268	1,010	-8,818
Cloverdale	1,014	-11,799	1,014	-11,484	1,016	-10,274	1,018	-8,844

Table 3.5 High Voltage grid Voltages depending on the DG production in the Medium Voltage grid

3.1.3.5 Distributed generation in Hancock at cos(φ)=0,95 lagging

The third test scenario simulates DG in the Medium Voltage grid in Hancock at three different production levels that operates at a power factor of 0,95 lagging. Figure 3.21 illustrates the three operation points.

3.1.3.5.1 Impact on the Medium Voltage grid

Figure 3.22, Figure 3.23 and Figure 3.24 show an illustration of the feeders in Hancock in this test scenario. In the test case P_{DG}= 0,1 p.u. and P_{DG}= 0,5 p.u. the bus bar voltages in Hancock stay within their limits. At a DG production level of P_{DG}= 1 p.u. the voltages in the feeders H2A and H2B fall below the lower voltage limit.
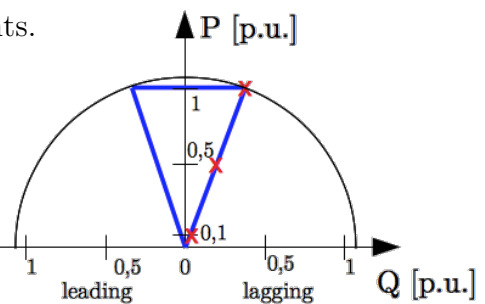
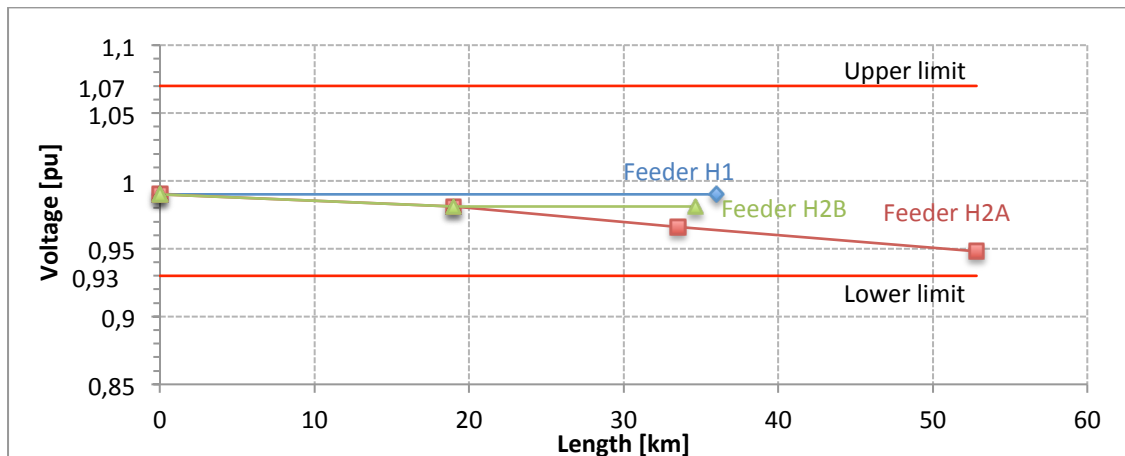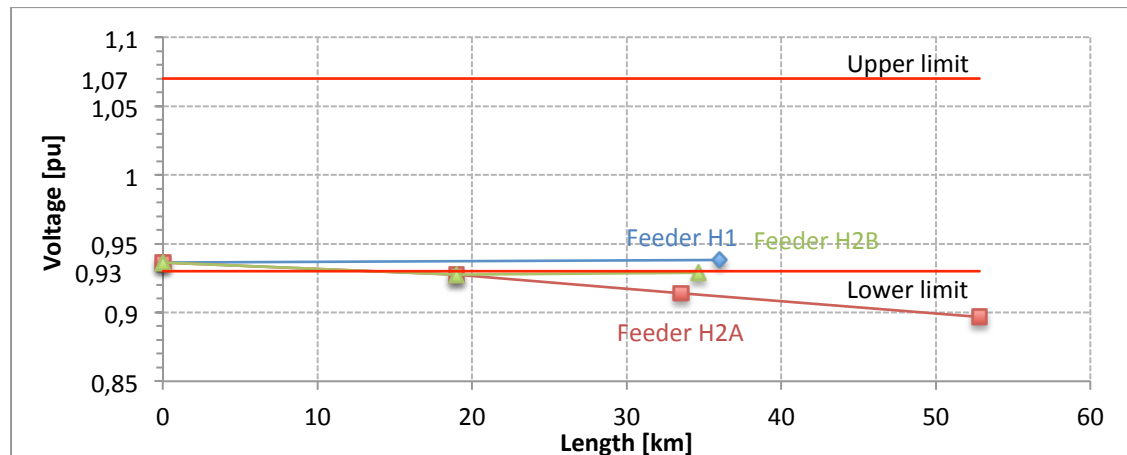Figure 3.21 *PQ* characteristic of the DG, red crosses mark the operation points
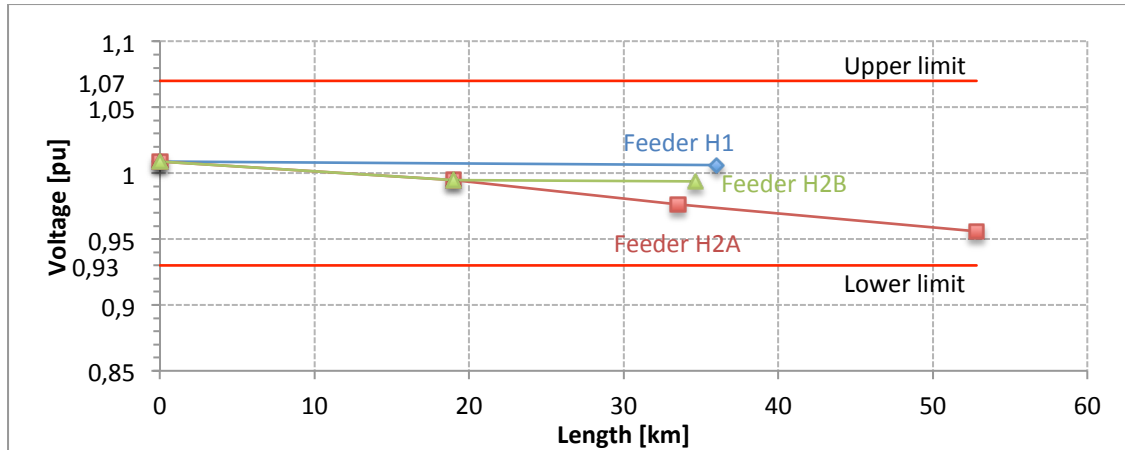
Figure 3.22 Voltage profile of all feeders supplied from the Hancock substation at the DG production level P_{DG}=0,1 p.u. at $cos(\varphi)$=0,95 lagging

Figure 3.22 illustrates that all three feeders in the Hancock region have the same behavior of a decreasing voltage with increasing distance from the HV/MV transformer. In comparison with Test Scenario 1 ($cos(\varphi)$=1) the voltage decrease along the feeder is more pronounced, even at this low DG production level. The voltage at the MV bus bar of the Hancock substation is $U_{Hancock}^{MV} = 1,009 \, p.u.$.

Figure 3.23 shows that the voltage for feeder H1 stays the same with increasing feeder length. The reactive power consumption from DG located at bus bar 14 has the effect that the voltage rise that occurs in Test Scenario 1 (feeder head voltage 1,032 p.u. rises to the feeder end voltage of 1,04 p.u.) is compensated. The voltage along the feeders H2A and H2B is decreasing with increasing feeder length. The voltage at the MV bus bar of the Hancock substation is $U_{Hancock}^{MV} = 0,99 \, p.u.$.

Figure 3.23 Voltage profile of all feeders supplied from the Hancock substation at the DG production level P_{DG}=0,5 p.u. at $cos(\varphi)$=0,95 lagging

Figure 3.24 illustrates that the feeder head voltage is only slightly above the lower voltage limit at $U_{Hancock}^{MV} = 0,936 \, p.u.$. Feeder H1 is also an exception at this production level, the voltage rises 0,2% to 0,938 p.u. from feeder head to the end of the feeder.

Feeder H2A and H2B show a behavior of decreasing voltage with increasing distance from the Hancock substation.

Figure 3.24 Voltage profile of all feeders supplied from the Hancock substation at the DG production level P_{DG}=1 p.u. at $cos(\varphi)$=0,95 lagging

The feeder head voltage declines from 1,009 p.u to 0,990 p.u. to 0,936 p.u at a DG production of P_{DG}=0,1 p.u., P_{DG}=0,5 p.u. and P_{DG}=1 p.u. respectively. This represents a voltage decline of 2458 V from no DG production to full DG production. The largest voltage decrease is along the H2A feeder. At P_{DG}=0,1 as shown in Figure 3.22 it is 5,32%, at P_{DG}=0,5 as shown in Figure 3.23 it is 4,22% and at P_{DG}=1 as shown in Figure 3.24 it is 3,96%. The active power supply from the DG compensates the load, which narrows the voltage decrease along the feeder. The reactive power consumption of the DG has the effect that the bus bar voltages decline with rising DG production. The exact voltages in the Medium Voltage grid in Hancock can be found in Table 3.6.

		no DG production		P_{DG}=0,1 pu, $cos(\varphi)$=0,95 lag		P_{DG}=0,5 pu, $cos(\varphi)$=0,95 lag		P_{DG}= 1 pu, $cos(\varphi)$=0,95 lag	
		Voltage [p.u.]	Angle [°]	Voltage [p.u.]	Angle [°]	Voltage [p.u.]	Angle [°]	Voltage [p.u.]	Angle [°]
Feeder	H1								
Bus bar	12	1,011	-15,316	1,009	-13,928	0,990	-8,518	0,936	-1,740
Bus bar	14	1,007	-16,328	1,006	-14,641	0,990	-8,000	0,938	0,604
Feeder	H2A								
Bus bar	12	1,011	-15,316	1,009	-13,928	0,990	-8,518	0,936	-1,740
Bus bar	15	0,995	-17,083	0,995	-15,256	0,981	-8,047	**0,928**	1,407
Bus bar	23	0,975	-18,316	0,976	-16,114	0,966	-7,387	**0,914**	4,325
Bus bar	24	0,954	-19,496	0,956	-17,003	0,948	-7,112	**0,897**	6,310
Feeder	H2B								
Bus bar	12	1,011	-15,316	1,009	-13,928	0,990	-8,518	0,936	-1,740
Bus bar	15	0,995	-17,083	0,995	-15,256	0,981	-8,047	**0,928**	1,407
Bus bar	18	0,993	-17,544	0,994	-15,585	0,981	-7,838	**0,929**	2,412

Table 3.6 Voltages in the Hancock Medium Voltage grid depending on the DG production, feeder head is shaded in grey, limit violations bold

3.1.3.5.2 Impact on the High Voltage grid

The power flow over the Transformer in Hancock is illustrated in Figure 3.25. Not only because of the reactive power consumption of the DG, but also because of the declining bus bar voltages in the Medium Voltage grid, which in turn has the effect that the cables produce less reactive power, leads to a rising reactive power flow (green curve) from the High Voltage grid to the Medium Voltage grid with rising DG supply. The active power flow however changes from a MV grid that consumes active power at no DG production to a MV grid that supplies the HV grid with active power at full DG production. The exact power flow data can be found in Table 3.7.
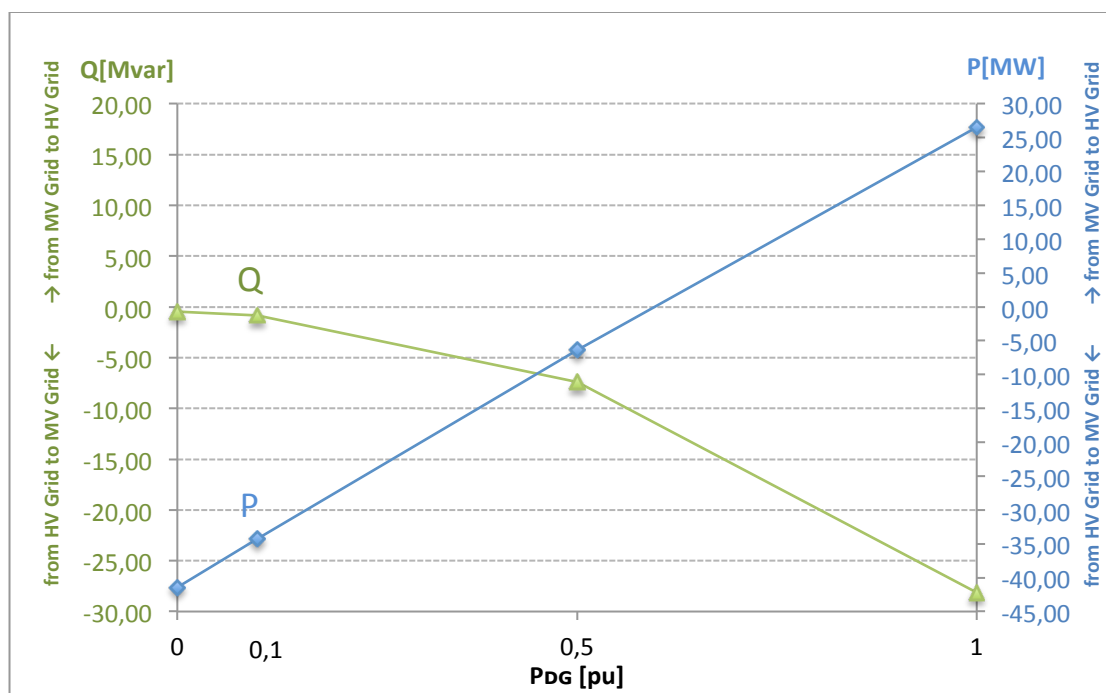
Figure 3.25 Power flow over the MV/HV transformer in Hancock for different DG production levels at $cos(\varphi)=0,95$ lagging

	no DG production	$P_{DG}=0,1$ pu, $cos(\varphi)=0,95$ lag	$P_{DG}=0,5$ pu, $cos(\varphi)=0,95$ lag	$P_{DG}=1$ pu, $cos(\varphi)=0,95$ lag
P [MW]	-41,44	-34,28	-6,39	26,53
Q [Mvar]	-0,46	-0,85	-7,40	-28,13

Table 3.7 Power flow over the Hancock substation in dependence of the DG

Figure 3.26 shows the High Voltage grid Voltages of this scenario. Again, as in the other test scenarios, the DG production has no impact on the voltage of the Fieldale and the Reusens bus bar. The voltage rises when increasing the DG production from $P_{DG}=0$ p.u. to $P_{DG}=0,1$ p.u. and furthermore to $P_{DG}=0,5$ p.u. and declines when increasing the production to $P_{DG}=1$ p.u. at HV bus bars in Kumis, Hancock, Cloverdale, Roanoke, and Blaine. The voltage at these five bus bars is always lower at full DG production than at no DG production. The voltage rise in the HV grid can be

explained with the increasing active power flow from the MV grid. Up until the DG production of P_{DG}=0,5 p.u. the reactive power flow into the HV grid is relatively small (7,4 Mvar). At full DG production the reactive power flow (28,13 Mvar) has the effect of the voltage decline in the HV grid.
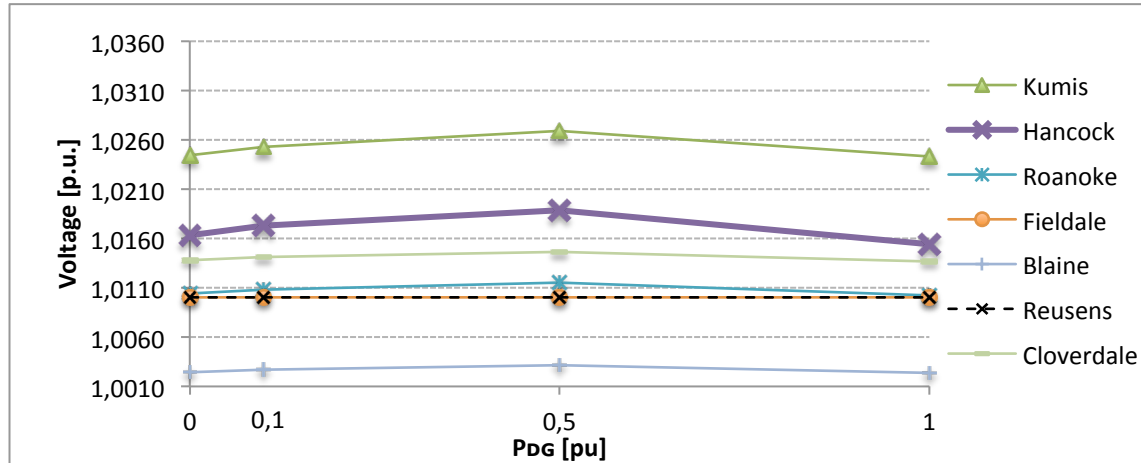
Figure 3.26 High Voltage grid (U_n=132kV) voltages depending on the DG production in the Medium Voltage grid at $cos(\varphi)$=0,95 lagging

	no DG production		P_{DG}=0,1 pu, $cos(\varphi)$=0,95 lag		P_{DG}=0,5 pu, $cos(\varphi)$=0,95 lag		P_{DG}=1 pu, $cos(\varphi)$=0,95 lag	
	Voltage [p.u.]	Angle [°]	Voltage [p.u.]	Angle [°]	Voltage [p.u.]	Angle [°]	Voltage [p.u.]	Angle [°]
Glen Lyn	1,060	0,000	1,060	0,000	1,060	0,000	1,060	0,000
Claytor	1,045	-5,389	1,045	-5,237	1,045	-4,654	1,045	-3,987
Kumis	1,024	-7,572	1,025	-7,287	1,027	-6,166	1,024	-4,797
Hancock	1,016	-9,329	1,017	-8,974	1,019	-7,579	1,015	-5,878
Roanoke	1,010	-11,098	1,011	-10,787	1,012	-9,585	1,010	-8,174
Fieldale	1,010	-14,178	1,010	-13,945	1,010	-13,056	1,010	-12,049
Blaine	1,002	-12,890	1,003	-12,610	1,003	-11,536	1,002	-10,291
Reusens	1,010	-11,836	1,010	-11,519	1,010	-10,303	1,010	-8,915
Cloverdale	1,014	-11,799	1,014	-11,486	1,015	-10,281	1,014	-8,875

Table 3.8 High Voltage grid voltages depending on the DG production in the Medium Voltage grid

As discussed in "2.2 Transformer secondary voltage dependence on the phase angle" the secondary voltage of the Transformer depends on the primary voltage and the phase angle. The construction of the secondary voltage referred to the primary side for the Hancock Transformer for the test cases no DG production, half DG production and full DG production can be found in Figure 3.27, Figure 3.28 and Figure 3.29. The primary side (index 1) of the transformer is connected to the MV grid, the secondary side (index 2) is connected to the HV grid.

Figure 3.27 shows the construction of the secondary voltage at no DG production. The voltage on the MV side (1,011 p.u.) is only slightly smaller than on the HV side (1,016 p.u.).
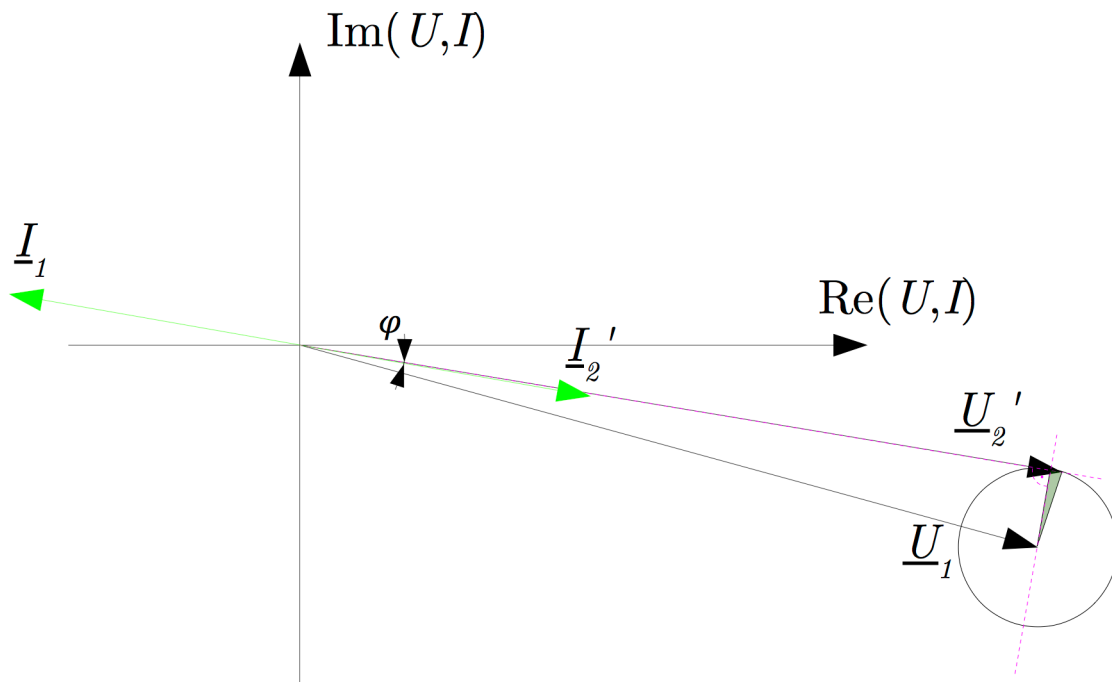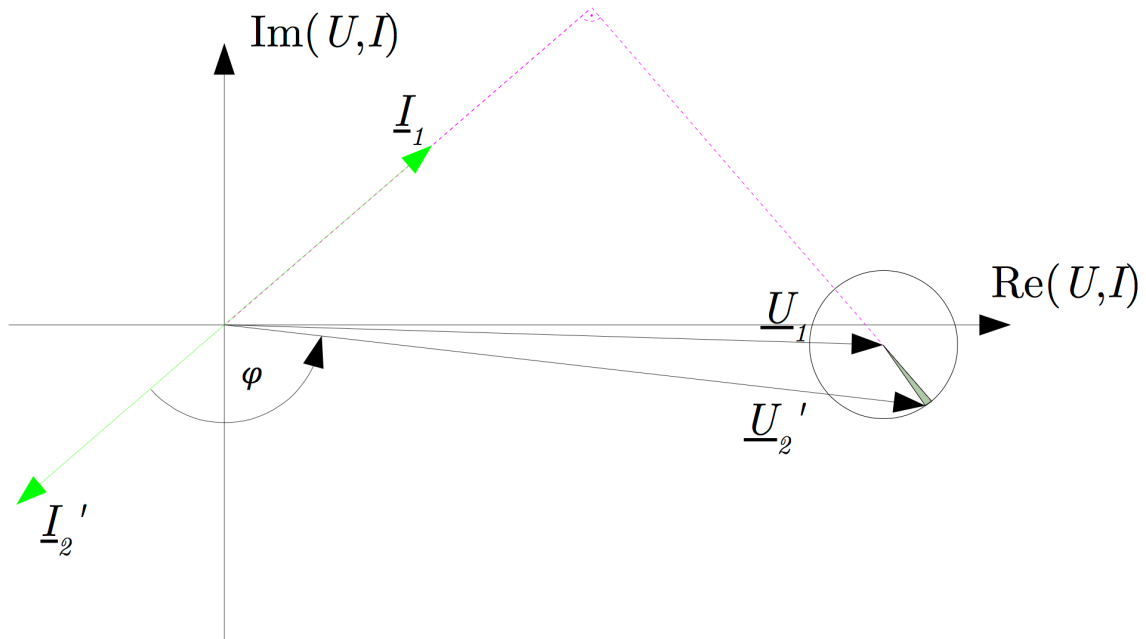

Figure 3.27 Construction of the secondary voltage referred to the primary side via the Kap- Triangle for the Transformer in Hancock at no DG production (P_{DG}=0 p.u.)

Figure 3.28 illustrates the construction of the secondary voltage at P_{DG}=0,5 p.u.. The voltage on the MV side declines to 0,99 p.u. but the HV side rises to 1,019 p.u.. The Kap-Triangle is smaller than at P_{DG}=0 p.u. and P_{DG}=1 p.u. because the Transformer current is smaller, the side ratio of the Kap-Triangle always stays the same.
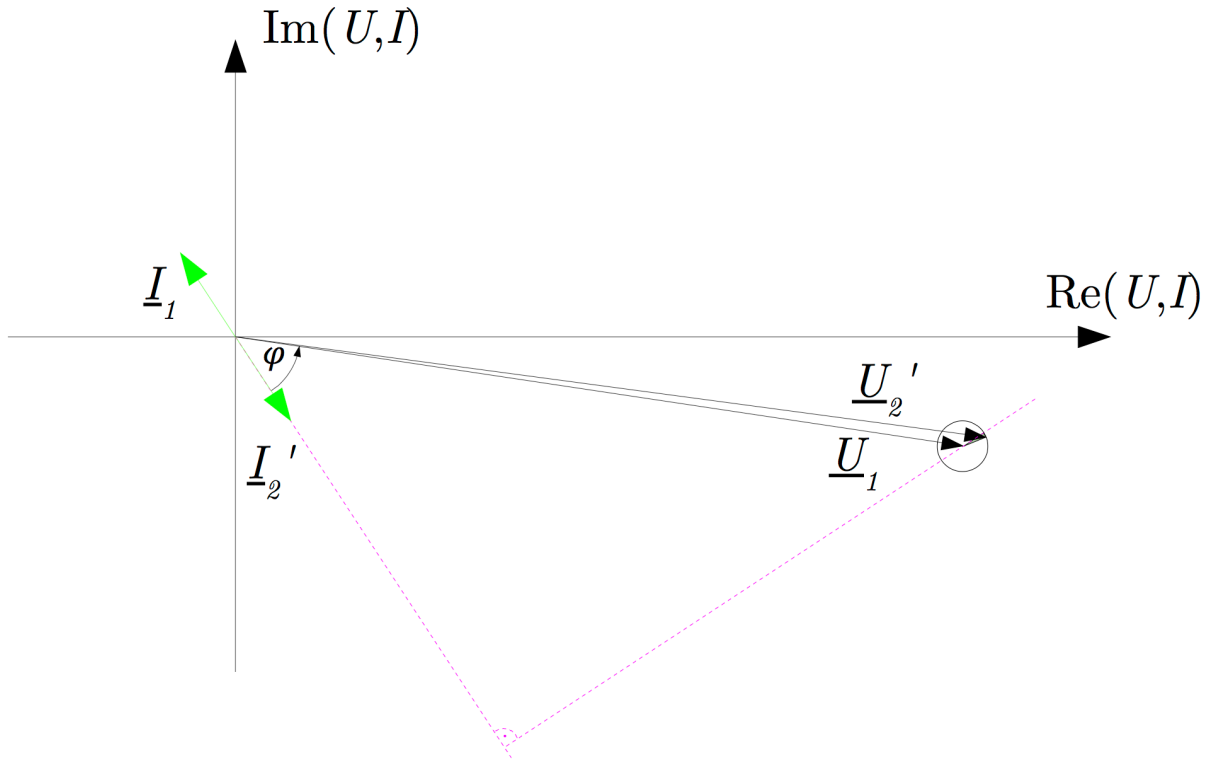
Figure 3.28 Construction of the secondary voltage referred to the primary side via the Kap- Triangle for the Transformer in Hancock at half DG production (P_{DG}=0,5 p.u.)

Figure 3.29 shows the construction of the secondary voltage at P_{DG}=1 p.u.. The voltage difference between the MV side and the HV side is even higher but because of the voltage decline to 0,936 p.u. on the MV side the voltage declines to 1,015 p.u. on the HV side which is less than at P_{DG}=0,5 p.u.. This voltage decline on the HV side also has an effect on the other HV bus bars as illustrated in Figure 3.26.

Figure 3.29 Construction of the secondary Voltage referred to the primary side via the Kap-Triangle for the Transformer in Hancock at full DG production (P_{DG}=1 p.u.)

3.1.3.6 Distributed generation in Hancock, Roanoke and Cloverdale at cos(φ)=1
The DG in this test scenario is enabled in Hancock, Roanoke and Cloverdale and operates at three different production levels (see Figure 3.14) at a power factor of 1.

3.1.3.6.1 Impact on the Medium Voltage grid
Table 3.9 presents the bus bar voltages of the MV grid in Hancock. In this Test Scenario 3 all feeders supplied by the Hancock substation show the same behavior at all three DG production levels as in Test Scenario 1 (DG operating at the same power factor but in Hancock only) but more pronounced. Therefore the voltage profiles will not be illustrated.

		no DG production		P_{DG}=0,1 pu, $cos(φ)$=1		P_{DG}=0,5 pu, $cos(φ)$=1		P_{DG}= 1 pu, $cos(φ)$=1	
		Voltage [p.u.]	Angle [°]	Voltage [p.u.]	Angle [°]	Voltage [p.u.]	Angle [°]	Voltage [p.u.]	Angle [°]
Feeder	H1								
Bus bar	12	1,011	-15,316	1,019	-13,329	1,039	-5,878	1,041	2,853
Bus bar	14	1,007	-16,328	1,018	-14,072	1,047	-5,628	1,059	4,291
Feeder	H2A								
Bus bar	12	1,011	-15,316	1,019	-13,329	1,039	-5,878	1,041	2,853
Bus bar	15	0,995	-17,083	1,008	-14,703	1,044	-5,815	1,061	4,616
Bus bar	23	0,975	-18,316	0,992	-15,598	1,041	-5,521	**1,071**	6,251
Bus bar	24	0,954	-19,496	0,973	-16,505	1,032	-5,504	**1,072**	7,257
Feeder	H2B								
Bus bar	12	1,011	-15,316	1,019	-13,329	1,039	-5,878	1,041	2,853
Bus bar	15	0,995	-17,083	1,008	-14,703	1,044	-5,815	1,061	4,616
Bus bar	18	0,993	-17,544	1,008	-15,044	1,048	-5,728	1,069	5,191

Table 3.9 Voltages in the Hancock Medium Voltage grid depending on the DG production, feeder head is shaded in grey, limit violations bold

Table 3.10 shows the voltage and angle difference between the Test Scenario 1 (DG in Hancock only at $cos(φ)$=1) and this Test Scenario 3 (DG in all three Medium Voltage regions at $cos(φ)$=1). The additional DG production in Roanoke and Cloverdale has the effect that the voltage in all Hancock bus bars raises about 1% at full DG production. Feeder H2A is already near the voltage limit in Test Scenario 1 but with the additional voltage rise in Test Scenario 3 the voltage exceeds the limit.

		no DG production		P_{DG}=0,1 pu, $cos(\varphi)$=1		P_{DG}=0,5 pu, $cos(\varphi)$=1		P_{DG}= 1 pu, $cos(\varphi)$=1	
		ΔVoltage	ΔAngle [°]	ΔVoltage	ΔAngle [°]	ΔVoltage	ΔAngle [°]	ΔVoltage	ΔAngle [°]
Feeder	H1								
Bus bar	12	0,00%	0,000	0,19%	0,562	0,70%	2,645	0,97%	5,040
Bus bar	14	0,00%	0,000	0,19%	0,564	0,70%	2,638	0,97%	5,009
Feeder	H2A								
Bus bar	12	0,00%	0,000	0,19%	0,562	0,70%	2,645	0,97%	5,040
Bus bar	15	0,00%	0,000	0,19%	0,565	0,72%	2,637	0,99%	4,997
Bus bar	23	0,00%	0,000	0,20%	0,567	0,74%	2,628	1,01%	4,959
Bus bar	24	0,00%	0,000	0,21%	0,570	0,76%	2,623	1,03%	4,935
Feeder	H2B								
Bus bar	12	0,00%	0,000	0,19%	0,562	0,70%	2,645	0,97%	5,040
Bus bar	15	0,00%	0,000	0,19%	0,565	0,72%	2,637	0,99%	4,997
Bus bar	18	0,00%	0,000	0,20%	0,566	0,72%	2,634	0,99%	4,984

Table 3.10 Voltage difference in the Hancock Medium Voltage grid depending on the DG production between Test Scenario 1 and Test Scenario 3, feeder head is shaded in grey

Table 3.11 shows the DG production impact on the bus bar voltages of the Roanoke MV grid. The rising DG production level causes a feeder head voltage rise. The voltage profile of the three feeders R1, R2 and R3 show no particular noteworthy behavior and are therefore not illustrated. They have the same feeder behavior as already described in Test Scenario 1 when adding DG with a $cos(\varphi)$=1. There are no voltage limit violations.

		no DG production		P_{DG}=0,1 pu, $cos(\varphi)$=1		P_{DG}=0,5 pu, $cos(\varphi)$=1		P_{DG}= 1 pu, $cos(\varphi)$=1	
		Voltage [p.u.]	Angle [°]	Voltage [p.u.]	Angle [°]	Voltage [p.u.]	Angle [°]	Voltage [p.u.]	Angle [°]
Feeder	R1								
Bus bar	10	0,988	-16,664	0,993	-14,708	1,006	-7,232	1,009	1,658
Bus bar	20	0,976	-18,117	0,984	-15,839	1,008	-7,152	1,021	3,183
Bus bar	19	0,971	-18,455	0,980	-16,111	1,005	-7,180	1,022	3,435
Feeder	R2								
Bus bar	10	0,988	-16,664	0,993	-14,708	1,006	-7,232	1,009	1,658
Bus bar	17	0,979	-17,182	0,985	-15,122	1,001	-7,250	1,007	2,116
Bus bar	16	0,974	-17,547	0,981	-15,425	0,998	-7,324	1,005	2,316
Feeder	R3								
Bus bar	10	0,988	-16,664	0,993	-14,708	1,006	-7,232	1,009	1,658
Bus bar	21	0,978	-17,348	0,984	-15,254	1,002	-7,255	1,010	2,265
Bus bar	22	0,979	-17,386	0,986	-15,278	1,004	-7,226	1,013	2,359

Table 3.11 Voltages in the Roanoke Medium Voltage grid depending on the DG production, feeder head is shaded in grey

Table 3.12 shows the DG production impact on the bus bar voltages of the Cloverdale MV grid. The three feeders supplied by the Cloverdale substation show no noteworthy behavior but the feeder head voltage does. It increases from 1,023 p.u. at P_{DG}=0,1 p.u. to 1,036 p.u. at P_{DG}=0,5 p.u.. But when increasing the DG production even more the feeder head voltage decreases to 1,029 p.u. at P_{DG}=1 p.u.. This is not an effect of a transformer tap position change because the tap position of all substations is fixed. There are no voltage limit violations.

		no DG production		P_{DG}=0,1 pu, $cos(\varphi)$=1		P_{DG}=0,5 pu, $cos(\varphi)$=1		P_{DG}= 1 pu, $cos(\varphi)$=1	
		Voltage [p.u.]	Angle [°]	Voltage [p.u.]	Angle [°]	Voltage [p.u.]	Angle [°]	Voltage [p.u.]	Angle [°]
Feeder	C1								
Bus bar	27	1,016	-15,693	1,023	-13,307	1,036	-4,242	1,029	6,593
Bus bar	29	1,030	-16,802	1,039	-14,188	1,061	-4,255	1,064	7,663
Feeder	C2								
Bus bar	27	1,016	-15,693	1,023	-13,307	1,036	-4,242	1,029	6,593
Bus bar	30	0,982	-19,437	0,997	-16,308	1,038	-4,550	1,060	9,437
Feeder	C3								
Bus bar	27	1,016	-15,693	1,023	-13,307	1,036	-4,242	1,029	6,593
Bus bar	25	1,017	-16,221	1,025	-13,605	1,047	-3,661	1,050	8,278
Bus bar	26	1,005	-16,884	1,017	-14,052	1,049	-3,307	1,064	9,595

Table 3.12 Voltages in the Cloverdale Medium Voltage grid depending on the DG production, feeder head is shaded in grey

3.1.3.6.2 Impact on the High Voltage grid
The *PQ* power flow chart over the Hancock substation is nearly identical to the one with the one from Test Scenario 1 and can be found in the Appendix in Figure 6.1.

In the analyzes of the impact on the MV grid in this Test Scenario a feeder head voltage decrease was observed in Cloverdale between P_{DG}= 0,5 p.u. and P_{DG}= 1 p.u.. Figure 3.30 and Table 3.13 show the active and reactive power flow over the Cloverdale substation. The high active power flow from the MV into the HV grid has the effect of decreasing the feeder head voltage in Cloverdale. This can be shown with the construction of the Kap-triangle.
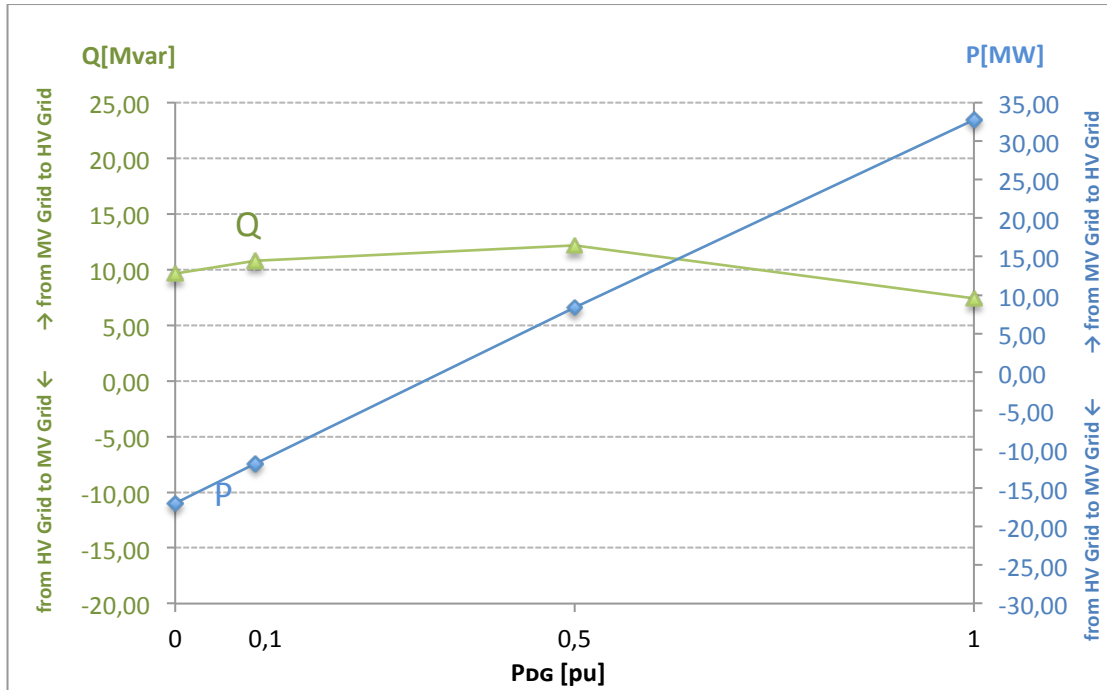
Figure 3.30 Power flow over the MV/HV transformer in Cloverdale for different DG production levels at $cos(\varphi)=1$

	no DG production	P_{DG}=0,1 pu, $cos(\varphi)$=1	P_{DG}=0,5 pu, $cos(\varphi)$=1	P_{DG}=1 pu, $cos(\varphi)$=1
P [MW]	-16,99	-11,82	8,37	32,14
Q [Mvar]	9,65	10,8	12,14	7,4

Table 3.13 Power flow over the Cloverdale substation in dependence of the DG

Figure 3.31 shows a chart of the HV grid voltages in dependence of the DG production. The HV bus bar voltage in Hancock rises 2,03% (1,19% in Test Scenario 1), 1,45% in Roanoke (0,49% in Test Scenario 1) and 1,66% in Cloverdale (0,39% in Test Scenario 1) from P_{DG}=0 p.u. to P_{DG}=1 p.u.. More DG production in the MV grid has a serious impact on the HV grid voltages.
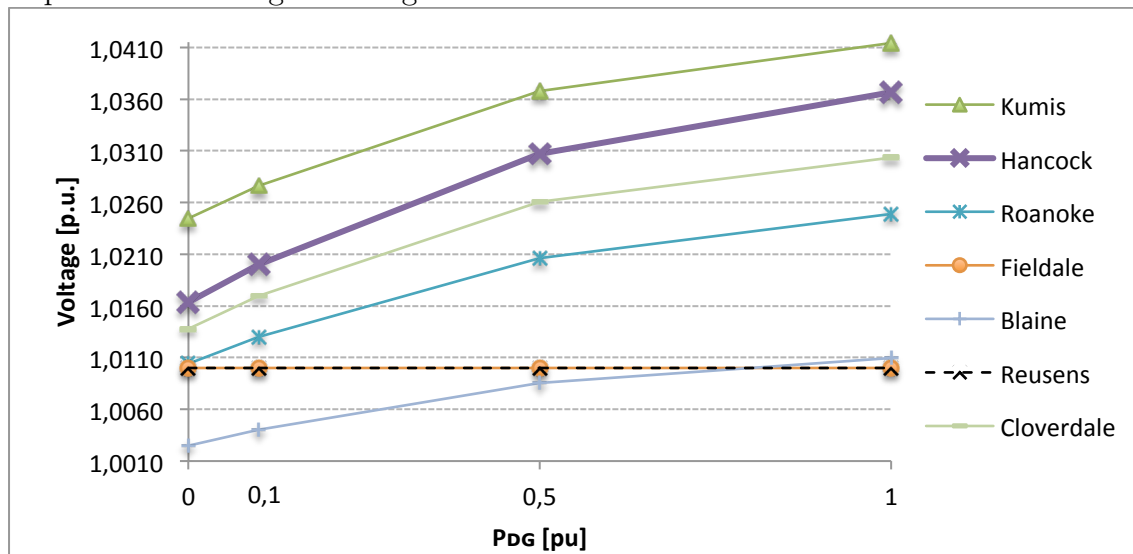
Figure 3.31 HV grid bus bar voltages depending on DG production in all three MV grids

Table 3.14 shows the HV grid bus bar voltages. The Generators and Synchronous Condensers in Glen Lyn, Claytor, Fieldale and Reusens are keeping the bus bar voltage to a pre-defined value so they are not exposed to the voltage changes in the grid.

	no DG production		P_{DG}=0,1 pu, $cos(\varphi)$=1		P_{DG}=0,5 pu, $cos(\varphi)$=1		P_{DG}=1 pu, $cos(\varphi)$=1	
	Voltage [p.u.]	Angle [°]	Voltage [p.u.]	Angle [°]	Voltage [p.u.]	Angle [°]	Voltage [p.u.]	Angle [°]
Glen Lyn	1,060	0,000	1,060	0,000	1,060	0,000	1,060	0,000
Claytor	1,045	-5,389	1,045	-4,931	1,045	-3,189	1,045	-1,174
Kumis	1,024	-7,572	1,028	-6,861	1,037	-4,104	1,041	-0,795
Hancock	1,016	-9,329	1,020	-8,442	1,031	-5,013	1,037	-0,910
Roanoke	1,010	-11,098	1,013	-10,066	1,021	-6,099	1,025	-1,394
Fieldale	1,010	-14,178	1,010	-13,413	1,010	-10,511	1,010	-7,161
Blaine	1,002	-12,890	1,004	-11,965	1,009	-8,427	1,011	-4,268
Reusens	1,010	-11,836	1,010	-10,734	1,010	-6,537	1,010	-1,643
Cloverdale	1,014	-11,799	1,017	-10,625	1,026	-6,101	1,030	-0,710

Table 3.14 HV grid bus bar voltages depending on the DG production in the Medium Voltage grid, areas with DG production are shaded in grey

Table 3.15 shows the difference between Test Scenario 1 and Test Scenario 3. The 0,85% voltage rise compared to Test Scenario 1 at the HV bus bar of Hancock has the effect that the voltage limits in the MV grid are violated.

	no DG production		P_{DG}=0,1 pu, $cos(\varphi)$=1		P_{DG}=0,5 pu, $cos(\varphi)$=1		P_{DG}=1 pu, $cos(\varphi)$=1	
	ΔVoltage	ΔAngle [°]	ΔVoltage	ΔAngle [°]	ΔVoltage	ΔAngle [°]	ΔVoltage	ΔAngle [°]
Glen Lyn	0,00%	0,00	0,00%	0,00	0,00%	0,00	0,00%	0,00
Claytor	0,00%	0,00	0,00%	0,30	0,00%	1,45	0,00%	2,77
Kumis	0,00%	0,00	0,14%	0,44	0,53%	2,12	0,68%	4,12
Hancock	0,00%	0,00	0,16%	0,54	0,62%	2,63	0,85%	5,10
Roanoke	0,00%	0,00	0,17%	0,72	0,68%	3,49	0,96%	6,77
Fieldale	0,00%	0,00	0,00%	0,53	0,00%	2,51	0,00%	4,80
Blaine	0,00%	0,00	0,10%	0,64	0,41%	3,10	0,56%	5,98
Reusens	0,00%	0,00	0,00%	0,78	0,00%	3,73	0,00%	7,18
Cloverdale	0,00%	0,00	0,25%	0,86	0,97%	4,17	1,27%	8,13

Table 3.15 Difference of the HV grid bus bar voltages between Test Scenario 1 (DG production in Hancock only) and Test Scenario 3 (DG production in all three MV grids), areas with DG production are shaded in grey

3.1.3.7 Distributed generation in Hancock, Roanoke and Cloverdale at *cos(φ)=0,95 lagging*

The DG in this test scenario is enabled in Hancock, Roanoke and Cloverdale and operates at three different production levels (see Figure 3.21) at a power factor of 0,95 lagging.

3.1.3.7.1 Impact on the Medium Voltage grid

Table 3.16 shows the bus bar voltages in Hancock. All three feeders show similar behavior to Test Scenario 2 where the DG is only activated along the Hancock feeders. Therefore the voltage profile of the feeders in Hancock is not illustrated. Similar to Test Scenario 2 the feeder head voltage declines with increasing DG production. The voltages of some bus bars of feeder H2A and H2B fall below the lower voltage limit in Test Scenario 2 as well as in Test Scenario 4 at full DG production.

		no DG production		P_{DG}=0,1 pu, $cos(\varphi)$=0,95 lag		P_{DG}=0,5 pu, $cos(\varphi)$=0,95 lag		P_{DG}= 1 pu, $cos(\varphi)$=0,95 lag	
		Voltage [p.u.]	Angle [°]	Voltage [p.u.]	Angle [°]	Voltage [p.u.]	Angle [°]	Voltage [p.u.]	Angle [°]
Feeder	H1								
Bus bar	12	1,011	-15,316	1,010	-13,365	0,994	-5,821	0,938	3,490
Bus bar	14	1,007	-16,328	1,007	-14,076	0,993	-5,308	0,940	5,827
Feeder	H2A								
Bus bar	12	1,011	-15,316	1,010	-13,365	0,994	-5,821	0,938	3,490
Bus bar	15	0,995	-17,083	0,996	-14,691	0,984	-5,357	**0,929**	6,625
Bus bar	23	0,975	-18,316	0,978	-15,548	0,970	-4,704	**0,915**	9,534
Bus bar	24	0,954	-19,496	0,957	-16,435	0,952	-4,434	**0,898**	11,510
Feeder	H2B								
Bus bar	12	1,011	-15,316	1,010	-13,365	0,994	-5,821	0,938	3,490
Bus bar	15	0,995	-17,083	0,996	-14,691	0,984	-5,357	**0,929**	6,625
Bus bar	18	0,993	-17,544	0,995	-15,019	0,985	-5,150	0,930	7,628

Table 3.16 Voltages in the Hancock Medium Voltage grid depending on the DG production, feeder head is shaded in grey, limit violations bold

Table 3.17 shows the voltage and angle difference between the Test Scenario 2 (DG in Hancock only at *cos(φ)*=0,95 lag) and this Test Scenario 4 (DG in all three Medium Voltage regions at *cos(φ)*=0,95). The additional DG production in Roanoke and Cloverdale has the effect that the voltage in all Hancock bus bars raises about 0,15% at full DG production which can be attributed to the voltage rise on the HV side of the Transformer.

		no DG production		P_{DG}=0,1 pu, $cos(\varphi)$=0,95 lag		P_{DG}=0,5 pu, $cos(\varphi)$=0,95 lag		P_{DG}= 1 pu, $cos(\varphi)$=0,95 lag	
		ΔVoltage	ΔAngle [°]	ΔVoltage	ΔAngle [°]	ΔVoltage	ΔAngle [°]	ΔVoltage	ΔAngle [°]
Feeder	H1								
Bus bar	12	0,00%	0,000	0,11%	0,564	0,34%	2,697	0,14%	5,230
Bus bar	14	0,00%	0,000	0,11%	0,565	0,34%	2,692	0,14%	5,222
Feeder	H2A								
Bus bar	12	0,00%	0,000	0,11%	0,564	0,34%	2,697	0,14%	5,230
Bus bar	15	0,00%	0,000	0,12%	0,565	0,35%	2,690	0,15%	5,219
Bus bar	23	0,00%	0,000	0,12%	0,567	0,37%	2,683	0,16%	5,208
Bus bar	24	0,00%	0,000	0,13%	0,568	0,38%	2,678	0,16%	5,200
Feeder	H2B								
Bus bar	12	0,00%	0,000	0,11%	0,564	0,34%	2,697	0,14%	5,230
Bus bar	15	0,00%	0,000	0,12%	0,565	0,35%	2,690	0,15%	5,219
Bus bar	18	0,00%	0,000	0,12%	0,566	0,36%	2,688	0,15%	5,215

Table 3.17 Voltage difference in the Hancock Medium Voltage grid depending on the DG production between Test Scenario 1 and Test Scenario 3, feeder head is shaded in grey

Table 3.18 shows the bus bar voltages in Roanoke. With increasing DG production the feeder head voltage decreases. The feeders supplied by the Roanoke substation have no noteworthy behavior. At full DG production there are voltage limit violations at the lower limit in all three feeders.

		no DG production		P_{DG}=0,1 pu, $cos(\varphi)$=0,95 lag		P_{DG}=0,5 pu, $cos(\varphi)$=0,95 lag		P_{DG}= 1 pu, $cos(\varphi)$=0,95 lag	
		Voltage [p.u.]	Angle [°]	Voltage [p.u.]	Angle [°]	Voltage [p.u.]	Angle [°]	Voltage [p.u.]	Angle [°]
Feeder	R1								
Bus bar	10	0,988	-16,664	0,986	-14,739	0,970	-7,208	0,930	2,117
Bus bar	20	0,976	-18,117	0,975	-15,839	0,961	-6,862	**0,923**	4,513
Bus bar	19	0,971	-18,455	0,970	-16,106	0,957	-6,840	**0,919**	4,940
Feeder	R2								
Bus bar	10	0,988	-16,664	0,986	-14,739	0,970	-7,208	0,930	2,117
Bus bar	17	0,979	-17,182	0,977	-15,146	0,961	-7,160	**0,921**	2,810
Bus bar	16	0,974	-17,547	0,972	-15,449	0,956	-7,211	**0,916**	3,111
Feeder	R3								
Bus bar	10	0,988	-16,664	0,986	-14,739	0,970	-7,208	0,930	2,117
Bus bar	21	0,978	-17,348	0,976	-15,271	0,961	-7,116	**0,922**	3,094
Bus bar	22	0,979	-17,386	0,978	-15,292	0,963	-7,069	**0,924**	3,241

Table 3.18 Voltages in the Roanoke Medium Voltage grid depending on the DG production, feeder head is shaded in grey, limit violations bold

Table 3.19 shows the bus bar voltages in Cloverdale. Similar to the effect at the Hancock and the Roanoke substation in this Test Scenario, again the voltage decreases with rising DG production.

		no DG production		P_{DG}=0,1 pu, $cos(\varphi)$=0,95 lag		P_{DG}=0,5 pu, $cos(\varphi)$=0,95 lag		P_{DG}= 1 pu, $cos(\varphi)$=0,95 lag	
		Voltage [p.u.]	Angle [°]	Voltage [p.u.]	Angle [°]	Voltage [p.u.]	Angle [°]	Voltage [p.u.]	Angle [°]
Feeder	C1								
Bus bar	27	1,016	-15,693	1,013	-13,317	0,988	-4,006	**0,919**	7,856
Bus bar	29	1,030	-16,802	1,028	-14,162	1,005	-3,736	0,938	9,891
Feeder	C2								
Bus bar	27	1,016	-15,693	1,013	-13,317	0,988	-4,006	**0,919**	7,856
Bus bar	30	0,982	-19,437	0,983	-16,256	0,968	-3,658	**0,904**	13,210
Feeder	C3								
Bus bar	27	1,016	-15,693	1,013	-13,317	0,988	-4,006	**0,919**	7,856
Bus bar	25	1,017	-16,221	1,014	-13,575	0,992	-3,122	**0,924**	10,563
Bus bar	26	1,005	-16,884	1,005	-13,979	0,987	-2,448	**0,924**	12,925

Table 3.19 Voltages in the Cloverdale Medium Voltage grid depending on the DG production, feeder head shaded in grey, limit violations bold

Figure 3.32 shows that at full DG production there are voltage limit violations at the lower limit in all three feeders. While the voltage decreases with increasing feeder length for feeder C2 and C3 the voltage increases slightly with increasing feeder length in feeder C1.
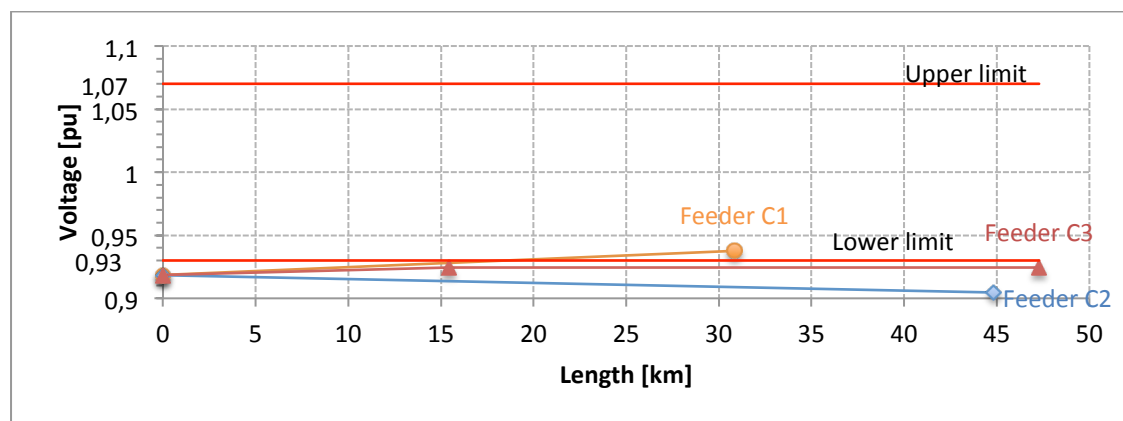
Figure 3.32 Voltage profile of all feeders supplied from the Cloverdale substation at the DG production level P_{DG}=1 p.u. at $cos(\varphi)$=0,95 lagging

3.1.3.7.2 Impact on the High Voltage grid

The chart describing the active and reactive power flow over the Hancock substation is very similar to Test Scenario 2 and can be found in the Appendix in Figure 6.3.

Table 3.20 shows the HV grid voltages. There are no voltage limit violations. As shown in Figure 3.33 the there is a minimal voltage rise of 0,01% (0,09% voltage decrease in Test Scenario 2) at the HV bus bar in Hancock between P_{DG}=0 p.u. and P_{DG}=1 p.u. The HV bus bar in Claytor experiences a voltage decrease of 0,56% (0,01% in Test Scenario 2) between P_{DG}=0 p.u. and P_{DG}=1 p.u.
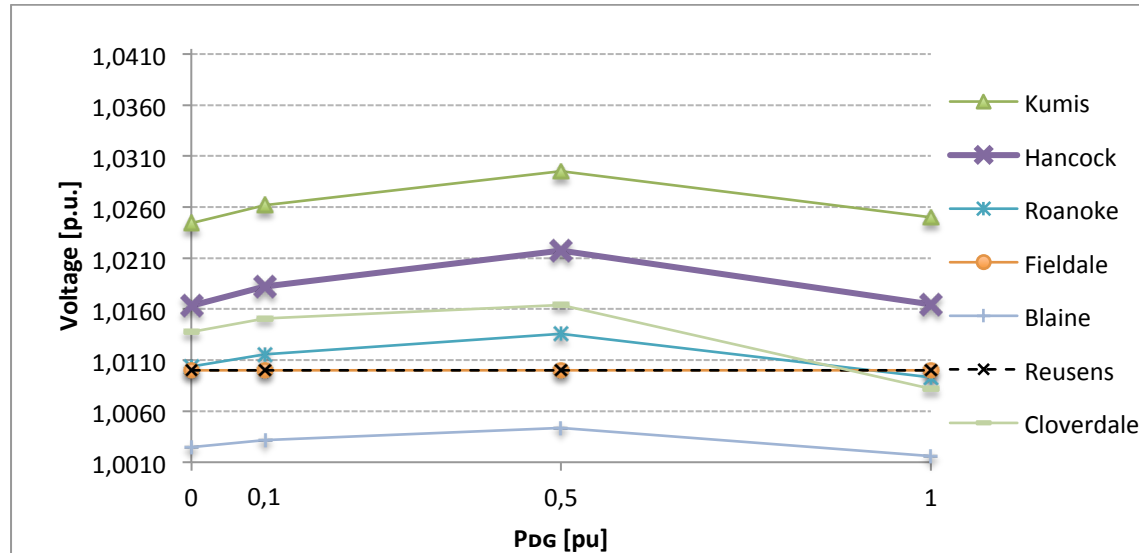
Figure 3.33 HV grid (U_n=132 kV) voltages depending on DG production in all three MV grids

	no DG production		P_{DG}=0,1 pu, $cos(\varphi)$= 0,95 lag		P_{DG}=0,5 pu, $cos(\varphi)$= 0,95 lag		P_{DG}=1 pu, $cos(\varphi)$= 0,95 lag	
	Voltage [p.u.]	Angle [°]	Voltage [p.u.]	Angle [°]	Voltage [p.u.]	Angle [°]	Voltage [p.u.]	Angle [°]
Glen Lyn	1,060	0,000	1,060	0,000	1,060	0,000	1,060	0,000
Claytor	1,045	-5,389	1,045	-4,935	1,045	-3,206	1,045	-1,232
Kumis	1,024	-7,572	1,026	-6,843	1,030	-4,003	1,025	-0,587
Hancock	1,016	-9,329	1,018	-8,421	1,022	-4,888	1,016	-0,638
Roanoke	1,010	-11,098	1,012	-10,054	1,014	-6,016	1,009	-1,209
Fieldale	1,010	-14,178	1,010	-13,426	1,010	-10,570	1,010	-7,314
Blaine	1,002	-12,890	1,003	-11,965	1,004	-8,408	1,002	-4,238
Reusens	1,010	-11,836	1,010	-10,746	1,010	-6,573	1,010	-1,722
Cloverdale	1,014	-11,799	1,015	-10,605	1,016	-5,971	1,008	-0,398

Table 3.20 HV grid (U_n=132 kV) voltages depending on DG production in all three MV grids

Table 3.21 shows the difference between Test Scenario 2 and Test Scenario 4. As already mentioned in Test Scenario 3, the Generators and Synchronous Condensers in Glen Lyn, Claytor, Fieldale and Reusens are keeping the bus bar voltage to a pre-defined value so the voltage difference is always 0%.

	no DG production		P_{DG}=0,1 pu, cos(φ)= 0,95 lag		P_{DG}=0,5 pu, cos(φ)= 0,95 lag		P_{DG}=1 pu, cos(φ)= 0,95 lag	
	ΔVoltage	ΔAngle [°]	ΔVoltage	ΔAngle [°]	ΔVoltage	ΔAngle [°]	ΔVoltage	ΔAngle [°]
Glen Lyn	0,00%	0,00	0,00%	0,00	0,00%	0,00	0,00%	0,00
Claytor	0,00%	0,00	0,00%	0,30	0,00%	1,45	0,00%	2,75
Kumis	0,00%	0,00	0,09%	0,44	0,26%	2,16	0,07%	4,21
Hancock	0,00%	0,00	0,09%	0,55	0,29%	2,69	0,11%	5,24
Roanoke	0,00%	0,00	0,08%	0,73	0,21%	3,57	-0,09%	6,96
Fieldale	0,00%	0,00	0,00%	0,52	0,00%	2,49	0,00%	4,74
Blaine	0,00%	0,00	0,05%	0,65	0,12%	3,13	-0,08%	6,05
Reusens	0,00%	0,00	0,00%	0,77	0,00%	3,73	0,00%	7,19
Cloverdale	0,00%	0,00	0,10%	0,88	0,17%	4,31	-0,54%	8,48

Table 3.21 Difference of the grid Voltages between Test Scenario 1 (DG production in Hancock only) and Test Scenario 3 (DG production in all three MV grids), areas with DG production are shaded in grey

The impact on the HV grid bus bar voltages of the changed power factor of the DG between Test Scenario 3 (*cos(φ)=1*) and Test Scenario 4 (*cos(φ)=0,95* lag) can be observed if Figure 3.26 and Figure 3.33 are compared. With more DG production the HV grid bus bar voltages always raises in the case of Test Scenario 3 and in the case of Test Scenario 4 there is a voltage rise between no DG production and half DG production and a voltage decline at full DG production. An explanation for this can be found if the power flow over the three substations where the DG production occurs are compared. This data can be found in Table 3.22. While there are only minor differences in the active power flow (which can be attributed to different cable losses at different voltage levels) between Test Scenario 3 and 4 there are, as expected, big differences in the reactive power flow. In Test Scenario 4 the at full DG production the reactive power flow from the HV grid to the MV grid has the effect that the voltage declines.

Power flow over MV/HV Substation		no DG production	P_{DG}=0,1 pu,	P_{DG}=0,5 pu,	P_{DG}= 1 pu,
Hancock	**P T3** [MW]	-41,44	-34,25	-6,25	27,40
	P T4 [MW]	-41,44	-34,28	-6,39	26,53
	Q T3 [Mvar]	-0,46	2,15	7,48	4,97
	Q T4 [Mvar]	-0,46	-0,78	-7,20	-28,02
Roanoke	**P T3** [MW]	-47,87	-40,25	-10,04	27,22
	P T4 [MW]	-47,87	-40,26	-10,11	26,93
	Q T3 [Mvar]	-13,57	-11,64	-7,35	-8,88
	Q T4 [Mvar]	-13,57	-14,59	-22,16	-40,34
Cloverdale	**P T3** [MW]	-16,99	-11,82	8,37	32,71
	P T4 [MW]	-16,99	-11,82	8,36	32,28
	Q T3 [Mvar]	9,65	10,80	12,14	7,40
	Q T4 [Mvar]	9,65	8,93	2,57	-14,79

Table 3.22 Comparison of the power flow over the three substations in Test Scenario 3 (T3) and Test Scenario 4 (T4), positive power flow from MV grid to HV grid

3.1.3.8 Distributed generation in Hancock, Q(U) controller active

A *Q(U)* controller was activated for every DG. The *Q(U)* characteristic of the DG is shown in Figure 3.34 and has been taken from [**24**].
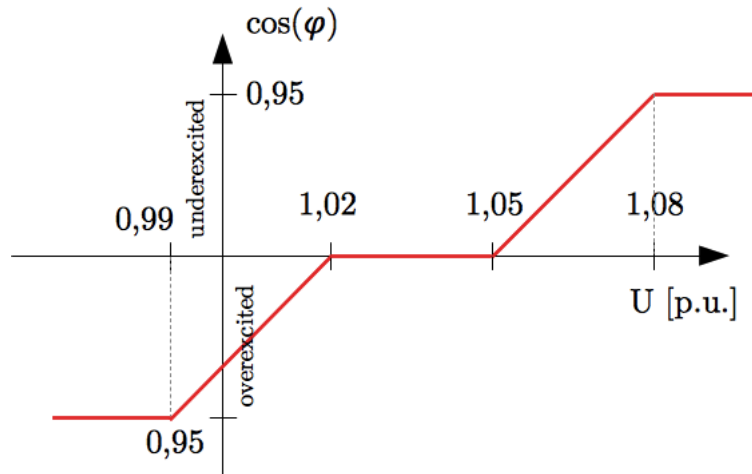
Figure 3.34 **Q(U) characteristic**

To get convergent results in this Test Scenario 5 and 6 the load flow calculation parameters in PSS Sincal were changed. Constant active and reactive loads are converted to ideal impedance behavior with a *P* and *Q* depending on the voltage.

In order to test the dependence on the voltage of this controller the four different DG production levels (0 p.u., 0,1 p.u., 0,5 p.u., 1 p.u.) were tested at 5 different transformer step positions (TSP) 10, 5, 0, -5 and -10 which results in 15 test cases for Test Scenario 5 (DG in Hancock only), 15 test cases for Test Scenario 6 (DG in Hancock, Roanoke and Cloverdale) and five test cases (P_{DG}=0 p.u.) which apply to Test Scenario 5 and 6.

Transformer taps happen on the HV side to keep the current and therefore the lightning arc small. Table 3.23 shows the impact of a transformer tap change to the voltage on the MV side.

Transformer step on the HV side	Voltage change on the MV side
+10	-10%
+5	-5%
0	0%
-5	+5%
-10	+10%

Table 3.23 Transformer step positions and their impact on the voltage

Because of the changed load modeling the change of the TSP has an effect on the active power flow over the substation, which is described and analyzed in the next sub chapter 3.1.3.8.1. After this the impact on the MV grid is discussed in sub chapter

3.1.3.8.2 and in the last sub chapter 3.1.3.8.3 there is a look on the impact on the HV grid.

3.1.3.8.1 Impact on the active power flow

With the loads modeled as ideal impedances the reactive and active power consumption are functions of the voltage to the power of two. In previous test scenarios the loads were modeled as constant P and Q consumers. The new method has the effect that the active power flow across the Transformer is changing with the change of the transformer step position. An illustration of this effect is lustrated in the charts Figure 6.6, Figure 6.8, Figure 6.10, Figure 6.12 and Figure 6.14. Table 3.24 shows the **change in active power flow** across the Hancock transformer between the TSPs. Table 3.25 shows **change in active power consumption** of the loads in Hancock between the TSPs. Table 3.26 is a comparison of the two tables and shows the difference in percent.

	no DG production	P_{DG}=0,1 pu	P_{DG}=0,5 pu	P_{DG}=1 pu
ΔP_{Tr}=P(Tsp:10)-P(Tsp:5) [MW]	3,31	3,33	1,71	0,94
ΔP_{Tr}=P(Tsp:5)-P(Tsp:0) [MW]	3,80	3,40	2,25	2,46
ΔP_{Tr}=P(Tsp:0-P(Tsp:-5) [MW]	4,39	3,83	2,45	1,22
ΔP_{Tr}=P(Tsp:-5)-P(Tsp:-10) [MW]	5,03	4,69	3,66	2,37

Table 3.24 Change in active power flow over the Transformer in Hancock between different TSPs

	no DG production	P_{DG}=0,1 pu	P_{DG}=0,5 pu	P_{DG}=1 pu
ΔP_{load}=P(Tsp:10)-P(Tsp:5) [MW]	3,25	3,28	1,77	1,04
ΔP_{load}=P(Tsp:5)-P(Tps:0) [MW]	3,74	3,35	2,26	2,59
ΔP_{load}=P(Tsp:0-P(Tsp:-5) [MW]	4,32	3,77	2,44	1,18
ΔP_{load}=P(Tsp:-5)-P(Tsp:-10) [MW]	4,95	4,61	3,58	2,28

Table 3.25 Change in active power consumption of all the loads in between different TSPs

	no DG production	P_{DG}=0,1 pu	P_{DG}=0,5 pu	P_{DG}=1 pu
ΔP_{load}=P(Tsp:10)-P(Tsp:5) [%]	1,65%	1,54%	-3,50%	-9,93%
ΔP_{load}=P(Tsp:5)-P(Tps:0) [%]	1,65%	1,37%	-0,53%	-5,15%
ΔP_{load}=P(Tsp:0-P(Tsp:-5) [%]	1,65%	1,58%	0,28%	3,40%
ΔP_{load}=P(Tsp:-5)-P(Tsp:-10) [%]	1,65%	1,72%	2,29%	4,26%

Table 3.26 Change in active power consumption of all the loads (Table 3.25) as a percentage of the change in reactive power flow (Table 3.24) in between different TSPs

With no DG production the difference is constant which can be attributed to cable losses. When DG supply is activated and especially at P_{DG}=1 p.u. in the MV grid an interesting effect can be observed. The change in active power flow at the Hancock transformer is smaller than the change of the active power consumption of the loads between the TSP 10 and 5, and 5 and 0. It is the other way around between the TSP

0 and -5, and -5 and -10. This behavior can again be explained with the cable losses, which are a function of the voltage to the power of 2. The voltage decrease at no DG production along the Hancock feeders stays nearly the same and only changes in a linear behaviour while at a DG supply of $P_{DG}=1$ p.u. it changes from a voltage rise at a TSP of 10 to a voltage decrease at a TSP of -10 (see Table 3.27).

	no DG production					$P_{DG}=1$ pu				
	TSP: 10	TSP: 5	TSP: 0	TSP: -5	TSP: -10	TSP: 10	TSP: 5	TSP: 0	TSP: -5	TSP: -10
Voltage Drop along Feeder H1 [%]	0,33	0,35	0,36	0,38	0,4	-2,91	-2,19	-1,72	-0,77	-0,23
Voltage Drop along Feeder H2A [%]	4,63	4,85	5,08	5,34	5,63	-4,33	-2,71	-1,79	0,17	2,37
Voltage Drop along Feeder H2B [%]	1,43	1,5	1,57	1,65	1,74	-3,88	-2,8	-2,06	0,89	0,22

Table 3.27 Voltage decrease along the feeders in Hancock depending on the TSP

3.1.3.8.2 Impact on the Medium Voltage grid

The positive effect of the *Q(U)* control can be seen in the voltage profiles of Hancock in Figure 3.35 - Figure 3.39 where the DG is set to half production. In the case of low bus bar voltages the *Q(U)* controller sets the DG to produce reactive power which has a voltage boost effect on the bus bars along the feeders. In the case of high bus bar voltages the *Q(U)* controller sets the DG to consume reactive power which has a voltage decreasing effect on the bus bars along the feeders. In the case of the TSP: -5 (Figure 3.38) some and in the case of the TSP: -10 (Figure 3.39) all bus bar voltages are not within the voltage limits.
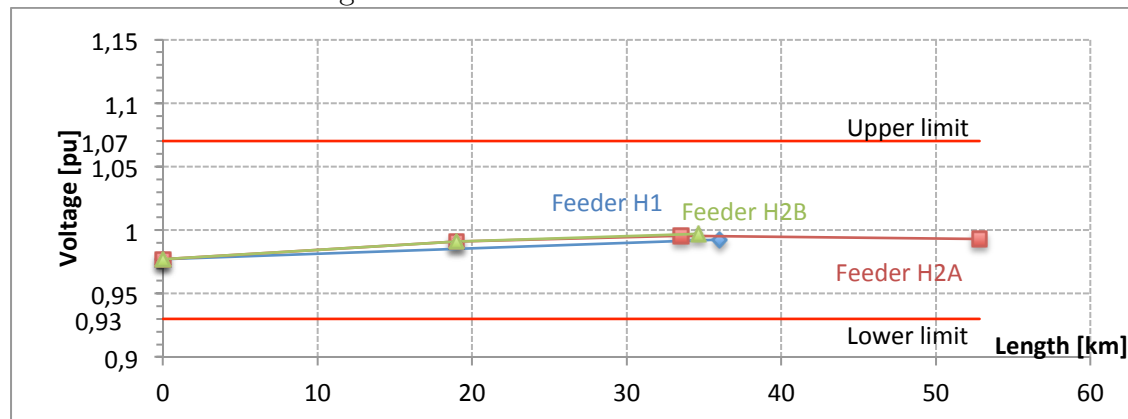
Figure 3.35 Voltage profile of all feeders supplied from the Hancock substation (U_n=33kV) at the DG production level of P_{DG}=0,5 p.u at the transformer step position TSP:10

Figure 3.35 shows the Hancock voltage profile at a TSP of 10 where all bus voltages are lower than 1 p.u. the local *Q(U)* controllers set the DG to inject reactive power at a power factor of 0,95 to 0,96 leading. The feeder head voltage is $U_{Hancock}^{MV} = 0,977\,p.u.$. With increasing feeder length the voltage is rising for feeder H1 and H2B. Feeder H2A shows the same behavior until bus bar 23. The voltage at bus bar 24 is 0,4% lower.

Figure 3.36 shows the voltage profile at a TSP of 5, the *Q(U)* controllers set the DG to a power factor of 0,98 leading to 1. The feeder behavior is the same as at a TSP of 10. The feeder head voltage is $U_{Hancock}^{MV} = 1,005\,p.u.$.
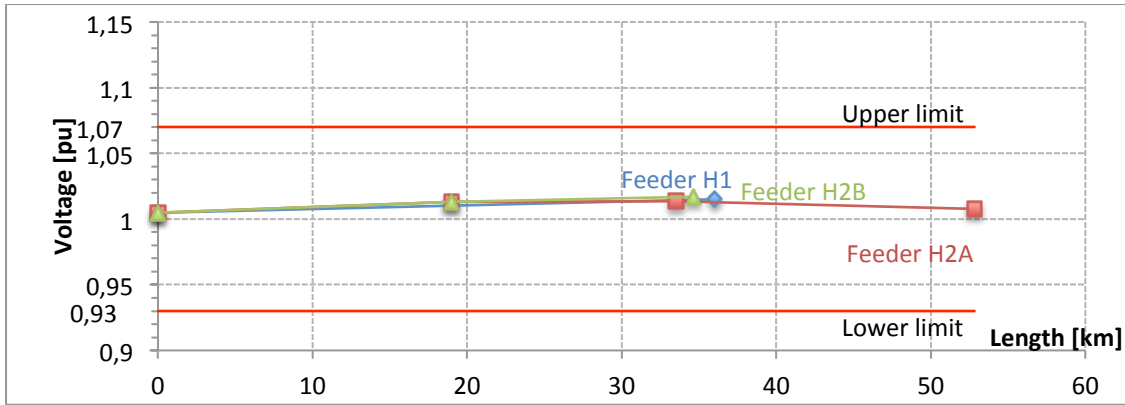
Figure 3.36 Voltage profile of all feeders supplied from the Hancock substation (U_n=33kV) at the DG production level of P_{DG}=0,5 p.u at the transformer step position TSP:5

Figure 3.37 shows the voltage profile at a TSP of 0, the *Q(U)* controllers set the DG to a power factor of 1. The voltage along the feeders H1 and H2B stay nearly constant with increasing feeder length. The voltage along feeder H2B is staying nearly constant until bus bar 15 and is decreasing after this. The feeder head voltage is $U^{MV}_{Hancock} = 1,038\,p\,u..$
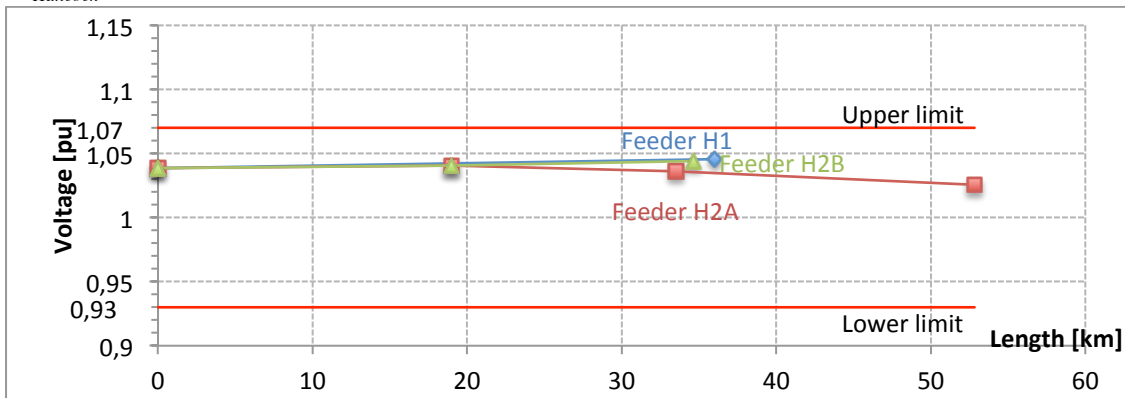
Figure 3.37 Voltage profile of all feeders supplied from the Hancock substation (U_n=33kV) at the DG production level of P_{DG}=0,5 p.u at the transformer step position TSP:0

Figure 3.38 shows the voltage profile at a TSP of -10, the *Q(U)* controllers set the DG to a power factor of 0,96 lagging to 1. Feeder H1 keeps has a constant voltage with increasing feeder length while the voltage of the feeders H2A and H2B is decreasing. The feeder head voltage is $U^{MV}_{Hancock} = 1,073\,p\,u..$
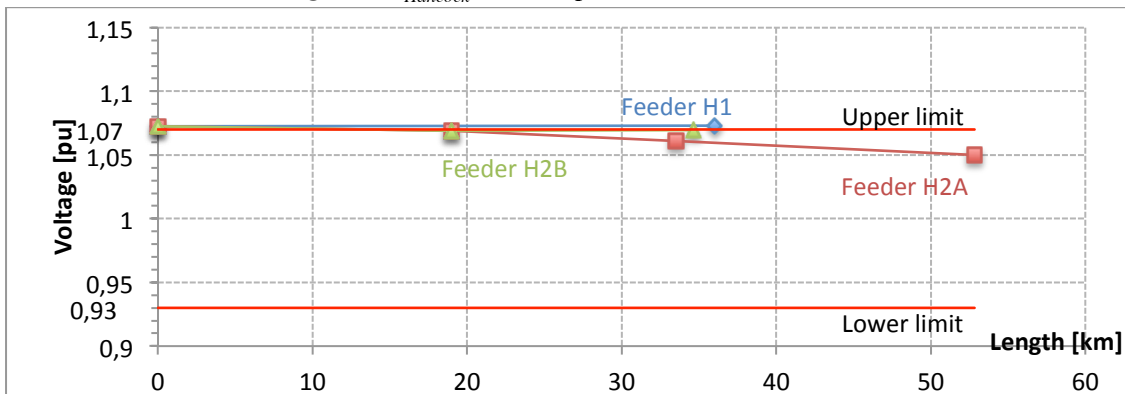
Figure 3.38 Voltage profile of all feeders supplied from the Hancock substation (U_n=33kV) at the DG production level of P_{DG}=0,5 p.u at the transformer step position TSP:-5

Figure 3.39 shows the voltage profile at a TSP of -10, the *Q(U)* controllers set the DG to a power factor of 0,95 lagging. The feeder behavior is the same as at a TSP of -5. The feeder head voltage is $U_{Hancock}^{MV} = 1,119\,p.u..$
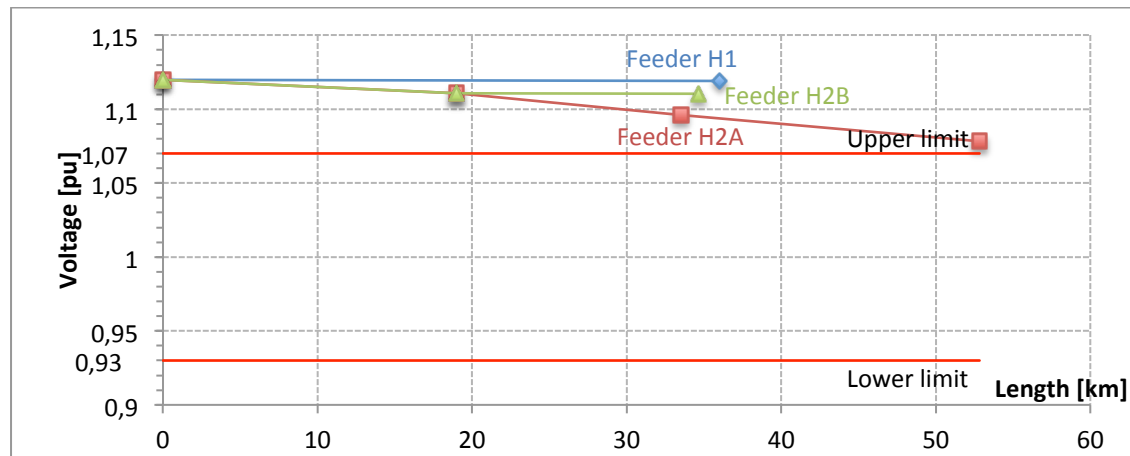
Figure 3.39 Voltage profile of all feeders supplied from the Hancock substation (U_n=33kV) at the DG production level of P_{DG}=0,5 p.u at the transformer step position TSP:-10

Table 3.28 shows the exact amount of reactive power production in dependence of the TSP and the active power production. The values reflect the *Q(U)* characteristic illustrated in Figure 3.34.

		P_{DG}=0,1 pu			P_{DG}=0,5 pu			P_{DG}=1 pu		
		U	$cos(\varphi)$	Q	U	$cos(\varphi)$	Q	U	$cos(\varphi)$	Q
		[p.u.]	[1]	[Mvar]	[p.u.]	[1]	[Mvar]	[p.u.]	[1]	[Mvar]
DG 18 (9 MW)	TSP:10	0,937	0,95	0,291	0,997	0,96	1,292	1,014	0,99	1,295
	TSP:5	0,979	0,95	0,296	1,017	1,00	0,437	1,024	1,00	0,003
	TSP:0	1,020	1,00	0,034	1,044	-1,00	-0,001	1,052	-1,00	-0,806
	TSP:-5	1,064	-0,98	-0,197	1,069	-0,97	-1,171	1,064	-0,98	-1,982
	TSP:-10	1,116	-0,95	-0,296	1,110	-0,95	-1,479	1,089	-0,95	-2,958
DG 14 (18 MW)	TSP:10	0,944	0,95	0,581	0,992	0,95	2,873	1,004	0,97	4,217
	TSP:5	0,987	0,95	0,586	1,015	0,99	1,153	1,018	1,00	1,552
	TSP:0	1,028	-1,00	-0,002	1,045	-1,00	-0,002	1,049	-1,00	-0,002
	TSP:-5	1,074	-0,96	-0,527	1,073	-0,96	-2,566	1,063	-0,98	-3,789
	TSP:-10	1,128	-0,95	-0,592	1,119	-0,95	-2,958	1,093	-0,95	-5,916
DG 15 (15 MW)	TSP:10	0,936	0,95	0,484	0,991	0,95	2,435	1,003	0,97	3,650
	TSP:5	0,979	0,95	0,493	1,013	0,99	1,157	1,016	0,99	1,757
	TSP:0	1,020	1,00	0,009	1,041	-1,00	-0,002	1,046	-1,00	-0,003
	TSP:-5	1,065	-0,98	-0,341	1,069	-0,97	-1,920	1,061	-0,98	-2,856
	TSP:-10	1,117	-0,95	-0,493	1,111	-0,95	-2,465	1,087	-0,95	-4,930
DG 23 (12 MW)	TSP:10	0,925	0,95	0,387	0,996	0,96	1,783	1,016	0,99	1,389
	TSP:5	0,966	0,95	0,394	1,014	0,99	0,885	1,024	1,00	0,003
	TSP:0	1,007	0,98	0,259	1,036	-1,00	-0,002	1,052	-1,00	-0,853
	TSP:-5	1,049	-1,00	-0,002	1,061	-0,98	-1,164	1,060	-0,98	-2,181
	TSP:-10	1,099	-0,95	-0,394	1,096	-0,95	-1,972	1,079	-0,95	-3,867
DG 24 (15 MW)	TSP:10	0,911	0,95	0,484	0,993	0,95	2,377	1,018	1,00	1,094
	TSP:5	0,951	0,95	0,484	1,008	0,98	1,532	1,023	1,00	0,003
	TSP:0	0,991	0,95	0,491	1,026	1,00	0,003	1,050	-1,00	-0,003
	TSP:-5	1,031	-1,00	-0,002	1,050	-1,00	-0,022	1,054	-0,99	-1,652
	TSP:-10	1,079	-0,95	-0,483	1,078	-0,95	-2,383	1,067	-0,97	-3,667

Table 3.28 Bus bar voltage (U_n=33kV), power factor and reactive power production in the Hancock MV grid, positive power factor values stand for leading operation, negative power factor values stand for lagging operation

3.1.3.8.3 Impact on the High Voltage grid

Note: Because of the sheer amount of charts and tables for this Test Scenario all the charts for this chapter have been moved to the chapter Appendix: Charts and Tables starting at page 97.

Reactive power production from the cables and from the DG is dependent on the voltage. At a TSP of 10 the DG in the MV grid in Hancock produces reactive power to elevate the voltage at every DG production level. Because of lower bus bar voltages at P_{DG}=0,5 p.u. compared to P_{DG}=1 p.u. the summed up DG reactive power production is nearly the same (10,759 Mvar at P_{DG}=0,5 p.u. and 11,645 Mvar at P_{DG}=1 p.u.). Slightly more reactive power gets produced by the cables at P_{DG}=0,5 p.u. than at P_{DG}=1 p.u. and combined with the less reactive power losses at P_{DG}=0,5 p.u. explains the higher reactive power flow into the HV grid at this DG production level (see Figure 6.6).

The described effect that there are higher reactive power losses in the Transformer at P_{DG}=1 p.u. than at P_{DG}=0,5 p.u. due to a higher load of the transformer is the same for all TSPs in this test scenario.

With decreasing TSP to 5, 0, -5 and -10 the bus bar voltages in the MV grid increase and therefore the *Q(U)* controller starts to have an inductive behavior (energy production is counted positive) and consumes reactive power. As illustrated in Figure 6.8, Figure 6.10, Figure 6.12 and Figure 6.14 the reactive power flow over the Hancock Transformer changes from reactive power flow into the HV grid at a TSP 5 and 0 to reactive power flow into the MV grid at a TSP of -5 and -10.

The effect on the HV grid (see Figure 6.7, Figure 6.9, Figure 6.11, Figure 6.13 and Figure 6.15) is similar to the test scenarios before. Bus bar voltages in Fieldale and Reusens are not affected by the active and reactive power change due to the synchronous condensers that are keeping a desired voltage. A higher reactive power flow from the MV grid to the HV grid results in higher bus bar voltages in the HV grid. Because of the changing active power flow, as discussed earlier in this test scenario, it is not possible to keep apart the effect of the active and the reactive power on the HV grid voltages.

3.1.3.9 Distributed generation in Hancock, Roanoke and Cloverdale, Q(U) controller active

In this test scenario the loads were modeled as ideal impedances and the same *Q(U)* controller was used for all DGs as in Test Scenario 5 (see Figure 3.34).

3.1.3.9.1 Impact on the active power flow

Due to the change of how the loads are modeled the active and reactive power consumption is a function of the voltage to the power of two. An analysis of this effect can be found in 3.1.3.8.1 Impact on the active power flow on page 56.

3.1.3.9.2 Impact on the Medium Voltage grid

The *Q(U)* controller of the DG helps to keep the voltage within the limits. At low bus bar voltages the DG produces reactive power to increase the voltage and at high bus bar voltages the DG consumes reactive power to decrease the voltage. This effect has been described in detail in Test Scenario 5 and can be found in chapter 3.1.3.8.2 Impact on the Medium Voltage grid on page 57.

3.1.3.9.3 Impact on the High Voltage grid

The impact on the High Voltage grid at a TSP of 10 is illustrated in Figure 6.19. The power flow over the Hancock Transformer is shown in Figure 6.16, over the Roanoke Transformer in Figure 6.17 and over the Cloverdale Transformer in Figure 6.18. Due to the low bus bar voltages at a TSP of 10 the *Q(U)* of the DG controller is set to supply reactive power to the grid which results in a reactive power flow into the HV grid from all three test regions. This adds up to a reactive power flow of 29,97 Mvar from the MV grid into the HV grid at a DG production level of P_{DG}=1 p.u.. At this production level the Synchronous Condenser in Reusens can't keep the desired bus bar voltage because it reached its the reactive power consumption limit of 10 Mvar.

With a decreasing TSP the reactive power flow changes its direction from MV grid supplies the HV grid to HV grid supplies the MV grid. This has the effect of lower HV grid bus bar voltages with a decreasing TSP (see Figure 6.23, Figure 6.27, Figure 6.31 and Figure 6.35). But comparing the HV grid bus bar voltages from Test Scenario 5 and Test Scenario 6 the HV bus bar voltages in Test Scenario 5 are always lower than in Test Scenario 6. The reactive power flow changes from being larger at a TSP of 10 and 5 in Test Scenario 6 than in Test Scenario 5, to being smaller at a TSP of 0, -5 and -10 (see Table 3.29). This shows the impact of the active power on the HV bus bar voltage increase. Otherwise the HV bus bar voltages would have been lower at in Test Scenario 6 for the TSPs 0, -5 and -10 than in Test Scenario 5.

Transformer step position	Test Scenario 5 *Q* [Mvar]	Test Scenario 6 *Q* [Mvar]
10	12,41	29,97
5	5,21	15,92
0	1,42	-3,68
-5	-9,12	-27,7
-10	-17,88	-53,52

Table 3.29 Cumulated reactive power flow from the HV grid to the MV grid at a DG production level of P_{DG}=1 p.u. in dependence of the TSP

3.1.4 Result summary for the IEEE 30 Bus Test Network

As described in Test Scenario 1, distributed generation supplying only active power located in the MV grid increases the bus bar voltages in the MV grid as well as in the HV grid. DG supplying active power and consuming reactive power without a controller, as simulated in Test Scenario 2, has the effect that the voltage boost in the MV grid and in the HV grid, originating from the active power supply, gets reduced. These effects from Test Scenario 1 and 2 get amplified when DG is installed not only in the MV test region Hancock, but also in the other two regions Roanoke and Cloverdale, as described in Test Scenario 3 and 4. The *Q(U)* controller that is used in Test Scenario 5 and 6 helps to intelligently keep the voltage within its limits depending on the voltage situation in the MV grid. But this also has an impact on the HV grid. With low MV grid bus bar voltages the *Q(U)* controller sets the DG to supply reactive power to the MV grid to boost the voltage. The reactive power flow from the MV grid to the HV grid has the effect of a voltage boost additionally to the voltage boost caused by the active power flow. This effect gets amplified with DG in all three test-regions, as tested in Test Scenario 6. However with high bus bar voltages in the MV grid the *Q(U)* controller sets the DG to consume reactive power. Because of the active power supply to the HV grid there is still a voltage increase compared to no DG production but with the reactive power consumption in the MV grid this effect is reduced.

3.2 Simulations in a real network

It is not allowed to publish this chapter due to privacy and security policies. Therefore page 63 to 84 is not available in this version.

4 Conclusion and Future Work

4.1 Conclusion

All effects described in this conclusion can be found in the IEEE Test network and in the real European distribution network, the only difference being that the effects were more pronounced in the real grid.

The supply of the MV grid with energy from DGs that are producing at a power factor of 1 boosts the voltage in the MV as well as in the HV grid, which can lead to voltage limit violations.

Local consumption of reactive power by the DGs is used to suppress the voltage limit violations in MV grid. In the case of lagging operation of the DGs, the reactive power flow from the MV grid into the HV grid is reduced. This has the effect of a reduction of the voltage boost in the MV grid as well as in the HV grid.

In the case of leading operation of the DGs, the reactive power flow from the MV grid into the HV grid gets increased. This leads to an increase of the voltage boost in the MV grid and equally in the HV grid.

The change of the transformer step position leads to a change in reactive power production by the cables. As a consequence there is a change in the reactive power flow over the HV/MV substation and this leads to the above-described effects in the HV grid (on a smaller scale).

In both simulated networks the reactive power flow changes have a higher impact on the HV grid voltages than active power flow changes of the same size.

The local reactive power control of the DGs does not only affect the voltage on the directly connected superordinate grid, but also of the other superior grids.

The impact of the DG integration on voltages in high- and medium voltage grids rises with the increase of the DG share.

4.2 Future Work

While this Thesis has shown the influence of a high share of DGs and the resulting interdependencies between the high- and medium voltage level, there are some opportunities to extend this work:

- The simulations in the real network are restricted to the case of only one subsystem with DG integration. To create the complete picture, the impact of a large-scale integration of DG in all existing MV-subsystems should be analyzed.
- Normally various kinds of DGs are connected to one subsystem, which have different PQ characteristics depending on the primary energy resource used. Therefore, it is important to investigate the impact of the ratio between the conventional DGs to the ones connected through an inverter on the voltage/reactive power behavior.

5 References

[1] European Commission. (2015, September) Europe 2020 targets. [Online]. http://ec.europa.eu/europe2020/europe-2020-in-a-nutshell/targets/index_en.htm

[2] The White House. (2015, August) Fact Sheet: President Obama to Announce Historic Carbon Pollution Standards for Power Plants. [Online]. https://www.whitehouse.gov/the-press-office/2015/08/03/fact-sheet-president-obama-announce-historic-carbon-pollution-standards

[3] Roger Harrabin. (2015, June) China 'deserves more credit' for renewable energy effort. [Online]. http://www.bbc.com/news/business-33143176

[4] Per Lund, "The Danish Cell Project - Part 1: Background and General Approach," pp. 1-6, 2007.

[5] Albana Ilo, Wolfgang Gawlik, Walter Schaffer, and Roland Eichler, "Uncontrolled reactive power flow due to local control of distributed generators," in *23rd International Conference on Electricity Distribution*, Lyon, 2015, pp. 1-5.

[6] Ebrahim Vaahedi, *Practical Power System Operation*, IEEE Press, Ed. New Jersey, United States: Wiley, 2014.

[7] CENELEC, EN 50160, 2011-02.

[8] Albana Ilo, Walter Schaffer, Rieder Thomas, and Izudin Dzafic, "Dynamische Optimierung der Verteilnetze – Closed loop Betriebergebnisse," in *VDE-Kongress 2012 - Intelligente Energieversorgung der Zukunft*, Stuttgart, 2012, pp. 184-189.

[9] E-Control. (2013, September) Technische und organisatorische Regeln für Betreiber und Benutzer von Netzen. [Online]. http://www.e-control.at/portal/page/portal/medienbibliothek/recht/dokumente/pdfs/TOR_D4_V2_2_040913-neu.pdf

[10] Christoph Winter, Martin Heidl, Benoit Bletterie, Serdar Kadam, and Andreas Abart, "morePV2grid: Spannungsregelung von PV- Wechselrichtern – Ergebnisse aus einem Feldtest," in *13. Symposium Energieinnovation*, Graz, 2014.

[11] Manfred Schrödl, *Unterlagen zur Vorlesung Elektrische Antriebe*, ESEA, Ed. Wien, 2013.

[12] Kerber Tobias, Kerber Georg, Werner Manfred, Finkel Michael, and Wiest Michael, "Optimierung der spannungsabhängigen Blindleistungsregelung Q(U) an dezentralen Erzeugungsanlagen zur Minimierung des Netzausbaus im 20 kV-Netz der LEW Verteilnetz GmbH," *9. Internationale Energiewirtschaftstagung an der TU Wien*, p. 3, 2015.

[13] Roland Bründlinger, "Advanced Inverter Functions," in *International workshop on PV and the electricity grid*, Sydney, 2013.

[14] Robert H. Miller and James H. Malinowski, *Power System Operation*, Third Edition ed. United States: Mc Graw Hill.

[15] Abraham Ellis et al. (2012, February) Reactive Power Interconnection Requirements for PV and Wind Plants – Recommendations to NERC. [Online]. http://renew-ne.org/wp-content/uploads/2012/05/Reactive-Power-Interconnection-Requirements.pdf

[16] Dan Zlatanovici, Pompiliu Budulan, and Rodica Zlatanovici, "DETERMINATION OF THE ACTUAL PQ DIAGRAM OF THE HYDROGENERATORS, BEING IN SERVICE, IN ORDER TO ESTABLISH THEIR MAXIMUM OPERATING DOMAINS AND THEIR CAPACITY TO PROVIDE SYSTEM SERVICES," in *Cigre Session 2004*, Icemenerg, 2004, p. 3.

[17] Andreas Binder, *Elektrische Maschinen und Antriebe.* Darmstadt, Deutschland: Springer , 2012.

[18] I. Niazy, H. Mortazavi, J. Ebadi, and S. Sabzevari, "Considering Synchronous Generator Capability Curve Variations for Reactive Power Market," , p. 2.

[19] University of Washington. (1993) Power Systems Test Case Archive. [Online]. http://www.ee.washington.edu/research/pstca/pf30/pg_tca30bus.htm

[20] O. Alsac and B. Stott, "Optimal Load Flow with steady-state Security," *IEEE Transactions on Power Apparatus and Systems*, vol. PAS-93, no. 3, p. 750, January 2007.

[21] Electric Engineering Portal. (2012, August) The Structure Of Power System. [Online]. http://electrical-engineering-portal.com/the-structure-of-power-system

[22] Pierre Cugnet, "Confidence Interval Estimation for Distribution Systems Power Consumption by using the Bootstrap Method," Virginia Polytechnic Institute and State University, Virginia, 1997.

[23] Ducab. Ducab Powerplus Medium Voltage Cables For Oil, Gas, and Petrochemical Industries. [Online]. http://www.ducab.com/cms_uploads/fck_files/file/Powerplus_Medium_Voltage_Cables_OGP.pdf

[24] Christian Elbs, Netzeinsparungsmöglichkeiten und Erfahrungen einer realen Q(U) - Einführung bei PV Wechselrichtern im Bundesland Vorarlberg, May 23, 2014.

[25] Working Group on a Common Format for the Exchange of Solved Load Flow Data, "Common Data Format for the Exchange of Solved Load Flow Data," *IEEE Transactions on Power Apparatus and Systems*, vol. 6, no. PAS-92, pp. 1916-1925, November/December 1973.

[26] University of Washington - Electrical Engineering. Partial Description of the IEEE Common Data Format for the Exchange of Solved Load Flow Data. [Online]. http://www.ee.washington.edu/research/pstca/formats/cdf.txt

[27] Liviu Constantinescu-Simon, *Handbuch Elektrische Energietechnik: Grundlagen · Anwendungen*. Wiesbaden: Springer, 1996.

[28] William Surles et al. (2009) Teach Engineering. [Online]. https://www.teachengineering.org/collection/cub_/lessons/cub_pveff/Attachments/cub_pveff_lesson02_fundamentalsarticle_v6_tedl_dwc.pdf

6 Appendix

6.1 Common Data Format

The working group for the "Exchange of Solved Load Flow Data" published the "Common Data Format for Exchange of Solved Load Flow Data" in November 1971. In the 1960's the meshed power systems were getting more and more complicated. Associated with that the number of load flow programs, which were used by a variety of study groups, was rising. The demand for exchanging data between this study groups grew which resulted in the Common Data Format. [25]

In the past there were two different options to supply the data. The data could either be sent on a magnetic tape or written on cards. Nowadays the data is in a simple text file. The Common Data Format file is split up into sections with lines that have up to 128 characters.

This appendix will pinpoint on the sections that were essential for this Master Thesis. For further information please see [25] [26].

The data types that are used in the file will be in brackets after the data:
A – alphanumeric (special characters are not allowed)
I – Integer
F – Floating point
* – Mandatory item

Case identification

In the first line of the file shows the Case identification. There the date when the file was created (in the format DD/MM/YY), the senders name (A), the MVA base (F*), the year the case describes (I), season the case describes (S – Summer, W – Winter), Case description or case number (A) can be found.

Bus Data

The Bus Data section is mandatory. It starts with the line *BUS DATA FOLLOWS* followed by *NNNN ITEMS* where NNNN is the number of items. After up to 9999 lines of Bus data the Bus Data section has to end with the line -999. Each Bus Data line contains information as described in Table 6.1.

Columns	Data
1-4	Bus Number (I*), number from 1 to 9999
6-17	Bus Name (A*), up to 12 characters, it is suggested to use the following name scheme: area name kV -- ------- ---
19-20	Bus Area (I*), number from 1 to 99 that indicates the responsible company, 0 means the data is not available
21-23	Loss zone (I), extension to the Area Number, if no data is available use zero
26	Bus Type (I*) 0 – This bus is unregulated (load) 1 – Keep the power generation within the given voltage limits 2 – Keep the bus voltage within the given power limits 3 – Keep bus voltage and angle (there must always be one of this type in the network)
28-33	Final Voltage in p.u. (F*), this must not be the same as the desired voltage
34-40	Final Angle in degrees (F*)
41-49	Load MW (F*)
50-59	Load MVAR (F*)
60-67	Generation MW (F*)
68-75	Generation MVAR (F*)
77-83	Base kV (F), if no data is available use zero
85-90	Desired voltage in p.u. (F)
91-98	Maximum MVAR/Voltage limit (F)
99-106	Minimum MVAR/Voltage limit (F)
107-114	Shunt conductance G in p.u. (F*)
115-122	Shunt susceptance B in p.u, (F*)
124-127	Remote controlled bus number (I)

Table 6.1 Bus Data [25] [26]

Branch Data

This section is also mandatory and starts similar to the section before with the line *BRANCH DATA FOLLOWS* followed by *NNNNN ITEMS* where NNNN is the number of items. The following lines contain the Branch Data as described in Table 6.2. The section ends with the line -999.

Columns	Data
1-4	From Bus Number (I*), for transformers or phase shifters this is the tap side: Tap Bus
6-9	To Bus Number (I*), for transformers or phase shifters this is where the impedance is: Z Bus
11-12	Bus area (I)
13-14	Loss zone (I), an integer from 1 to 999 to define zone of loss calculation, 0 means the data is not available
17	Circuit (I*), this number from 1 to 9 represents the number of parallel lines
19	Branch Type (I*) 0 – Transmission line 1 – Transformer with fixed voltage ratio and/or fixed phase angle 2 – Transformer with fixed phase angle and variable voltage ratio with voltage control 3 - Transformer with fixed phase angle and variable voltage ratio with apparent power control 4 - Transformer with fixed voltage ratio and variable phase angle with active power control
20-29	Branch resistance in p.u. (F*)
30-40	Branch reactance in p.u. (F*)
41-50	Line charging (susceptance B) in p.u. (F*), for transformers this value has to be zero unless the transformer has been combined with a transmission line
51-55	Line rating Number 1 (I), these Line rating values are not of any concern for this Master Thesis
57-61	Line rating Number 2 (I)
63-67	Line rating Number 3 (I)
69-72	Controlled Bus Number (I), This value is mandatory for Transformers. This is the bus number whose voltage/power is to be controlled.
74	Side code (I), required for "type 2" Transformers 0 – The controlled bus is one of the terminals (see Controlled Bus Number) 1 – The controlled bus is near the tap side (see From Bus Number) 2 – The controlled bus is near the impedance side (see To Bus Number)
77-82	Final Voltage Ratio (F), the final Transformers ratio from the solved load flow case
84-90	Final Phase Angle (F), the final Transformers phase angle from the solved load flow case

91-97	Minimum tap or phase shift (F)
98-104	Maximum tap or phase shift (F)
106-111	Step size
113-119	Minimum voltage, apparent/active power limit
120-126	Maximum voltage, apparent/active power limit

Table 6.2 Branch Data [25] [26]

The other sections of the Common Data Format were not relevant for this Master Thesis.

6.2 Appendix: Charts and Tables

6.2.1 IEEE 30 Bus Test grid

Branch Number	From	To	Power Rating [MVA]	Type
1	1	2	130	Transmission Line
2	1	3	130	Transmission Line
3	2	4	65	Transmission Line
4	3	4	130	Transmission Line
5	2	5	130	Transmission Line
6	2	6	65	Transmission Line
7	4	6	90	Transmission Line
8	5	7	70	Transmission Line
9	6	7	130	Transmission Line
10	6	8	32	Transmission Line
11	6	9	65	Transformer
12	6	10	32	Transformer
13	9	11	65	Transformer
14	9	10	65	Transformer
15	4	12	65	Transformer
16	12	13	65	Transformer
17	12	14	32	Transmission Line
18	12	15	32	Transmission Line
19	12	16	32	Transmission Line
20	14	15	16	Transmission Line
21	16	17	16	Transmission Line
22	15	18	16	Transmission Line
23	18	19	16	Transmission Line
24	19	20	32	Transmission Line
25	10	20	32	Transmission Line
26	10	17	32	Transmission Line
27	10	21	32	Transmission Line
28	10	22	32	Transmission Line
29	21	22	32	Transmission Line
30	15	23	16	Transmission Line
31	22	24	16	Transmission Line
32	23	24	16	Transmission Line
33	24	25	16	Transmission Line
34	25	26	16	Transmission Line
35	25	27	16	Transmission Line
36	28	27	65	Transformer
37	27	29	16	Transmission Line
38	27	30	16	Transmission Line
39	29	30	16	Transmission Line
40	8	28	32	Transmission Line
41	6	28	32	Transmission Line

Table 6.3 Branch data [20]

6.2.2 Charts for Distributed generation in Hancock, Roanoke and Cloverdale at $cos(\varphi){=}1$

	no DG production	$P_{DG}{=}0,1$ pu, $cos(\varphi){=}1$	$P_{DG}{=}0,5$ pu, $cos(\varphi){=}1$	$P_{DG}{=}1$ pu, $cos(\varphi){=}1$
Q [Mvar]	-0,46	2,15	7,48	4,97
P [MW]	-41,44	-34,25	-6,25	27,40
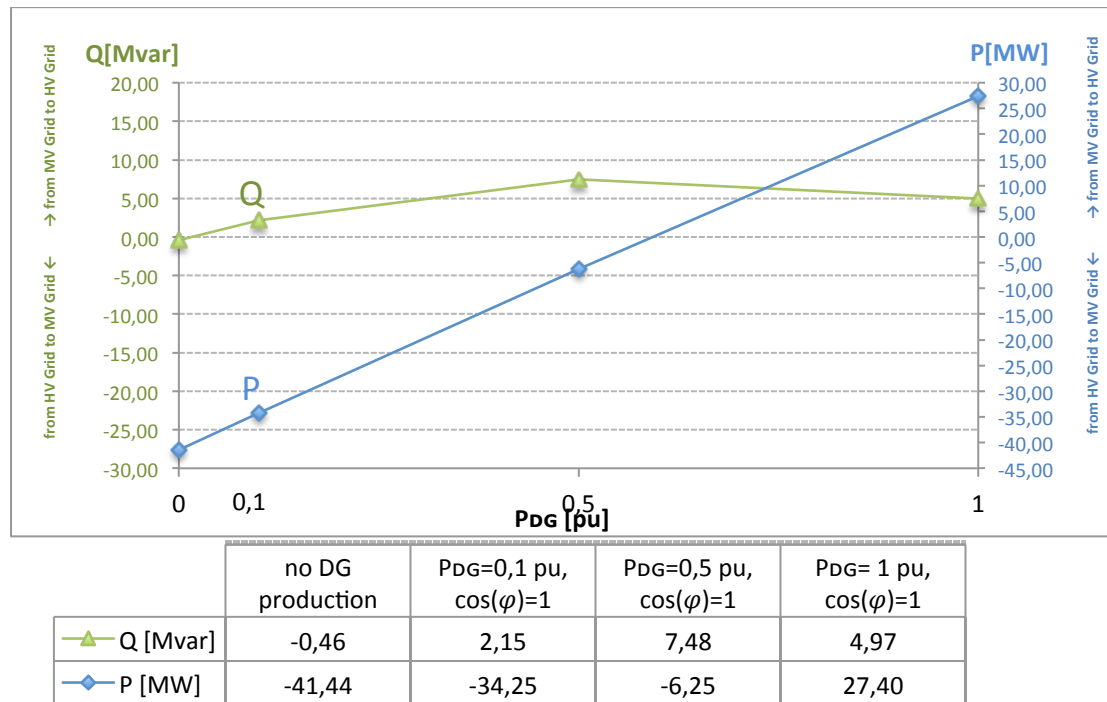
Figure 6.1 Power flow over the MV/HV transformer in Hancock for different DG production levels at $cos(\varphi){=}1$

	no DG production	$P_{DG}{=}0,1$ pu, $cos(\varphi){=}1$	$P_{DG}{=}0,5$ pu, $cos(\varphi){=}1$	$P_{DG}{=}1$ pu, $cos(\varphi){=}1$
Q [Mvar]	-13,57	-11,64	-7,35	-8,88
P [MW]	-47,87	-40,25	-10,04	27,22
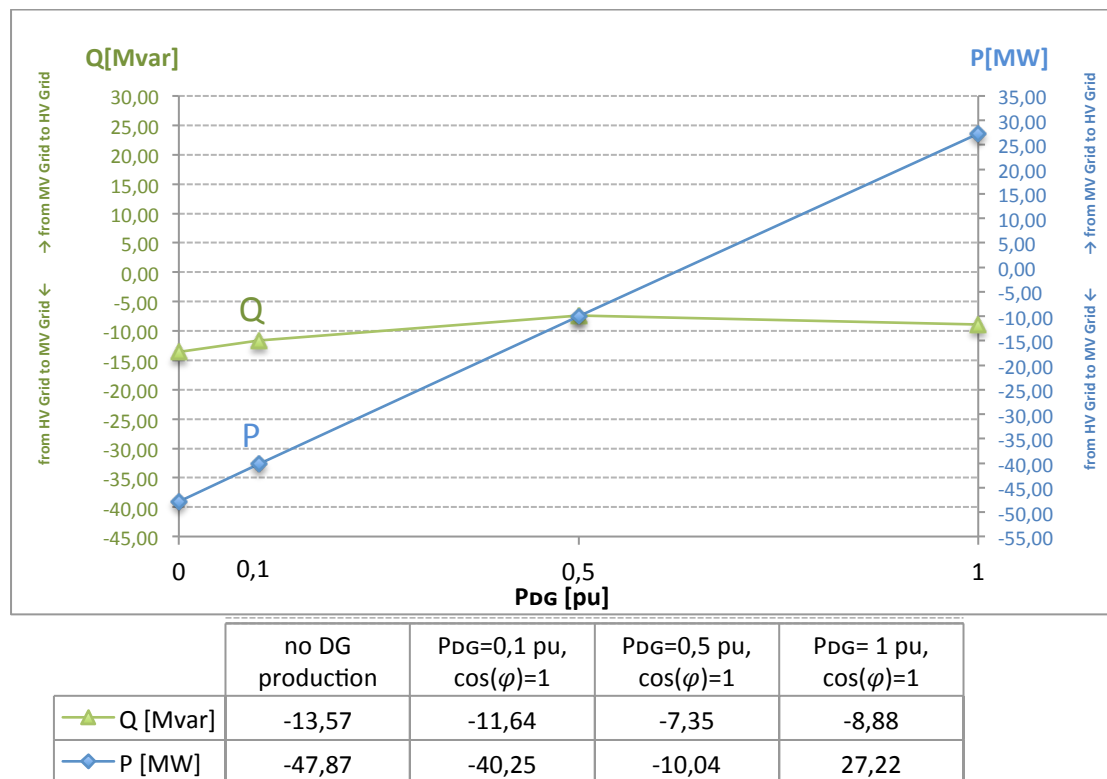
Figure 6.2 Power flow over the MV/HV transformer in Roanoke for different DG production levels at $cos(\varphi){=}1$

6.2.3 Charts for Distributed generation in Hancock, Roanoke and Cloverdale at $cos(\varphi)=0,95$ lagging
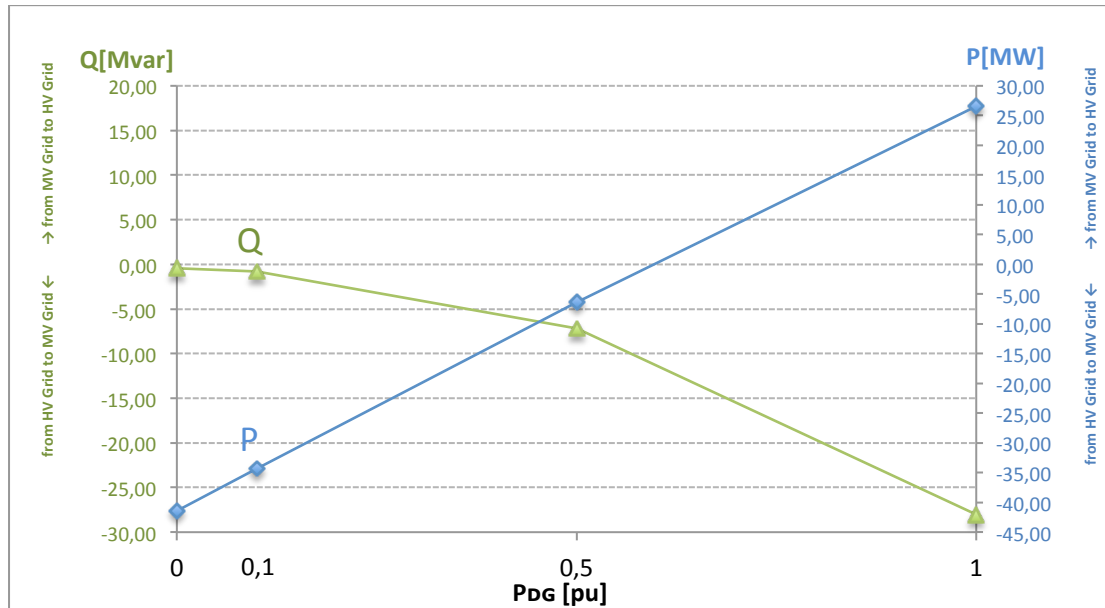
	no DG production	PDG=0,1 pu, cos(φ)=0,95 lag	PDG=0,5 pu, cos(φ)=0,95 lag	PDG=1 pu, cos(φ)=0,95 lag
Q [Mvar]	-0,46	-0,78	-7,20	-28,02
P [MW]	-41,44	-34,28	-6,39	26,53

Figure 6.3 Power flow over the MV/HV transformer in Hancock for different DG production levels at $cos(\varphi)=0,95$ lagging
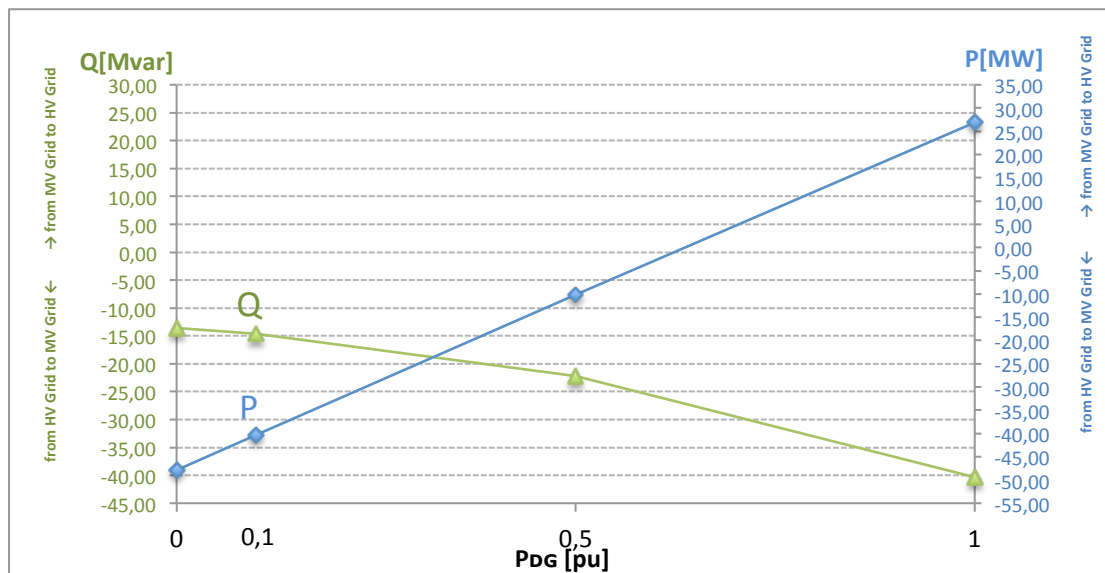
	no DG production	PDG=0,1 pu, cos(φ)=0,95 lag	PDG=0,5 pu, cos(φ)=0,95 lag	PDG=1 pu, cos(φ)=0,95 lag
Q [Mvar]	-13,57	-14,59	-22,16	-40,34
P [MW]	-47,87	-40,26	-10,11	26,93

Figure 6.4 Power flow over the MV/HV transformer in Roanoke for different DG production levels at $cos(\varphi)=0,95$ lagging
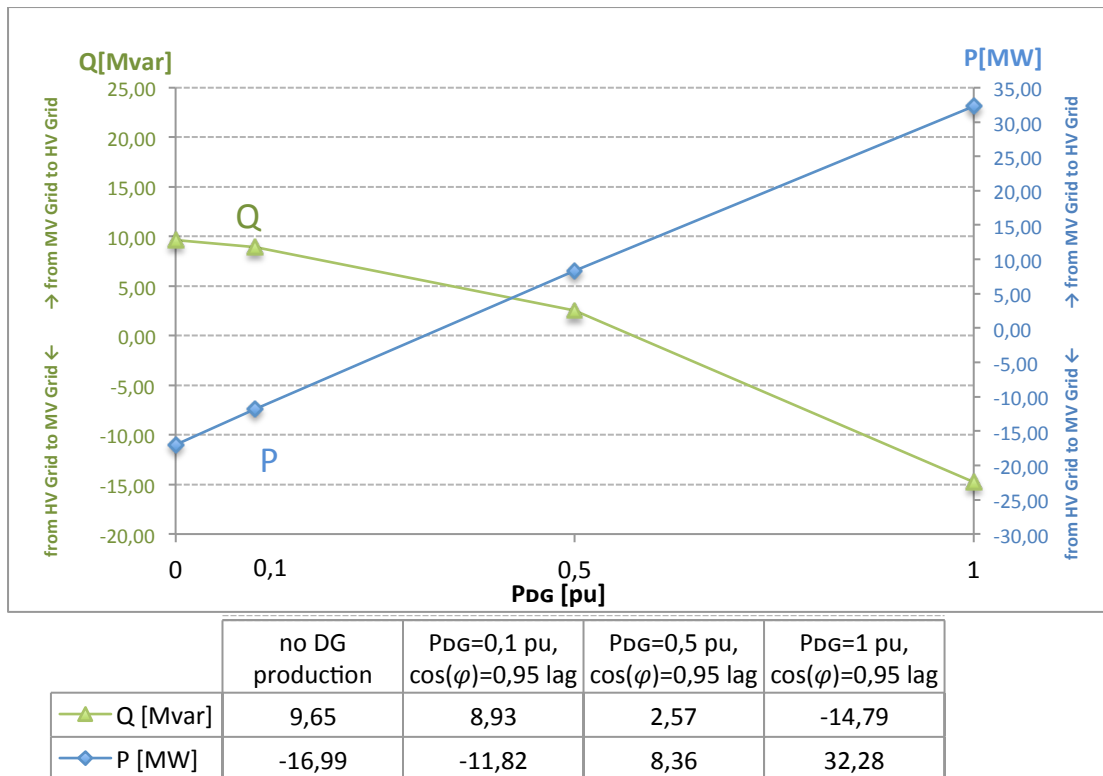
Figure 6.5 Power flow over the MV/HV transformer in Cloverdale for different DG production levels at $cos(\varphi)=0{,}95$ lagging

	no DG production	PDG=0,1 pu, cos(φ)=0,95 lag	PDG=0,5 pu, cos(φ)=0,95 lag	PDG=1 pu, cos(φ)=0,95 lag
Q [Mvar]	9,65	8,93	2,57	-14,79
P [MW]	-16,99	-11,82	8,36	32,28

6.2.4 Charts for Distributed generation in Hancock, $Q(U)$ controller

	no DG production TSP: 10	PDG=0,1 pu; TSP:10	PDG=0,5 pu; TSP:10	PDG=1 pu; TSP:10
Q [Mvar]	0,29	4,13	15,20	12,41
P [MW]	-34,70	-28,87	-5,40	27,20
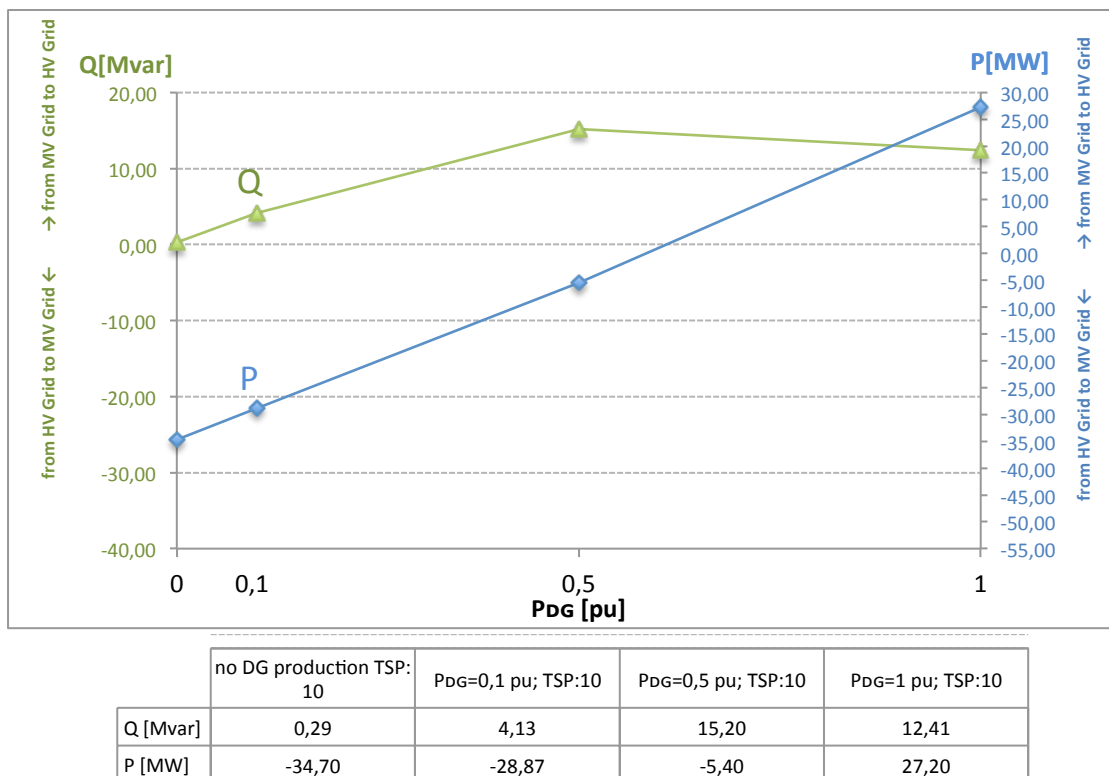
Figure 6.6 Active- and Reactive power flow over Hancock Transformer at the TSP:10
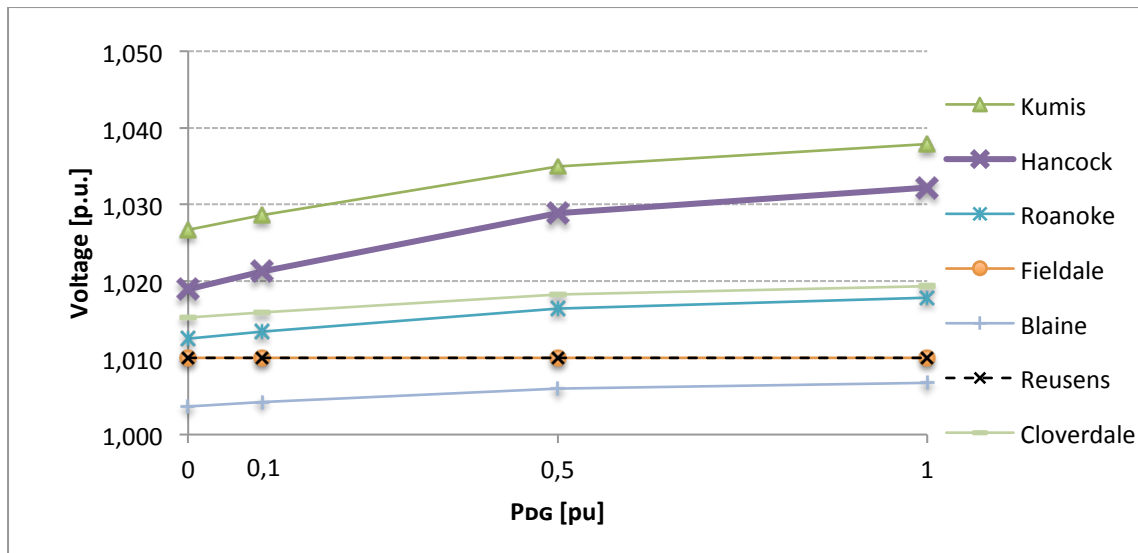
	no DG production TSP: 10	P_{DG}=0,1 pu; TSP:10	P_{DG}=0,5 pu; TSP:10	P_{DG}=1 pu; TSP:10
Kumis	1,027	1,029	1,035	1,038
Hancock	1,019	1,021	1,029	1,032
Roanoke	1,013	1,013	1,016	1,018
Fieldale	1,010	1,010	1,010	1,010
Blaine	1,004	1,004	1,006	1,007
Reusens	1,010	1,010	1,010	1,010
Cloverdale	1,015	1,016	1,018	1,019

Figure 6.7 Voltages in the HV grid (U_n=132 kV) depending on DG production at the TSP:10
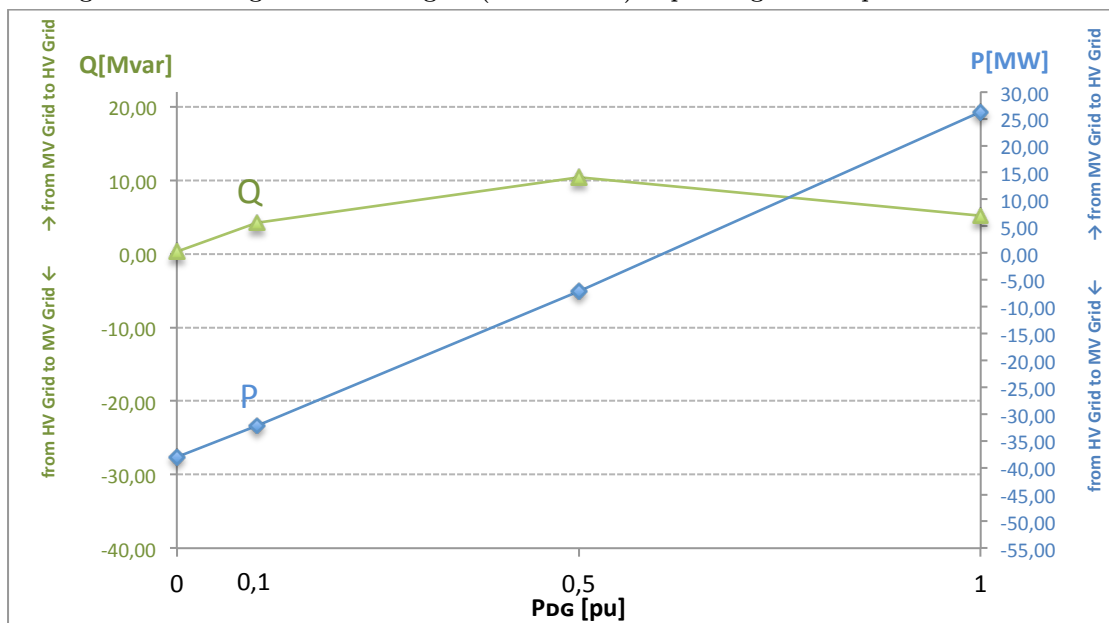
	no DG production TSP: 5	P_{DG}=0,1 pu; TSP:5	P_{DG}=0,5 pu; TSP:5	P_{DG}=1 pu; TSP:5
Q [Mvar]	0,31	4,20	10,38	5,21
P [MW]	-38,00	-32,20	-7,11	26,26

Figure 6.8 Active- and Reactive power flow over Hancock Transformer at the TSP:5
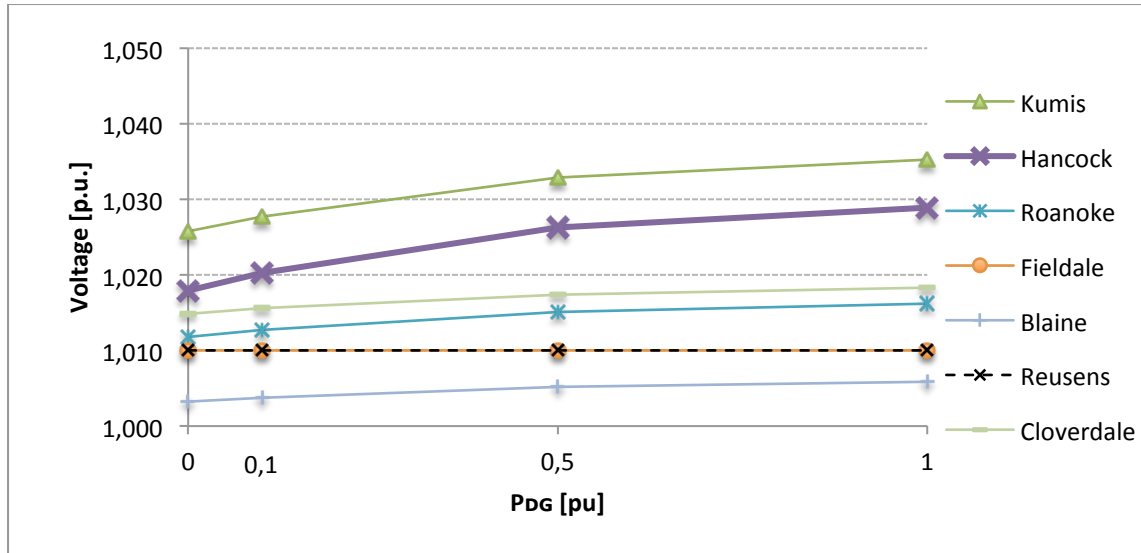
	no DG production TSP:5	PDG=0,1 pu; TSP:5	PDG=0,5 pu; TSP:5	PDG=1 pu; TSP:5
Kumis	1,026	1,028	1,033	1,035
Hancock	1,018	1,020	1,026	1,029
Roanoke	1,012	1,013	1,015	1,016
Fieldale	1,010	1,010	1,010	1,010
Blaine	1,003	1,004	1,005	1,006
Reusens	1,010	1,010	1,010	1,010
Cloverdale	1,015	1,016	1,017	1,018

Figure 6.9 Voltages in the HV grid (U_n=132 kV) depending on DG production at the TSP:5
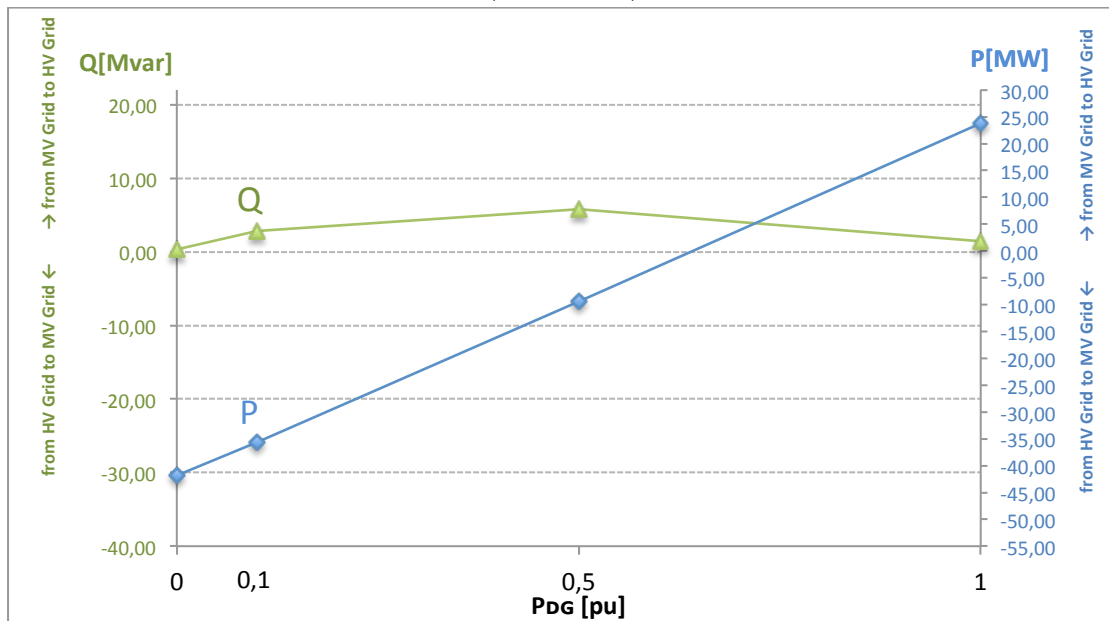
	no DG production TSP: 0	PDG=0,1 pu; TSP:0	PDG=0,5 pu; TSP:0	PDG=1 pu; TSP:0
Q [Mvar]	0,34	2,86	5,78	1,42
P [MW]	-41,80	-35,60	-9,35	23,80

Figure 6.10 Active- and Reactive power flow over Hancock Transformer at the TSP:0
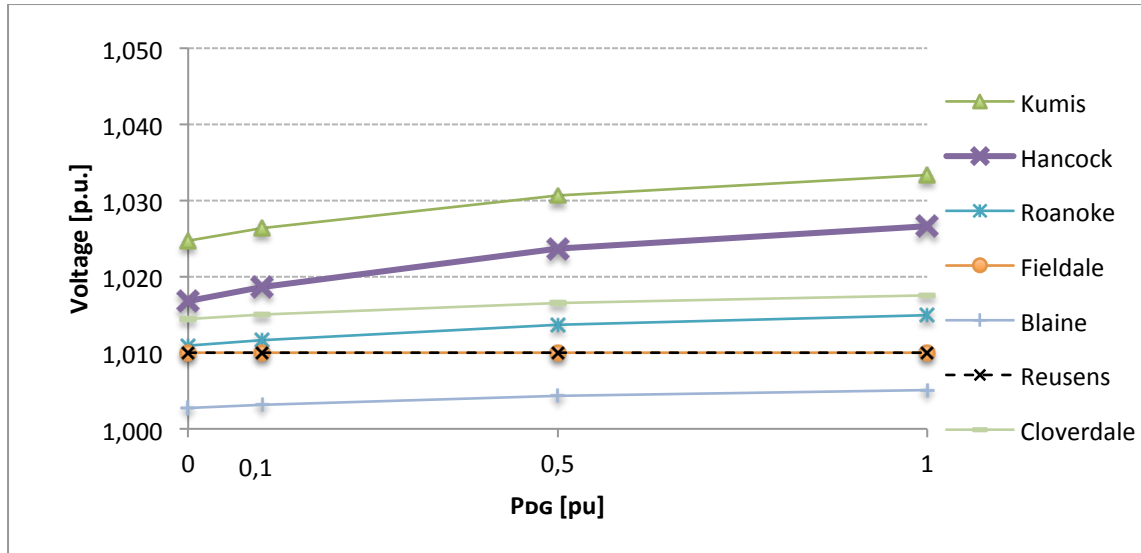
	no DG production TSP:0	PDG=0,1 pu; TSP:0	PDG=0,5 pu; TSP:0	PDG=1 pu; TSP:0
Claytor	1,045	1,045	1,045	1,045
Kumis	1,025	1,026	1,031	1,033
Hancock	1,017	1,019	1,024	1,027
Roanoke	1,011	1,012	1,014	1,015
Fieldale	1,010	1,010	1,010	1,010
Blaine	1,003	1,003	1,004	1,005
Reusens	1,010	1,010	1,010	1,010

Figure 6.11 Voltages in the HV grid (U_n=132 kV) depending on DG production at the TSP:0
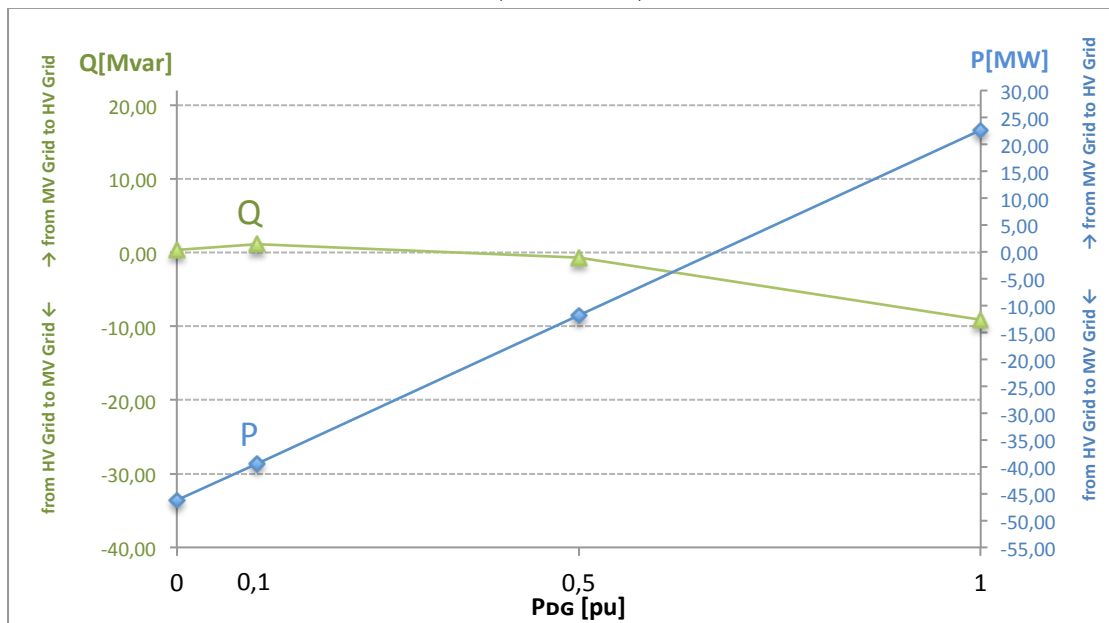
	no DG production TSP:-5	PDG=0,1 pu; TSP:-5	PDG=0,5 pu; TSP:-5	PDG=1 pu; TSP:-5
Q [Mvar]	0,38	1,12	-0,71	-9,12
P [MW]	-46,19	-39,43	-11,80	22,58

Figure 6.12 Active- and Reactive power flow over Hancock Transformer at the TSP:-5

	no DG production TSP:-5	PDG=0,1 pu; TSP:-5	PDG=0,5 pu; TSP:-5	PDG=1 pu; TSP:-5
Claytor	1,045	1,045	1,045	1,045
Kumis	1,023	1,025	1,028	1,029
Hancock	1,015	1,017	1,020	1,022
Roanoke	1,010	1,010	1,012	1,013
Fieldale	1,010	1,010	1,010	1,010
Blaine	1,002	1,002	1,003	1,004
Reusens	1,010	1,010	1,010	1,010
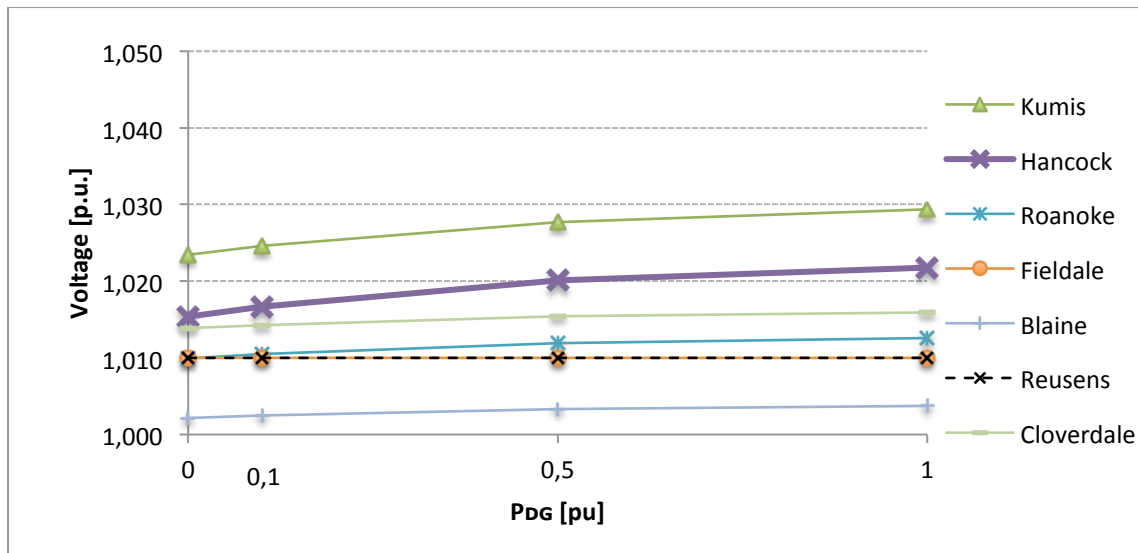
Figure 6.13 Voltages in the HV grid (U_{n}=132 kV) depending on DG production at the TSP:-5

	no DG production TSP:-10	PDG=0,1 pu; TSP:-10	PDG=0,5 pu; TSP:-10	PDG=1 pu; TSP:-10
Q [Mvar]	0,42	0,04	-4,86	-17,88
P [MW]	-51,22	-44,12	-15,46	20,21
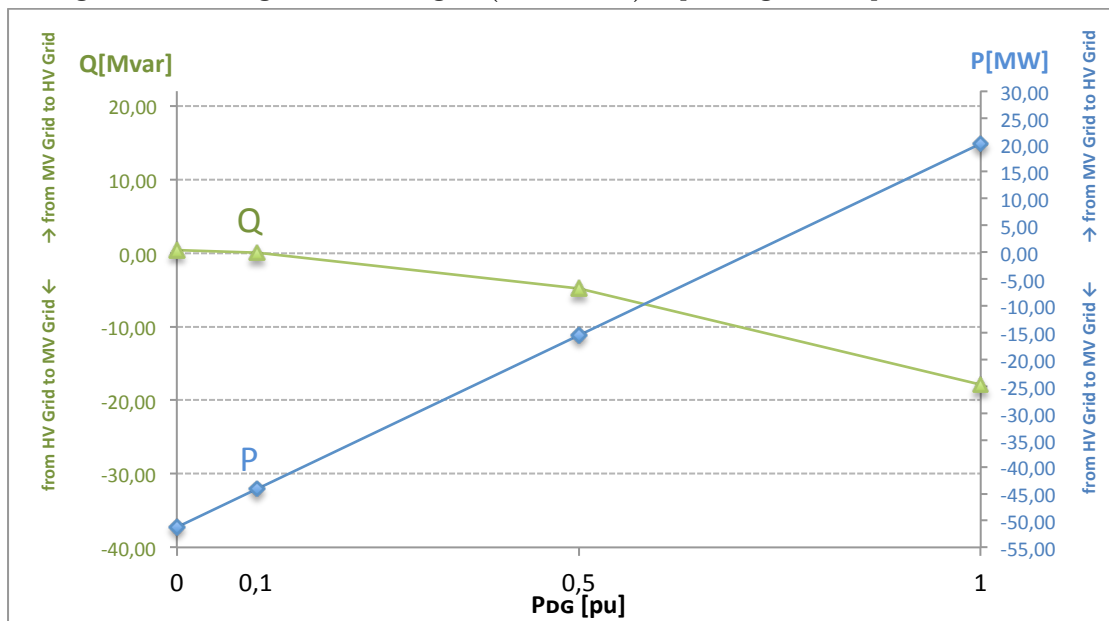
Figure 6.14 Active- and Reactive power flow over Hancock Transformer at the TSP:-10
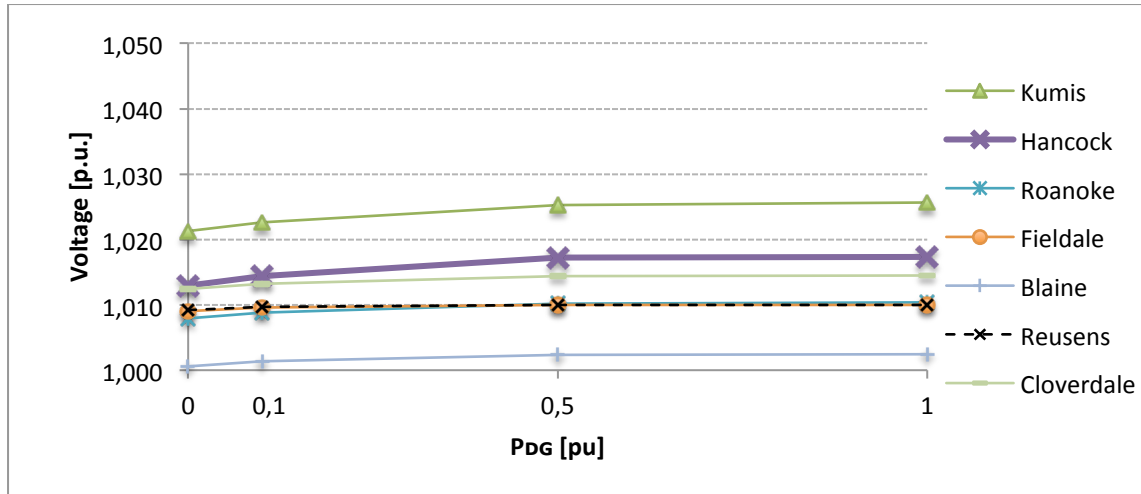
	no DG production TSP:-10	P_DG=0,1 pu; TSP:-10	P_DG=0,5 pu; TSP:-10	P_DG=1 pu; TSP:-10
Kumis	1,021	1,023	1,025	1,026
Hancock	1,013	1,014	1,017	1,017
Roanoke	1,008	1,009	1,010	1,010
Fieldale	1,009	1,010	1,010	1,010
Blaine	1,001	1,001	1,002	1,002
Reusens	1,009	1,010	1,010	1,010
Cloverdale	1,012	1,013	1,014	1,014

Figure 6.15 Voltages in the HV grid (U_n=132 kV) depending on DG production at the TSP:-10

6.2.5 Charts for Distributed generation in Hancock, Roanoke and Cloverdale, $Q(U)$ controller
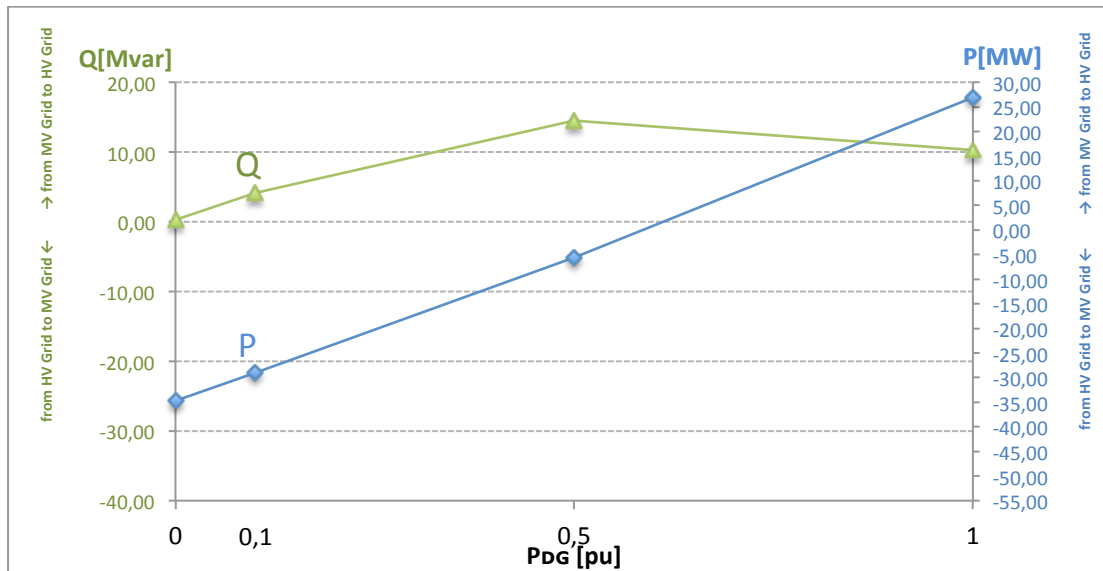
	no DG production TSP:10	P_DG=0,1 pu; TSP:10	P_DG=0,5 pu; TSP:10	P_DG=1 pu; TSP:10
Q [Mvar]	0,29	4,13	14,54	10,27
P [MW]	-34,70	-28,99	-5,65	26,92

Figure 6.16 Active- and Reactive power flow over Hancock Transformer at the TSP:10
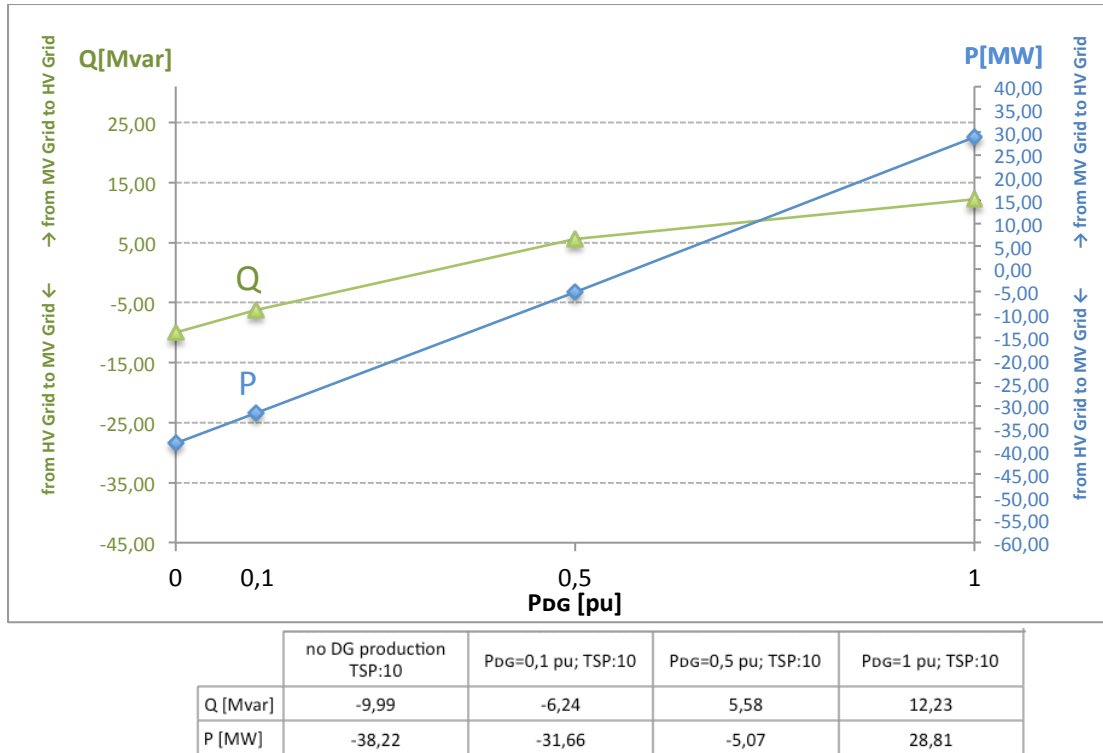
Figure 6.17 Active- and Reactive power flow over Roanoke Transformer at the TSP:10

	no DG production TSP:10	PDG=0,1 pu; TSP:10	PDG=0,5 pu; TSP:10	PDG=1 pu; TSP:10
Q [Mvar]	-9,99	-6,24	5,58	12,23
P [MW]	-38,22	-31,66	-5,07	28,81
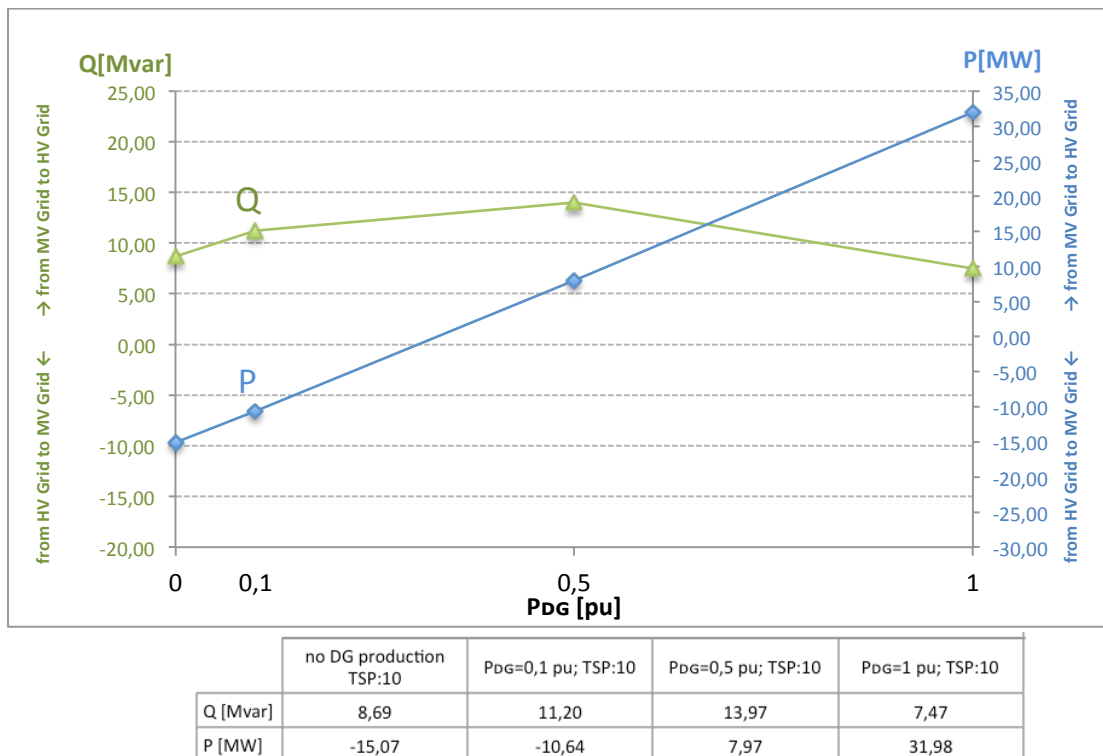
Figure 6.18 Active- and Reactive power flow over Cloverdale Transformer at the TSP:10

	no DG production TSP:10	PDG=0,1 pu; TSP:10	PDG=0,5 pu; TSP:10	PDG=1 pu; TSP:10
Q [Mvar]	8,69	11,20	13,97	7,47
P [MW]	-15,07	-10,64	7,97	31,98
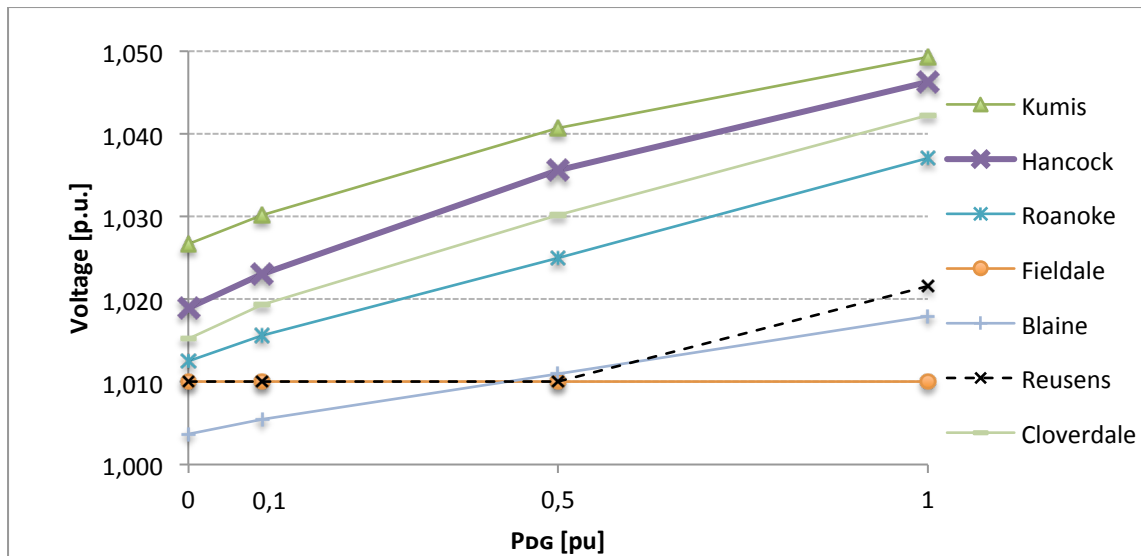
	no DG production TSP: 10	PDG=0,1 pu; TSP:10	PDG=0,5 pu; TSP:10	PDG=1 pu; TSP:10
Kumis	1,027	1,030	1,041	1,049
Hancock	1,019	1,023	1,036	1,046
Roanoke	1,013	1,016	1,025	1,037
Fieldale	1,010	1,010	1,010	1,010
Blaine	1,004	1,005	1,011	1,018
Reusens	1,010	1,010	1,010	1,022
Cloverdale	1,015	1,019	1,030	1,042

Figure 6.19 Voltages in the HV grid (U_n=132 kV) depending on DG production at the TSP:10
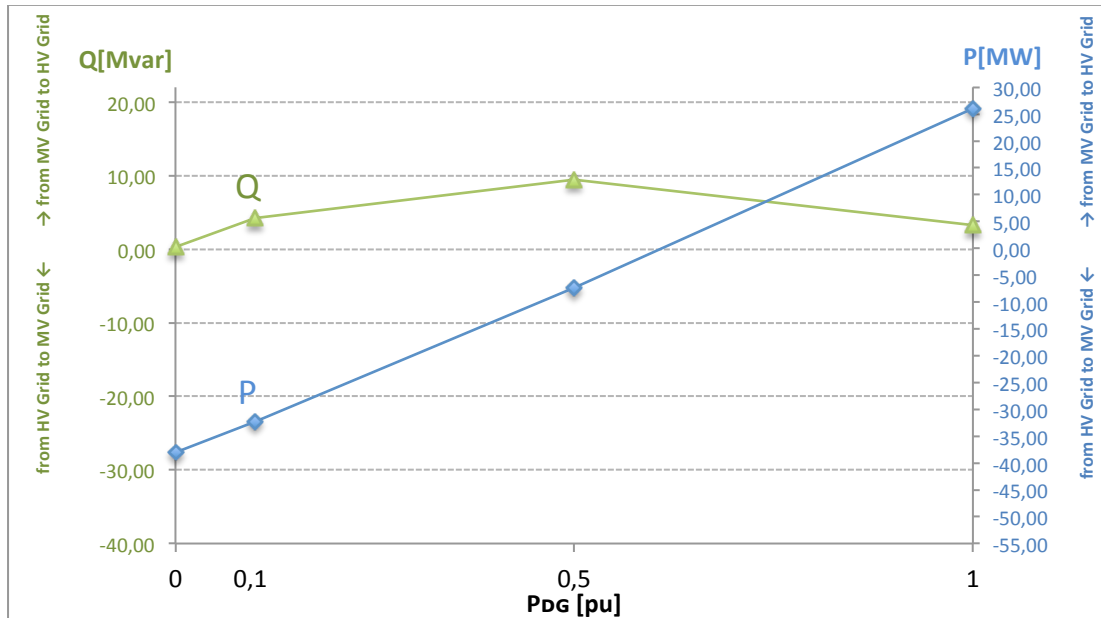
	no DG production TSP:5	PDG=0,1 pu; TSP:5	PDG=0,5 pu; TSP:5	PDG=1 pu; TSP:5
Q [Mvar]	0,31	4,20	9,42	3,23
P [MW]	-38,00	-32,33	-7,31	25,99

Figure 6.20 Active- and Reactive power flow over Hancock Transformer at the TSP:5
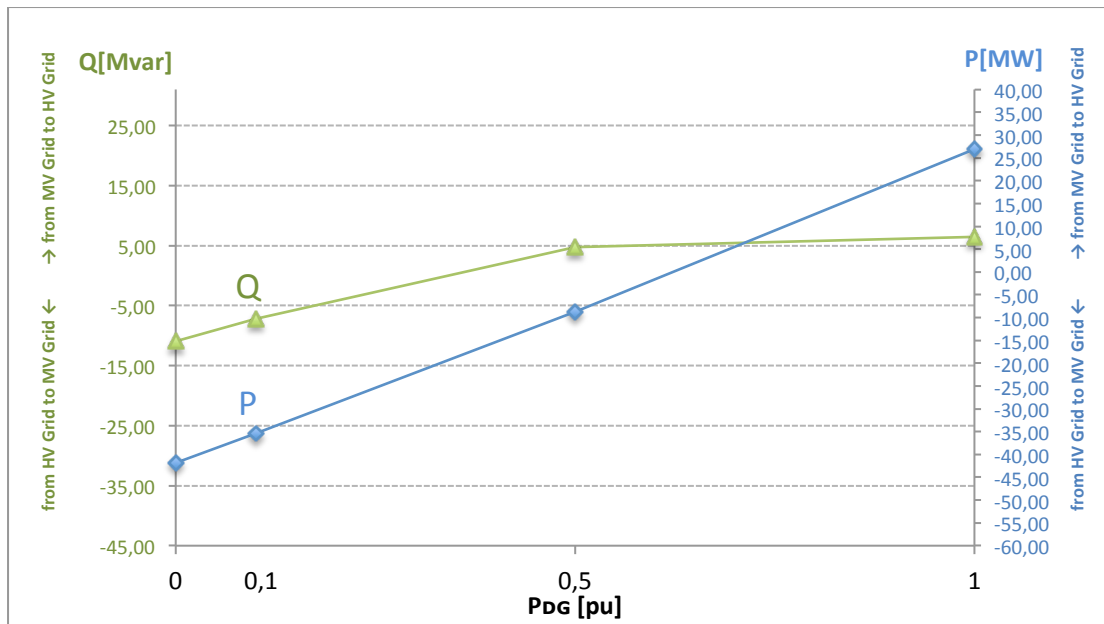
	no DG production TSP:5	PDG=0,1 pu; TSP:5	PDG=0,5 pu; TSP:5	PDG=1 pu; TSP:5
Q [Mvar]	-10,95	-7,18	4,76	6,39
P [MW]	-41,89	-35,34	-8,71	26,86

Figure 6.21 Active- and Reactive power flow over Roanoke Transformer at the TSP:5
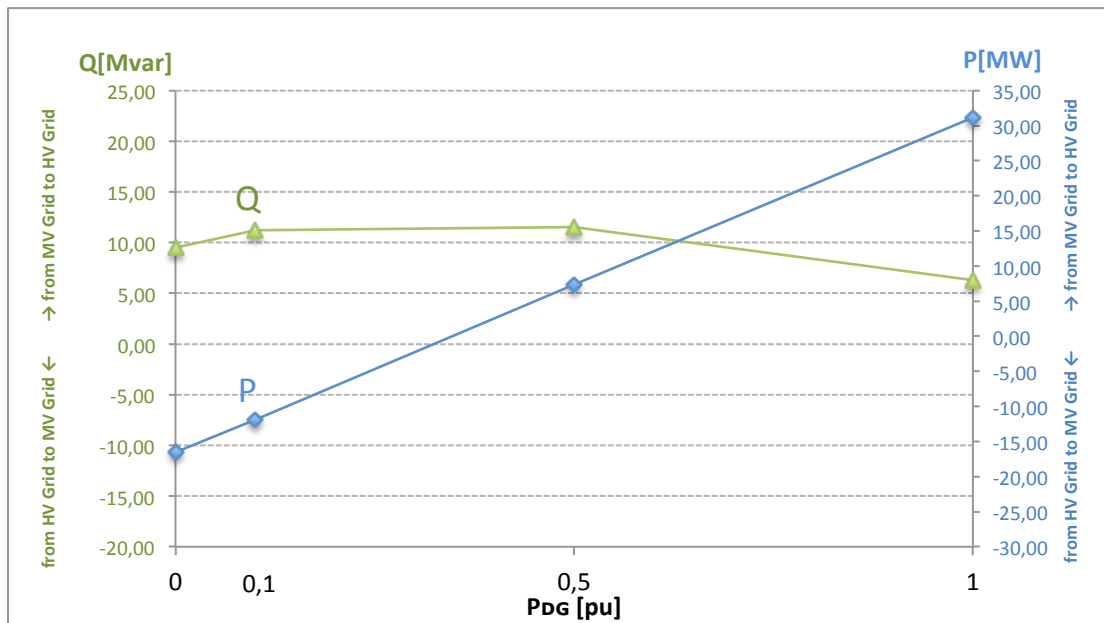
	no DG production TSP:5	PDG=0,1 pu; TSP:5	PDG=0,5 pu; TSP:5	PDG=1 pu; TSP:5
Q [Mvar]	9,54	11,24	11,52	6,30
P [MW]	-16,52	-11,95	7,33	31,17

Figure 6.22 Active- and Reactive power flow over Cloverdale Transformer at the TSP:5
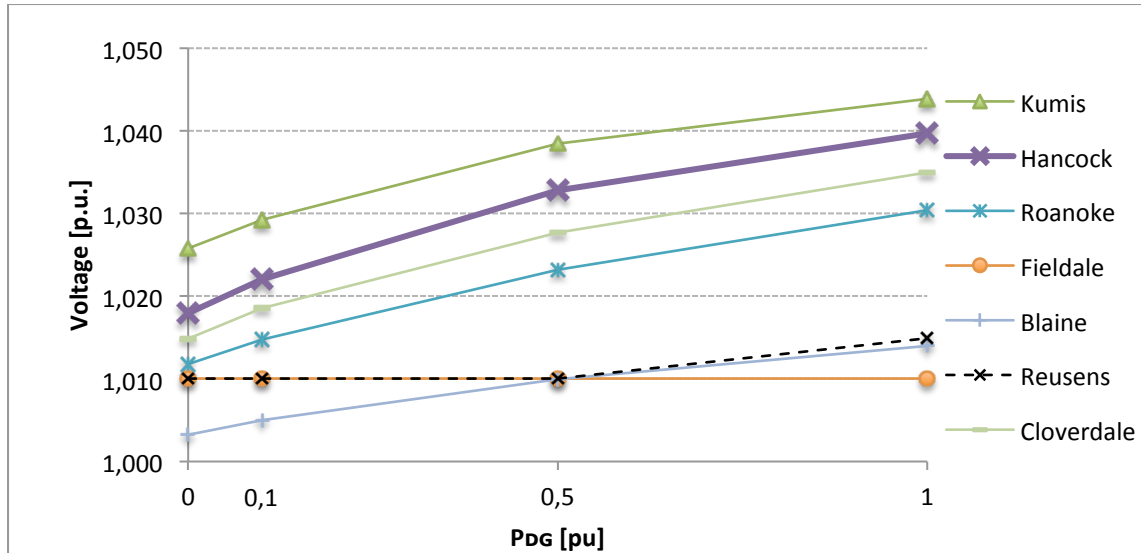
	no DG production TSP:5	PDG=0,1 pu; TSP:5	PDG=0,5 pu; TSP:5	PDG=1 pu; TSP:5
Kumis	1,026	1,029	1,038	1,044
Hancock	1,018	1,022	1,033	1,040
Roanoke	1,012	1,015	1,023	1,030
Fieldale	1,010	1,010	1,010	1,010
Blaine	1,003	1,005	1,010	1,014
Reusens	1,010	1,010	1,010	1,015
Cloverdale	1,015	1,019	1,028	1,035

Figure 6.23 Voltages in the HV grid (U_n=132 kV) depending on DG production at the TSP:5
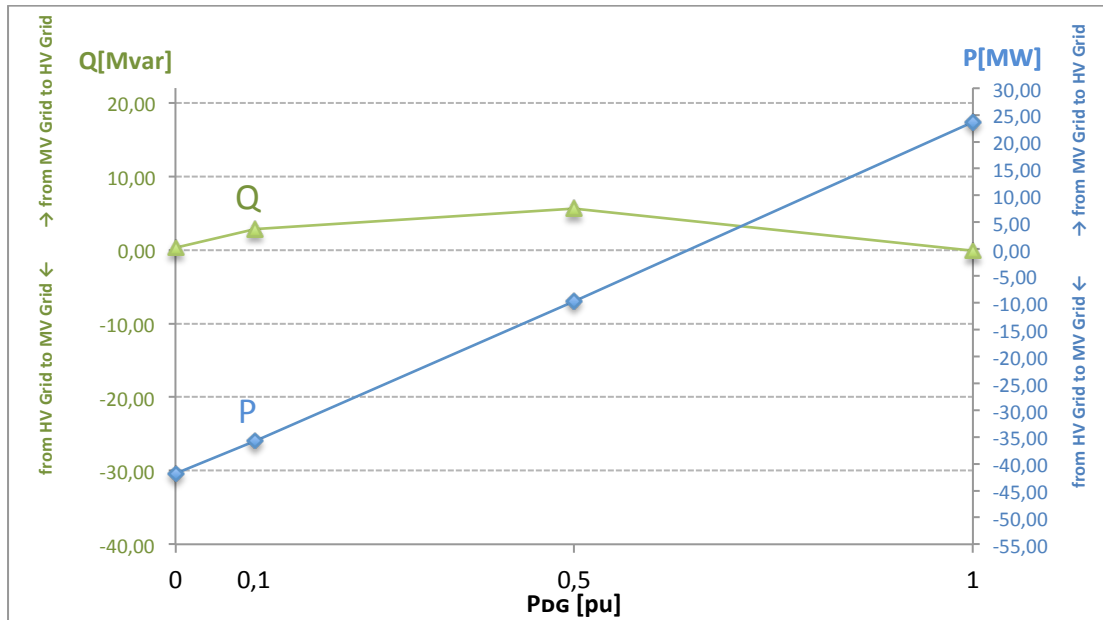
	no DG production TSP:0	PDG=0,1 pu; TSP:0	PDG=0,5 pu; TSP:0	PDG=1 pu; TSP:0
Q [Mvar]	0,34	2,80	5,63	-0,10
P [MW]	-41,80	-35,72	-9,78	23,64

Figure 6.24 Active- and Reactive power flow over Hancock Transformer at the TSP:0

Figure 6.25 Active- and Reactive power flow over Roanoke Transformer at the TSP:0
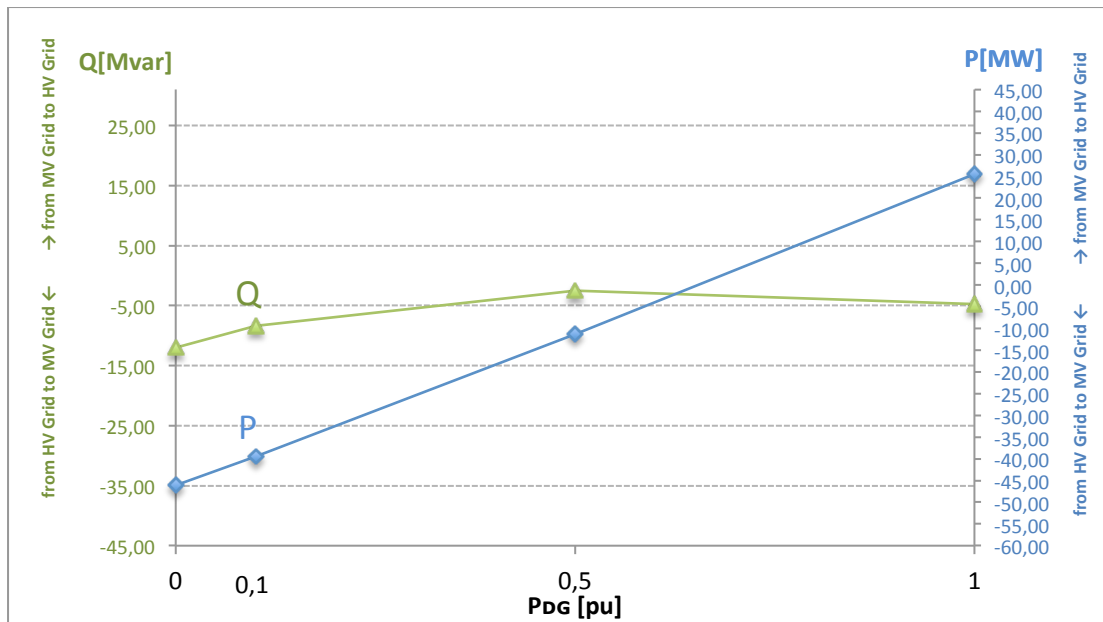
	no DG production TSP:0	PDG=0,1 pu; TSP:0	PDG=0,5 pu; TSP:0	PDG=1 pu; TSP:0
Q [Mvar]	-12,05	-8,33	-2,50	-4,75
P [MW]	-46,10	-39,53	-11,34	25,45

Figure 6.26 Active- and Reactive power flow over Cloverdale Transformer at the TSP:0
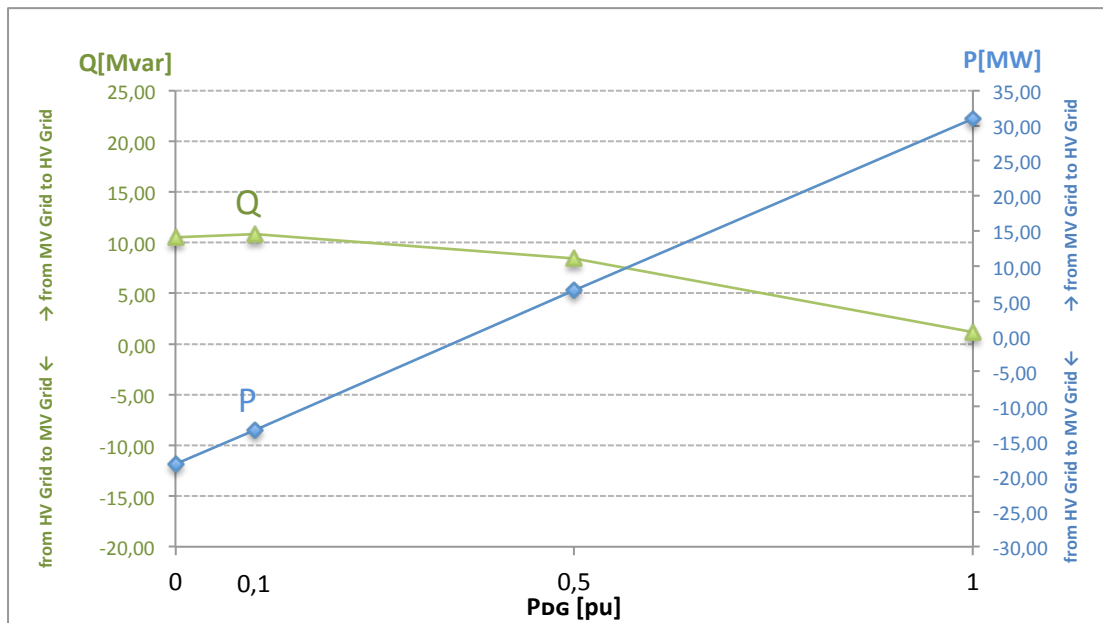
	no DG production TSP:0	PDG=0,1 pu; TSP:0	PDG=0,5 pu; TSP:0	PDG=1 pu; TSP:0
Q [Mvar]	10,50	10,86	8,46	1,17
P [MW]	-18,20	-13,32	6,49	30,94
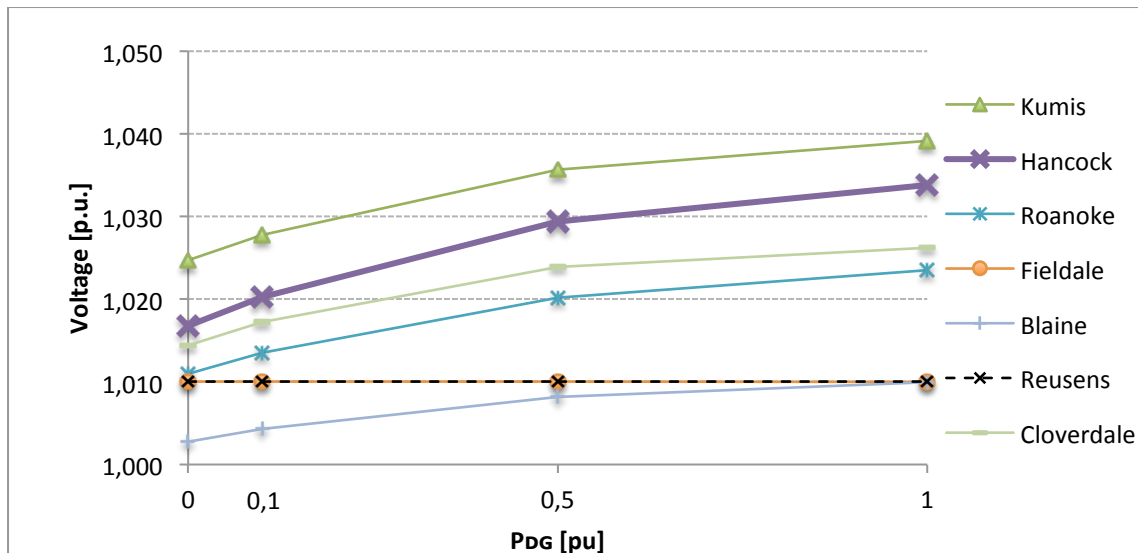
	no DG production TSP:0	PDG=0,1 pu; TSP:0	PDG=0,5 pu; TSP:0	PDG=1 pu; TSP:0
Kumis	1,025	1,028	1,036	1,039
Hancock	1,017	1,020	1,029	1,034
Roanoke	1,011	1,014	1,020	1,024
Fieldale	1,010	1,010	1,010	1,010
Blaine	1,003	1,004	1,008	1,010
Reusens	1,010	1,010	1,010	1,010
Cloverdale	1,014	1,017	1,024	1,026

Figure 6.27 Voltages in the HV grid (U_n=132 kV) depending on DG production at the TSP:0
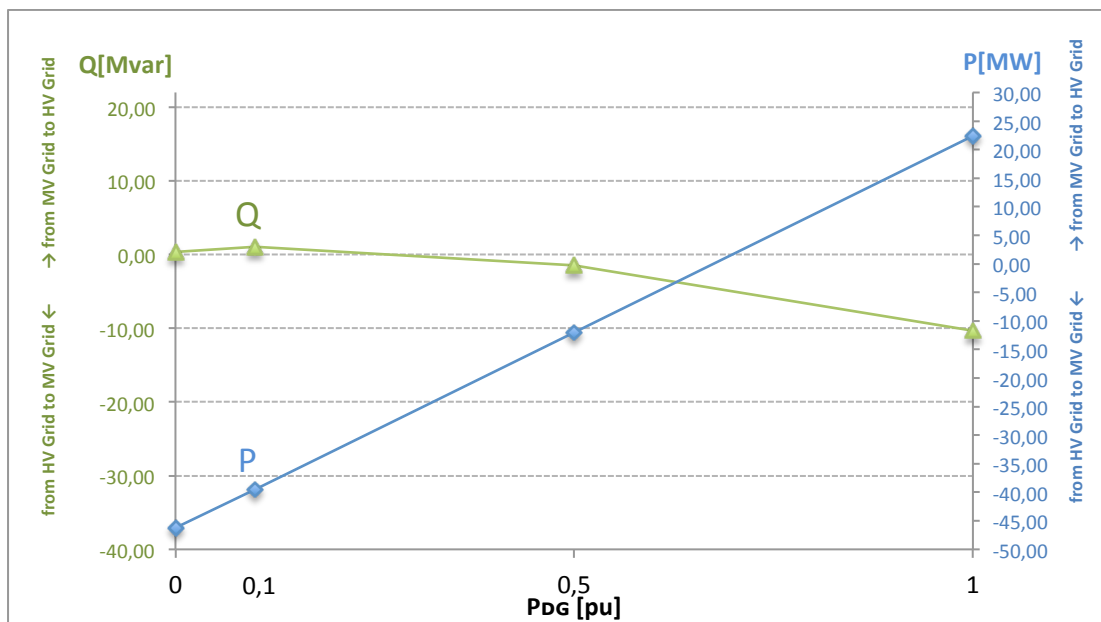
	no DG production TSP:-5	PDG=0,1 pu; TSP:-5	PDG=0,5 pu; TSP:-5	PDG=1 pu; TSP:-5
Q [Mvar]	0,38	1,07	-1,45	-10,34
P [MW]	-46,19	-39,53	-12,00	22,37

Figure 6.28 Active- and Reactive power flow over Hancock Transformer at the TSP:-5

	no DG production TSP:-5	PDG=0,1 pu; TSP:-5	PDG=0,5 pu; TSP:-5	PDG=1 pu; TSP:-5
Q [Mvar]	-13,33	-11,88	-9,10	-12,90
P [MW]	-50,98	-43,84	-14,83	22,48
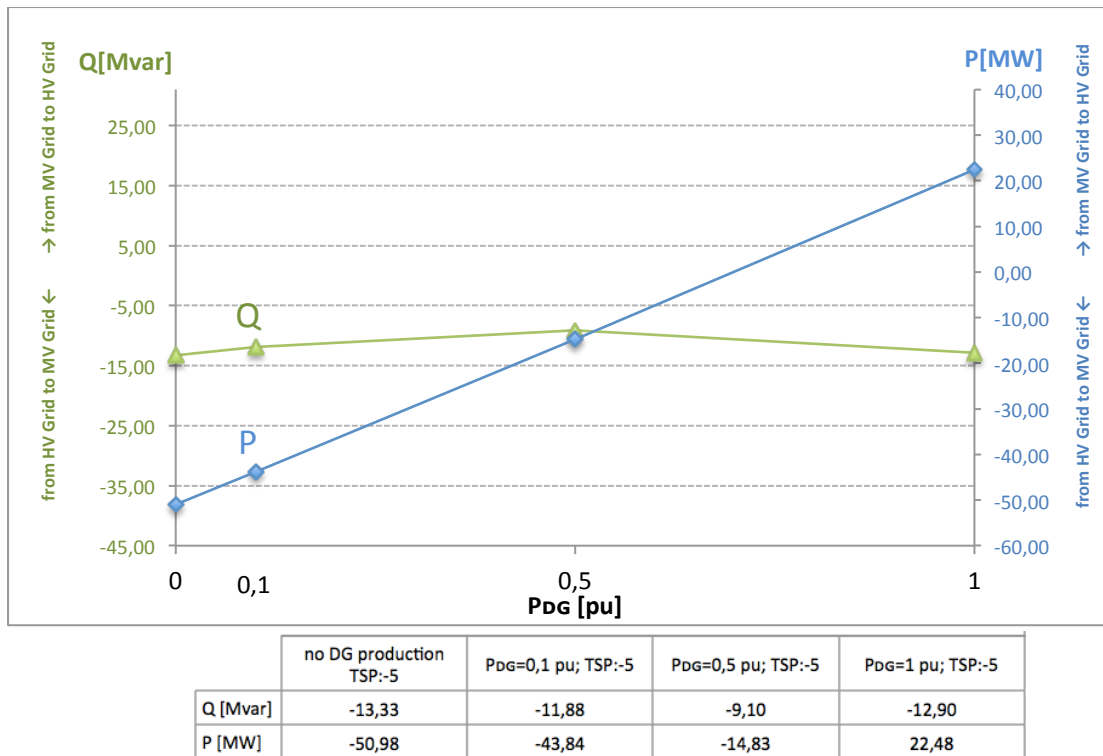
Figure 6.29 Active- and Reactive power flow over Roanoke Transformer at the TSP:-5

	no DG production TSP:-5	PDG=0,1 pu; TSP:-5	PDG=0,5 pu; TSP:-5	PDG=1 pu; TSP:-5
Q [Mvar]	11,63	10,96	5,81	-4,46
P [MW]	-20,15	-15,01	5,48	30,45
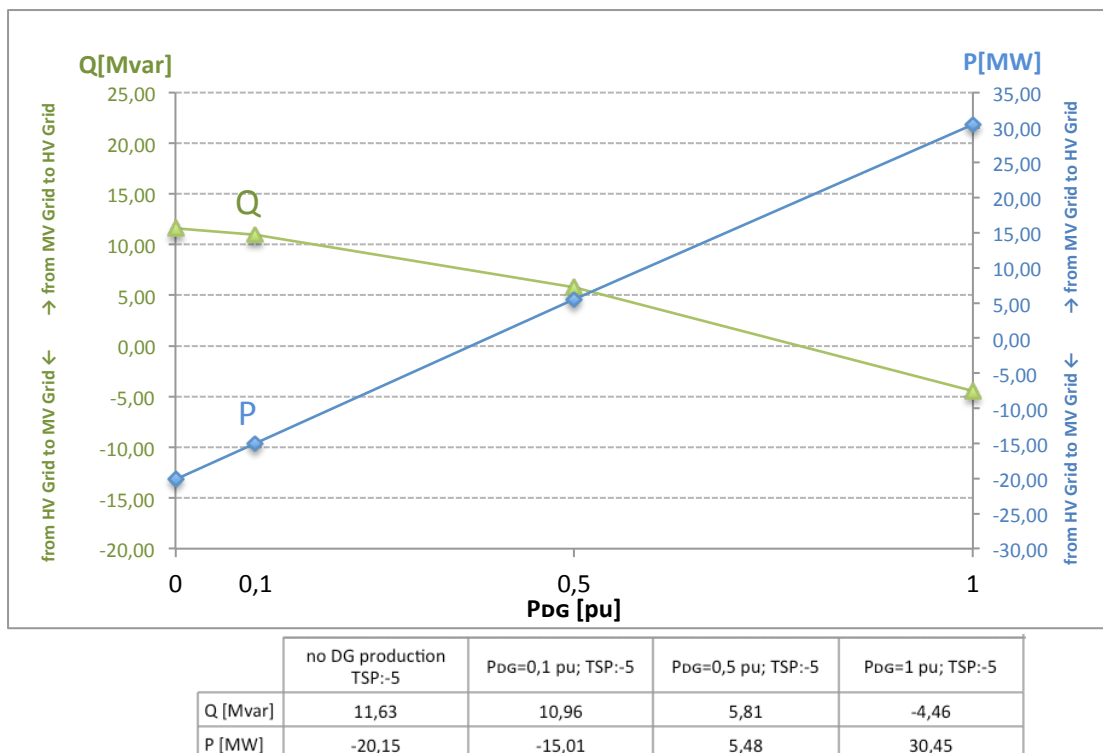
Figure 6.30 Active- and Reactive power flow over Cloverdale Transformer at the TSP:-5
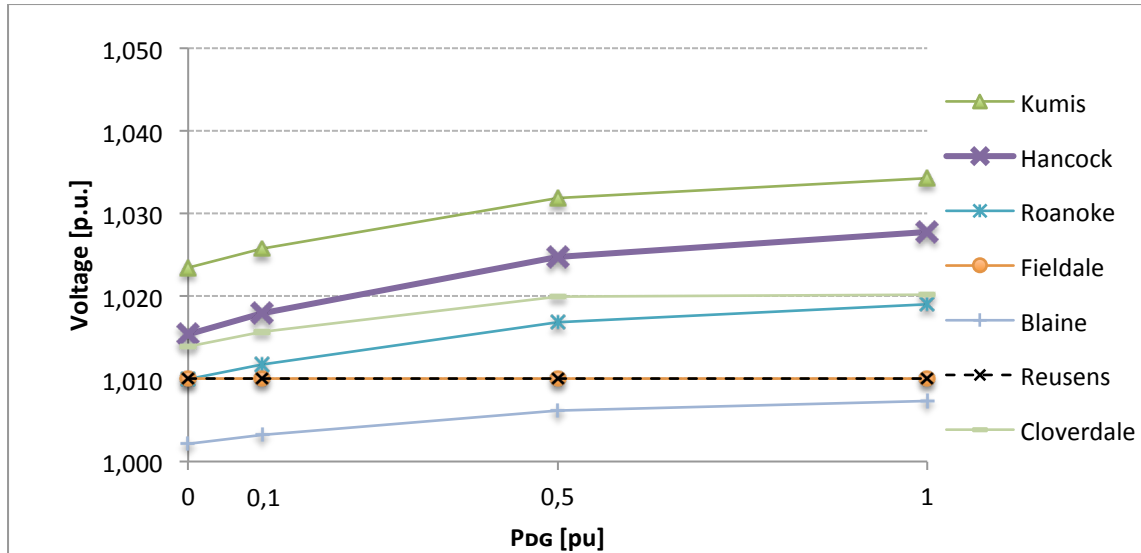
	no DG production TSP:-5	PDG=0,1 pu; TSP:-5	PDG=0,5 pu; TSP:-5	PDG=1 pu; TSP:-5
Kumis	1,023	1,026	1,032	1,034
Hancock	1,015	1,018	1,025	1,028
Roanoke	1,010	1,012	1,017	1,019
Fieldale	1,010	1,010	1,010	1,010
Blaine	1,002	1,003	1,006	1,007
Reusens	1,010	1,010	1,010	1,010
Cloverdale	1,014	1,016	1,020	1,020

Figure 6.31 Voltages in the HV grid (U_n=132 kV) depending on DG production at the TSP:-5
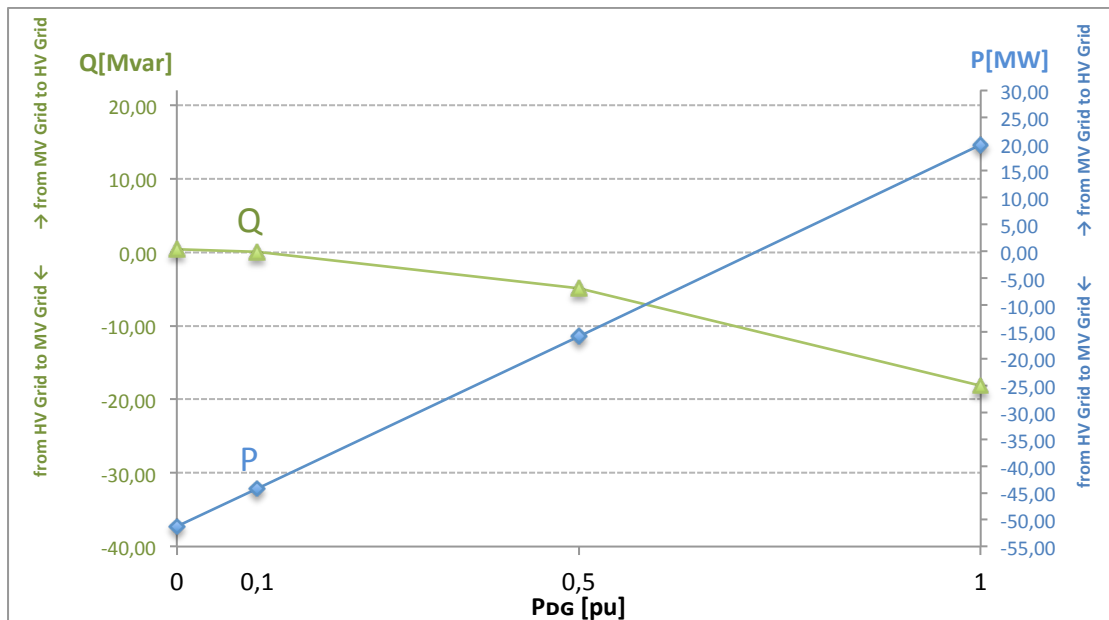
	no DG production TSP:-10	PDG=0,1 pu; TSP:-10	PDG=0,5 pu; TSP:-10	PDG=1 pu; TSP:-10
Q [Mvar]	0,42	0,03	-4,91	-18,13
P [MW]	-51,22	-44,25	-15,81	19,88

Figure 6.32 Active- and Reactive power flow over Hancock Transformer at the TSP:-10
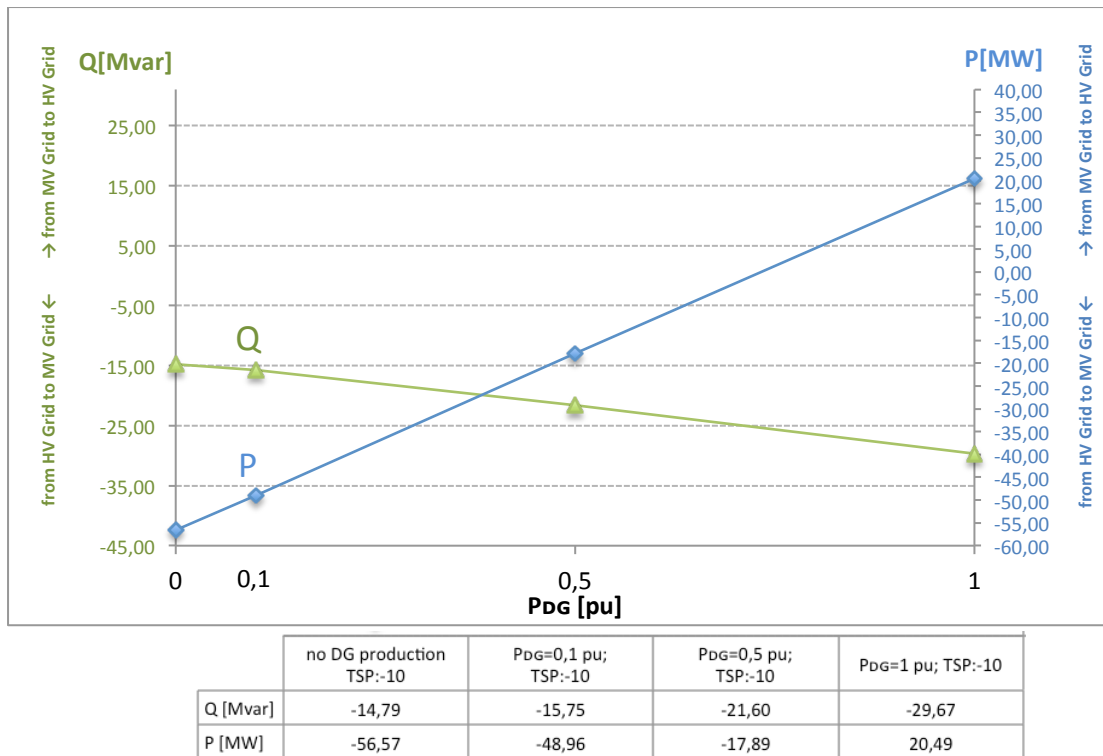
Figure 6.33 Active- and Reactive power flow over Roanoke Transformer at the TSP:-10

	no DG production TSP:-10	P$_{DG}$=0,1 pu; TSP:-10	P$_{DG}$=0,5 pu; TSP:-10	P$_{DG}$=1 pu; TSP:-10
Q [Mvar]	-14,79	-15,75	-21,60	-29,67
P [MW]	-56,57	-48,96	-17,89	20,49
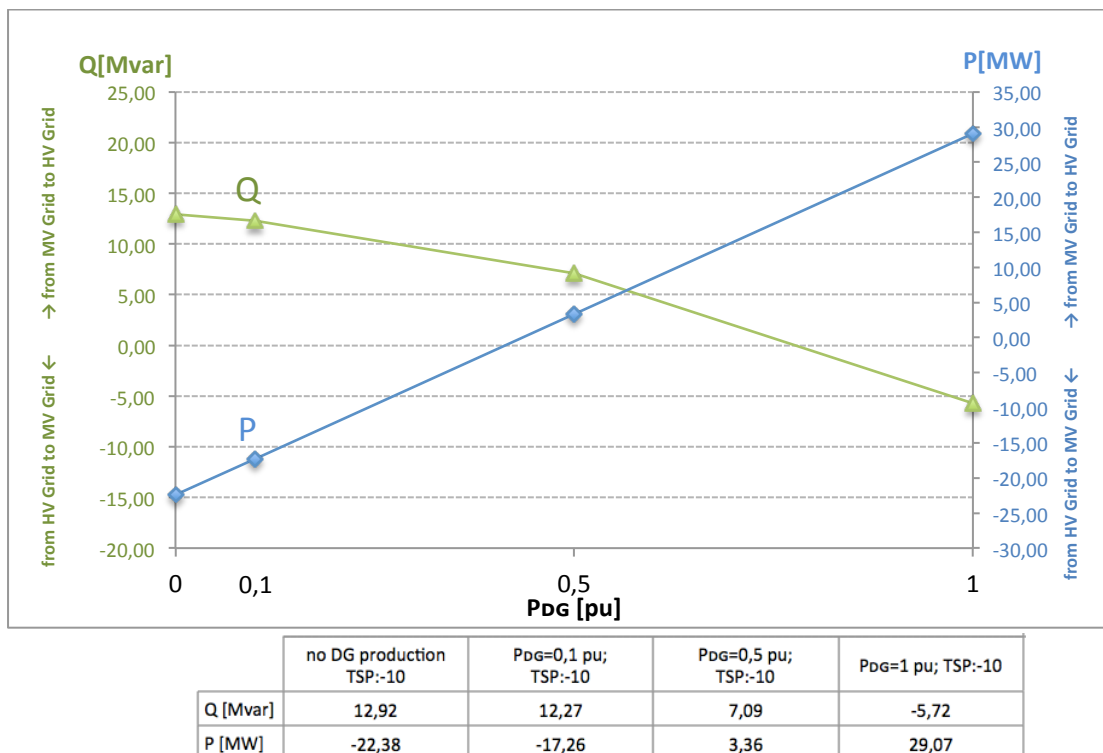
Figure 6.34 Active- and Reactive power flow over Cloverdale Transformer at the TSP:-10

	no DG production TSP:-10	P$_{DG}$=0,1 pu; TSP:-10	P$_{DG}$=0,5 pu; TSP:-10	P$_{DG}$=1 pu; TSP:-10
Q [Mvar]	12,92	12,27	7,09	-5,72
P [MW]	-22,38	-17,26	3,36	29,07
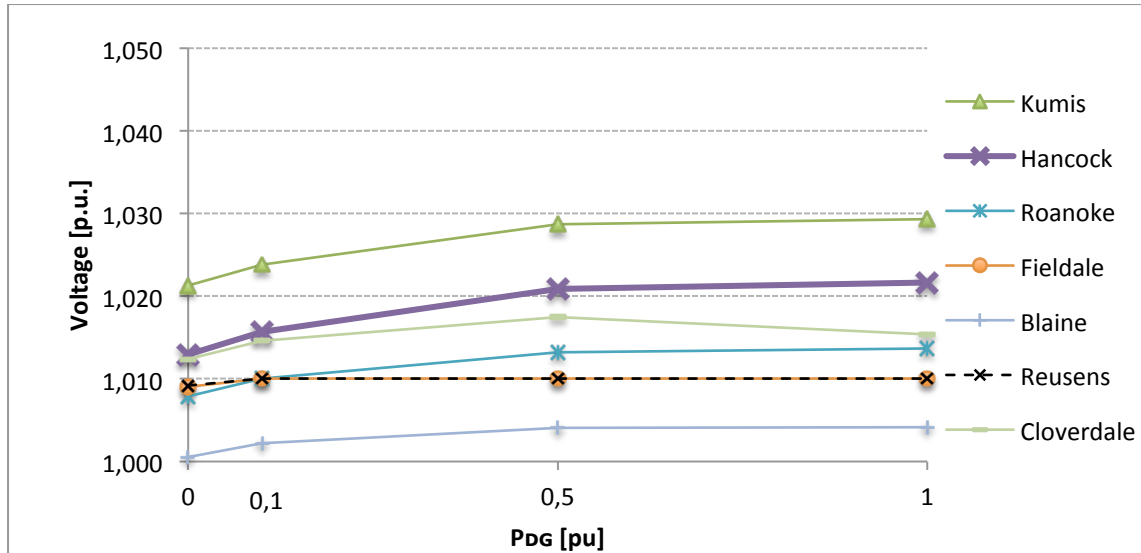
	no DG production TSP:-10	PDG=0,1 pu; TSP:-10	PDG=0,5 pu; TSP:-10	PDG=1 pu; TSP:-10
Kumis	1,021	1,024	1,029	1,029
Hancock	1,013	1,016	1,021	1,022
Roanoke	1,008	1,010	1,013	1,014
Fieldale	1,009	1,010	1,010	1,010
Blaine	1,001	1,002	1,004	1,004
Reusens	1,009	1,010	1,010	1,010
Cloverdale	1,012	1,015	1,018	1,015

Figure 6.35 Voltages in the HV grid (U_n=132 kV) depending on DG production at the TSP:-10

List of figures

List of tables

Eidstattliche Erklärung

Hiermit erkläre ich, dass die vorliegende Arbeit gemäß dem Code of Conduct – Regeln zur Sicherung guter wissenschaftlicher Praxis (in der aktuellen Fassung des jeweiligen Mitteilungsblattes der TU Wien), insbesondere ohne unzulässige Hilfe Dritter und ohne Benutzung anderer als der angegebenen Hilfsmittel, angefertigt wurde. Die aus anderen Quellen direkt oder indirekt übernommenen Daten und Konzepte sind unter Angabe der Quelle gekennzeichnet.

Die Arbeit wurde bisher weder im In– noch im Ausland in gleicher oder in ähnlicher Form in anderen Prüfungsverfahren vorgelegt.

Wien, am 25.9.2015

_____

Alexander Oman, BSc.